Advances in Solvent Extraction: Separation and Purification of Adjacent Trivalent Lanthanides Using the Electroneutral Solvating Extractant N,N,N',N'-Tetraoctyl Diglycolamide

A Dissertation

Presented in Partial Fulfillment of the Requirements for the

Degree of Doctor of Philosophy

with a

Major in Chemical Engineering

in the

College of Graduate Studies

University of Idaho

by

Kevin L. Lyon

Major Professor: Vivek Utgikar, Ph.D., P.E.

Committee Members: Matthew Bernards, Ph.D.; Haiyan Zhao, Ph.D.; Terry Todd, Ph.D.

Department Administrator: D. Eric Aston, Ph.D.

May 2020

AUTHORIZATION TO SUBMIT DISSERTATION

This dissertation of Kevin L. Lyon, submitted for the degree of Doctor of Philosophy with a Major in Chemical Engineering and titled, "Advances in Solvent Extraction: Separation and Purification of Adjacent Trivalent Lanthanides Using the Electroneutral Solvating Extractant N,N,N',N'-Tetraoctyl Diglycolamide," has been reviewed in final form. Permission, as indicated by the signatures and dates below, is now granted to submit final copies to the College of Graduate Studies for approval.

Major Professor: _____ Date: _____

Vivek Utgikar, Ph.D., P.E.

Committee Members: _____ Date: _____

Matthew Bernards, Ph.D.

_____ Date: _____

Haiyan Zhao, Ph.D.

_____ Date: _____

Terry Todd, Ph.D.

Department

Administrator: _____ Date: _____

D. Eric Aston, Ph.D.

ABSTRACT

Rare earth elements have become essential materials in advanced clean energy technologies and national security applications due to their unique properties. Despite their importance, the United States remains almost completely dependent upon foreign supply chains, notably imports from China, for both raw and finished commodities containing rare earth elements. This dissertation explores the implementation of a neutral ligand, N, N, N', N' tetraoctyl diglycolamide (TODGA), for the separation of rare earth elements. TODGA offers distinct advantages over traditional phosphonic acid extractants, notably the elimination of saponification to achieve high recovery in a solvent extraction circuit and improved adjacent lanthanide separation factors, ultimately requiring fewer solvent extraction stages to achieve high degrees of purity and recovery. This work marks the first use of TODGA's unique chemistry to separate and purify the rare earths from each other in hydrochloric acid media using counter-current solvent extraction.

Chapter 1 introduces the concept of rare earths as a critical material and highlights historic and future challenges associated with the rare earth supply chain. Separations remains as one of the greatest challenges due to high capital and operating costs to purify individual rare earth elements, thus emphasizing the need for advances in solvent extraction to enable a viable domestic supply chain in the United States.

Chapters 2 and 3 provide background context that motivated the research by describing commercial rare earth separation processes and an overview of TODGA's known applications and uses for trivalent lanthanide extraction and separation. While TODGA's lanthanide extraction chemistry has been studied extensively for separations relevant to the nuclear fuel cycle, it has not been successfully applied in the field of rare earth mining and hydrometallurgy to separate individual lanthanides with high degrees of recovery and purity in a continuous counter-current solvent extraction cascade. TODGA exhibits a unique extraction trend among "light" low molecular weight lanthanides, with an observed 50% increase in adjacent light lanthanide separation factors as compared to the industry standard phosphonic acid PC88A. This suggests that a counter-current solvent extraction cascade with a reduced number of stages may be implemented for the purification of light rare earth elements.

Chapter 4 outlines the various experimental methods that were utilized to conduct this research. A variety of techniques were utilized in the approach, including laboratory batch equilibrium solvent extraction experiments, counter-current mixer-settler testing, and process modeling and simulation using MATLAB/Simulink.

Chapter 5 provides the rationale behind counter-current solvent extraction modeling and simulation for process design. Mass balances around a solvent extraction cascade may be written as a system of ordinary differential equations and coupled with empirical laboratory equilibrium data to model the approach to steady state. Alternative techniques for steady state cascade modeling using algebraic equations written in the form of a tridiagonal matrix and solved using the Thomas Algorithm are discussed. This approach may also be coupled with empirical expressions for calculating distribution ratios as a function of free TODGA and aqueous phase chloride concentration at equilibrium.

Chapter 6 describes experimental results that were used to evaluate the feasibility of TODGA's extraction chemistry in a counter-current solvent extraction circuit. While TODGA demonstrates improved light rare earth separation factors, they are still relatively low, implying that neighboring lanthanides essentially co-extract. Commercially, high degrees of purity and recovery are achieved by implementing a selective scrubbing technique through which the purified REE product stream is refluxed into the scrub section. Batch solvent extraction experiments and simplified counter-current solvent extraction experiments in mixer-settlers revealed that TODGA is indeed capable of selective scrubbing to purify REEs under proper solvent loading conditions.

Chapter 7 describes the applied culmination of TODGA's extraction chemistry through the design and experimental testing of a solvent extraction process to produce the permanent magnet precursor material didymium (75% neodymium and 25% praseodymium by mass), from a mixed light rare earth chloride feed representative of that produced from the processing of bastnäsite ore. The chapter includes single metal extraction data with empirically determined expressions for calculating distribution ratios, followed by batch counter-current extraction experiments for light REE separations. Batch experimental results were used to design a 24-stage counter-current solvent extraction cascade to purify PrNd from a mixture of La, Ce, Pr, and Nd. While experimental results of the cascade design did

not achieve optimum recovery or purity, they indicate that TODGA can successfully be used to for the continuous separation and purification of light rare earths. Single metal distribution ratio correlations did not accurately model cascade behavior; a "pseudo single-metal" approach is presented to calculate distribution ratios under saturated loading conditions in a solvent extraction cascade.

Chapter 8 discusses the implications of utilizing TODGA in an industrial setting. While the use of a neutral ligand has distinct benefits over phosphonic acids, there are several limitations to the solvent system that require additional research efforts to address. Furthermore, implementing TODGA chemistry has economic impacts that may potentially limit its commercial viability. Notable limitations discussed include organic phase loading capacity, ligand synthesis and production costs, and high molarity salt-bearing raffinate streams that must be recycled or disposed of. A structure/property relationship was identified for DGA extractants with varying alkyl chain substituents, indicating that short alkyl chains make stronger, more selective extractants but are prone to gelling and third phase formation. Longer alkyl chains maintain selectivity and slightly reduce overall extraction strength. Branched alkyl chains prevent gelling and third phase formation but comes at the cost of poor selectivity due to steric hindrance caused by the branched alkyl chains in the outer coordination sphere.

Chapter 9 summarizes the general conclusion of this work: TODGA is capable of performing industrially relevant rare earth separations in continuous counter-current solvent extraction equipment, achieving high degrees of REE recovery and purity. However, its practical application is limited at this time due to its low organic phase loading. Ongoing research in collaboration with Oak Ridge National Laboratory is currently underway to synthesize and test novel DGA extractants with tailored alkyl chain substituents that achieve high degrees of organic phase loading capacity, maintain enhanced adjacent lanthanide selectivity among light rare earths, and demonstrate acceptable hydrodynamic behavior suitable for use in solvent extraction equipment.

ACKNOWLEDGEMENTS

First and foremost, I would like to thank my major professor, Dr. Vivek Utgikar, for advising me throughout my graduate studies. Vivek has become a great mentor, collaborator, and friend over the last eight years. I would like to thank my committee members, Dr. Matthew Bernards, Dr. Haiyan Zhao, and Dr. Terry Todd for their time and effort to read and evaluate this dissertation. I would like to thank Alice Allen for all her hard work to support and advise me throughout my graduate studies. I would like to thank Mitch Greenhalgh, Dr. R. Scott Herbst, and my Idaho National Laboratory (INL) colleagues for mentoring, guidance, and collaboration during my research. I would like to provide special thanks to INL intern Paige Brimley for her hard work and dedication conducting laboratory experiments to support this work. This project has been a multi-laboratory collaboration between Idaho National Laboratory (INL), Oak Ridge National Laboratory (ORNL), and Colorado School of Mines (CSM); I would like to thank Dr. Bruce Moyer, Dr. Derek Brigham, Dr. Ross Ellis, Dr. Santa Jansone-Papova, Dr. Mary Healy, and Brock O'Kelley for their contributions both intellectually and experimentally. Finally, I would like to thank the Critical Materials Institute and Idaho National Laboratory's Laboratory Directed Research and Development program for providing the funding that made this research possible.

DEDICATION

For Lauren and Zachary, my beautiful family. You are the purpose in life that drives me, and this would not have been possible without your love, support, and dedication. I love you more than you will know!

In loving memory of Dr. R. Scott Herbst, a beloved colleague, mentor, and friend. Scott opened endless doors of opportunity for me and empowered me with the tools to succeed in my professional career. I will be forever grateful for Scott's mentorship and giving me the opportunities to succeed.

TABLE OF CONTENTS

LIST OF FIGURES

LIST OF TABLES

CHAPTER 1: INTRODUCTION AND PROBLEM STATEMENT

The Rare Earth Problem

Rare earth elements (REE) are comprised of the lanthanide (Ln) series (lanthanum through lutetium) and typically include yttrium. Unique properties of REEs have made them indispensable for a vast range of applications in clean energy and national security technologies including hybrid electric vehicles, wind turbines, high efficiency lighting phosphors, military guidance and sonar systems, photovoltaic thin films, magnets, optics, and lasers. As electrification of our society expands, it is anticipated that future demand for REEs will continue to grow. Despite the importance of REEs in modern technologies, the United States is nearly 100% reliant on raw and finished REE product imports, with Chinese rare earth compounds and metals accounting for 80% of U.S. import sources in 2019 [1]. Chinese domination of the REE supply chain was made evident beginning in 2009 when China began to impose export restrictions on rare earths, citing the needs for conservation of its exhaustible natural resources and pollution reduction related to mining operations. This caused a tumultuous global response in the rare earth industry that has garnered international attention ever since, triggering unprecedented price spikes for REEs in 2011 and sparking supply chain uncertainty across clean energy manufacturing sectors.

The infamous REE price spike of 2011 initiated a revitalization in the domestic REE industry, with Molycorp resuming rare earth oxide (REO) production at their mining facility located at Mountain Pass, CA in 2012. Exploration efforts to develop rare earth projects ramped up both domestically and globally. Notable domestic exploration projects included Bear Lodge, WY, Bokan, AK, Diamond Creek, ID, Elk Creek, NE, La Paz, AZ, Lemhi Pass, ID/MT, Pea Ridge, MO, Round Top, TX, and Thor, NV [2]. Vulnerability of the REE supply chain also caught the attention of the federal government; the U.S. Department of Energy (DOE) published a Critical Materials Strategy in 2011 that defined a material as being critical if it is of high strategic importance for clean energy technologies and highly susceptible to supply chain disruption [3]. REEs Nd, Dy, Eu, Tb, and Y rose to the top of the strategy's published list of critical materials. In 2013, the DOE Advanced Manufacturing Office (AMO) established the Critical Materials Institute (CMI), a DOE Energy Innovation Hub tasked with providing innovative solutions to ensure a viable domestic supply of critical

materials that are crucial to U.S. manufacturing and energy security. Global trade issues surrounding critical materials ultimately culminated in a World Trade Organization lawsuit that ruled in 2014 Chinese trading practices were unfair, stating that export control cannot be used to protect and nurture domestic industry [4].

As quickly as the prices of REEs skyrocketed in the aftermath of Chinese export restrictions, they tumbled dramatically in the coming years. Over-supply, coupled with speculation that Chinese producers undercut competitor pricing, ultimately stagnated investment and interest in domestic rare earth production. Molycorp filed for bankruptcy protection in 2015 [5], halting mining operations at Mountain Pass altogether shortly thereafter. While import reliance and Chinese production dominance were still widely recognized as a vulnerability to the United States, the rare earths seemed to slowly fade away from the international spotlight.

The rare earth supply chain is further complicated when considering market conditions and production practices. First, the rare earths are often produced as a co-product or byproduct of a primary ore. For example, China's Baotou Rare Earth and Steel plant produces rare earths as a byproduct of an iron ore mine [6]. Co-production offers significant advantages not available to primary producers, such as bearing primary mining costs, overburden rock removal and management, and co-located infrastructure such as power, water, transportation and roadways, waste disposal, and capital equipment. Second, many operations overseas do not abide by the regulatory conduct and standards that would be enforced in the United States. Environmental pollution and unacceptable waste disposal practices are employed in an effort to reduce costs. Third, it can be argued that the rare earths and many other critical mineral commodities do not truly operate in a free market economy due to supply control and subsequent price manipulation by state-backed entities. While there is certainly a policy perspective that must be addressed at the federal government level to overcome market uncertainties and trading practices, competitive economic advantages can certainly be obtained through technical advancements in mineral processing operations that will help enable a domestic supply chain of critical materials.

Recent tensions on the international stage, particularly surrounding trade disputes with China, have brought the susceptibility of the REE supply chain back into focus. In an effort to address the vulnerability of critical minerals deemed strategic to the United States,

President Donald J. Trump issued Executive Order 13817, A Federal Strategy to Ensure Secure and Reliable Supplies of Critical Minerals, on December 20, 2017 [7]. The Executive Order strategy contained six calls to action: 1) Advance Transformational Research, Development, and Deployment Across Critical Mineral Supply Chains, 2) Strengthen America's Critical Mineral Supply Chains and Defense Industrial Base, 3) Enhance International Trade and Cooperation Related to Critical Minerals, 4) Improve Understanding of Domestic Critical Mineral Resources, 5) Improve Access to Domestic Critical Mineral Resources on Federal Lands and Reduce Federal Permitting Timeframes, and 6) Grow the American Critical Minerals Workforce. Furthermore, President Trump issued five presidential determinations under Section 303 of the Defense Production Act of 1950 on July 22, 2019. The five determinations specifically identified the need for the production of rare earth metals and alloys, separation and processing of heavy rare earth elements, separation and processing of light rare earth elements, production of neodymium-iron-boron rare earth permanent magnets, and production of samarium-cobalt rare earth permanent magnets [8]. These capabilities were determined by the President to be essential to national defense.

Expansion and diversification of the domestic rare earth supply chain requires economically viable technical advancements to mining and separation practices to compete and ensure responsible stewardship of the environment in today's economy. The rare earths are typically found in ore types such as monazite and bastnäsite, and the entire lanthanide series is usually present to some extent in a given ore body (although most rare earth ore deposits primarily consist of "light" atomic weight lanthanides) [9]. Industrial solvent extraction separation processes used to obtain individual rare earth elements are not only complex but also notorious for being costly, inefficient, and having adverse environmental impacts. The CMI deemed the separation of rare earths as a "Grand Challenge"- a problem that has the potential to cause adverse effects in a matter of months, whereas the solution could potentially take years or decades to be resolved and implemented [10].

Problem Statement

Improved separation processing techniques and/or solvent extraction ligands will reduce economic and environmental barriers to enable sustainable domestic REE supply chains. Reductions in capital and operating costs may be realized using solvent extraction

chemistries that minimize the consumption of chemical reagents and offer improved selectivity. In order to provide significant improvements over existing state of the art phosphonic acid solvent extraction processes, it is proposed to use an electroneutral solvating ligand, N,N,N',N'-tetraoctyl diglycolamide (herein referred to as TODGA). Available literature suggests that TODGA may offer enhanced light rare earth separation factors, thereby reducing capital and operating costs of a solvent extraction plant [11]. It is hypothesized that utilizing a neutral ligand will eliminate the need for saponification and the wasteful acid-base consumption characteristic of phosphonic acids. Furthermore, the solvent's promising REE selectivity improvements when compared to phosphonic acids may significantly reduce the number of equilibrium stages required to facilitate the necessary separations.

Consequently, the purpose of this research is to examine the applied solvent extraction chemistry of TODGA in detail and demonstrate for the first-time novel chloride-based REE separations using an electroneutral ligand through the design and testing of continuous counter-current solvent extraction processes. The primary focus will be on separations relevant to the processing of bastnäsite ore, with a specific emphasis on separations required for the production of the rare earth permanent magnet precursor material didymium oxide (a blend of 75% neodymium oxide and 25% praseodymium oxide by mass) [12]. Experimental results will be used to evaluate the performance of TODGA as compared to the current industry standard phosphonic acid. Primary criteria for evaluation will include equilibrium stage implications, chemical reagent consumption, process configurations, throughput, and impacts to the mineral processing facility.

CHAPTER 2: A REVIEW OF INDUSTRIAL RARE EARTH SEPARATION PROCESSES

Domestic Resources of Rare Earth Elements

The lanthanide series, while frequently referred to as rare earth elements, are actually far from rare. Consider Figure 2.1: the rare earth elements are actually more abundant in the earth's crust than many of the common transition metals. However, REEs are usually present in very low concentrations in the majority of REE-bearing ore bodies, making economic extraction and purification challenging due to the significant amounts of overburden and gangue material associated with the mineralogy.

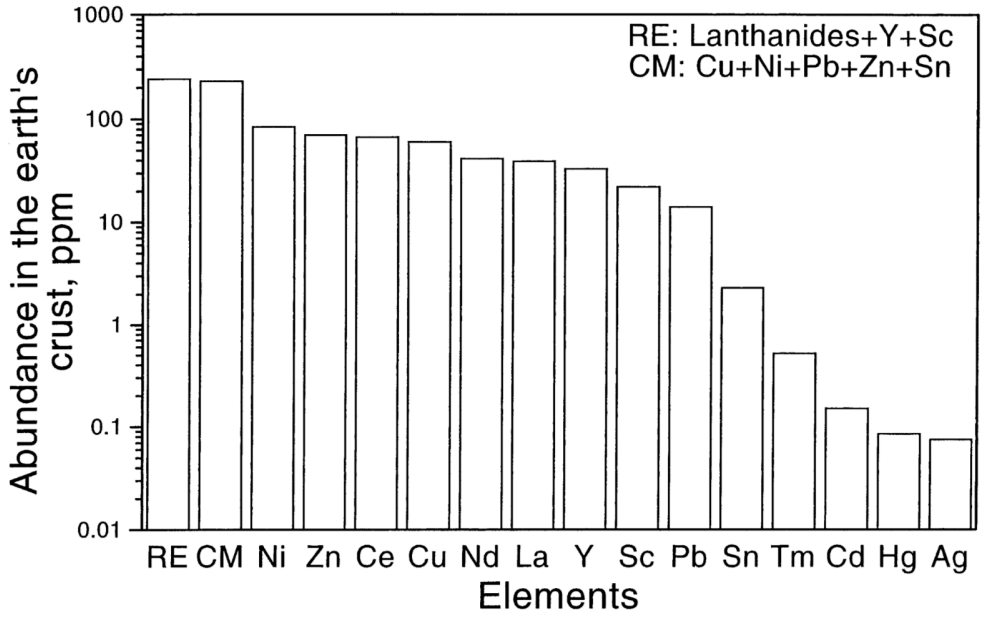

Figure 2.1: Crustal distribution of rare earths and other common elements [9].

The United States contains a vast number of domestic REE resources, with some estimates accounting for almost 12% of global REO reserves from placer and hard rock sources [13]. Host rock mineralogy is vast and complex across the known reserves, with notable REE minerals including bastnäsite, monazite, xenotime, apatite, and eudialyte [9]. While an exhaustive list of domestic REO reserves exists, there are only a handful of resources that are being actively pursued in the private sector for exploitation. Notable deposits under development include Rare Element Resources' Bear Lodge Project in northeastern Wyoming

and Ucore's Bokan-Dotson Ridge REE Project in southeastern Alaska [14, 15]. Other non-traditional resources have also been investigated recently through public-private partnerships, notably the recovery of REEs as a co-product or byproduct from coal and phosphate rock processing [16, 17].

To date, only one established mine exists in the United States, located at Mountain Pass, California. Originally discovered in 1949, the mining claims were purchased by The Molybdenum Corporation (later renamed Molycorp in 1974), which commenced rare earth production from the mine in 1952. Production expanded dramatically in the 1960s as driven by the demand for europium, used as a red phosphor in color televisions. After expansion in the 1960s, Mountain Pass dominated as the leading global producer of rare earths for nearly 30 years. However, mining operations slowly curtailed in the late nineties, and eventually ceased in 2002 due to competition from emerging Chinese producers and environmental restrictions [18].

As the rare earth crisis described in Chapter 1 unfolded, efforts were undertaken to modernize Mountain Pass, with investments exceeding 1.5 billion USD. Unfortunately, as rare earth production resumed at the mine market prices for rare earths continued to plummet. Molycorp, struggling with production issues and stiff competition from Chinese producers, eventually filed for bankruptcy in 2015 and the mine was placed in shutdown standby. U.S. investors JHL Capital Group and QVT Financial LP, backed by Chinese-owned Shenghe Resources Holding Company, acquired Mountain Pass in 2017 and resumed operations under the name MP Materials. Current production practices at the mine produce a rare earth concentrate that is currently being shipped overseas for downstream separations and purification. MP Materials has announced plans to resume downstream separations aimed at the production of didymium oxide by 2020 [18].

The mineralogy of Mountain Pass primarily contains bastnäsite with smaller fractions of monazite. The REE-bearing minerals are primarily co-mineralized with allanite, barite and quartz [9]. Bastnäsite is a rare earth fluorocarbonate of the general chemical form $(Ce,La)CO_3F$. The mass percentages of the individual REEs contained in Mountain Pass bastnäsite ore are shown in Figure 2.2.

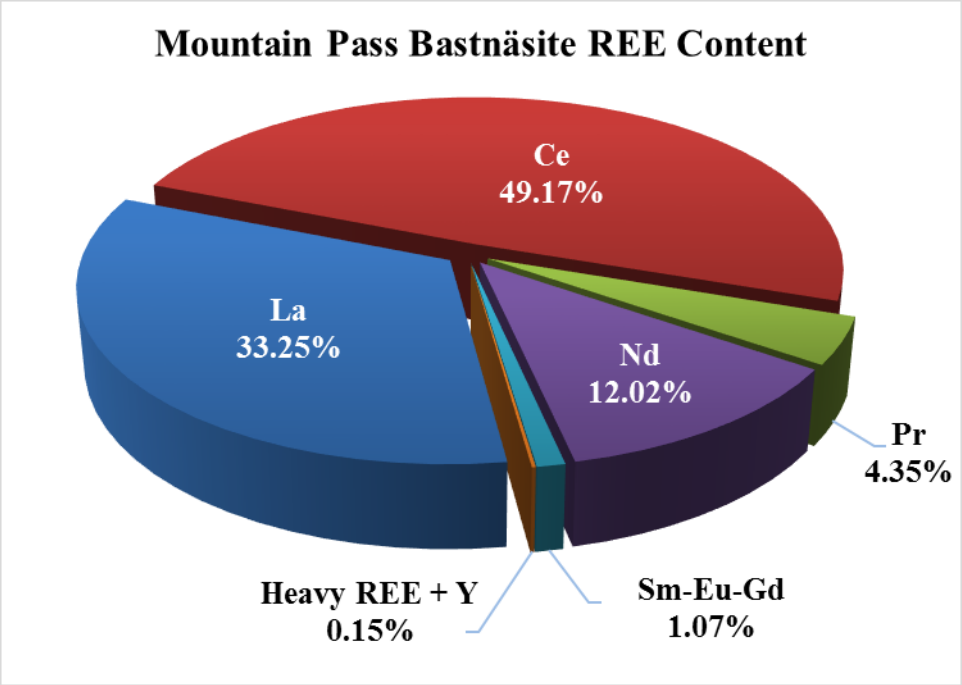

Figure 2.2: Bastnäsite ore rare earth content at Mountain Pass, CA [9].

The composition of Mountain Pass bastnäsite highlights the challenge of processing REEs that are deemed most critical for clean energy applications such as Nd, Dy, and Y. Nearly half of the rare earth content is cerium, with another third being comprised of lanthanum. Nd and Pr together account for an additional 16%, with the remaining distribution of heavy REEs (Sm-Lu+Y) totaling less than 1.5%. Significant overproduction of low-value Ce and La must occur in order to produce meaningful quantities of the most critical REEs. A detailed breakdown of the heavy REE composition of bastnäsite is shown in Table 2.1:

Table 2.1: Heavy REE composition of Mountain Pass bastnäsite [9].

Element	wt %
Sm	64.59%
Eu	9.66%
Gd	13.59%
Tb	1.30%
Dy	2.55%
Ho	0.42%
Er	0.29%
Tm	0.07%
Yb	0.05%
Lu	0.01%
Y	7.47%

Heavy REEs, accounting for less than 1.5% of the total REE content in bastnäsite, primarily consist of Sm. The balance is predominantly Gd, Eu, Y, Dy, and Tb. Bastnäsite, for all practical purposes, has negligible quantities of Ho-Lu. As such, the mineralogy of Mountain Pass characterizes it as a light rare earth mine, with operations targeting production of didymium oxide in the era of critical minerals as a precursor material for rare earth permanent magnet production.

Bastnäsite Beneficiation and Hydrometallurgical Processing

Upstream beneficiation of bastnäsite ore is typically performed through mining, milling, and froth flotation followed by acid leaching to produce an aqueous rare earth chloride solution [9, 13]. Due to the inherent chemical similarities of the lanthanide series, the rare earth distribution remains largely unaltered through beneficiation and dissolution unless specific measures are taken to manage cerium in the process. For example, historic operations at Mountain Pass (and existing operations within China) involve a roast/leach process by which cerium is oxidized to its tetravalent oxidation state. Tetravalent cerium does not readily dissolve in mineral acid solutions, generating a solid cerium residue that can either be sold as a commercial ceria product or sent to waste tailing impoundment. A process flow diagram of the historic Molycorp bastnäsite process is shown in Figure 2.3 [9].

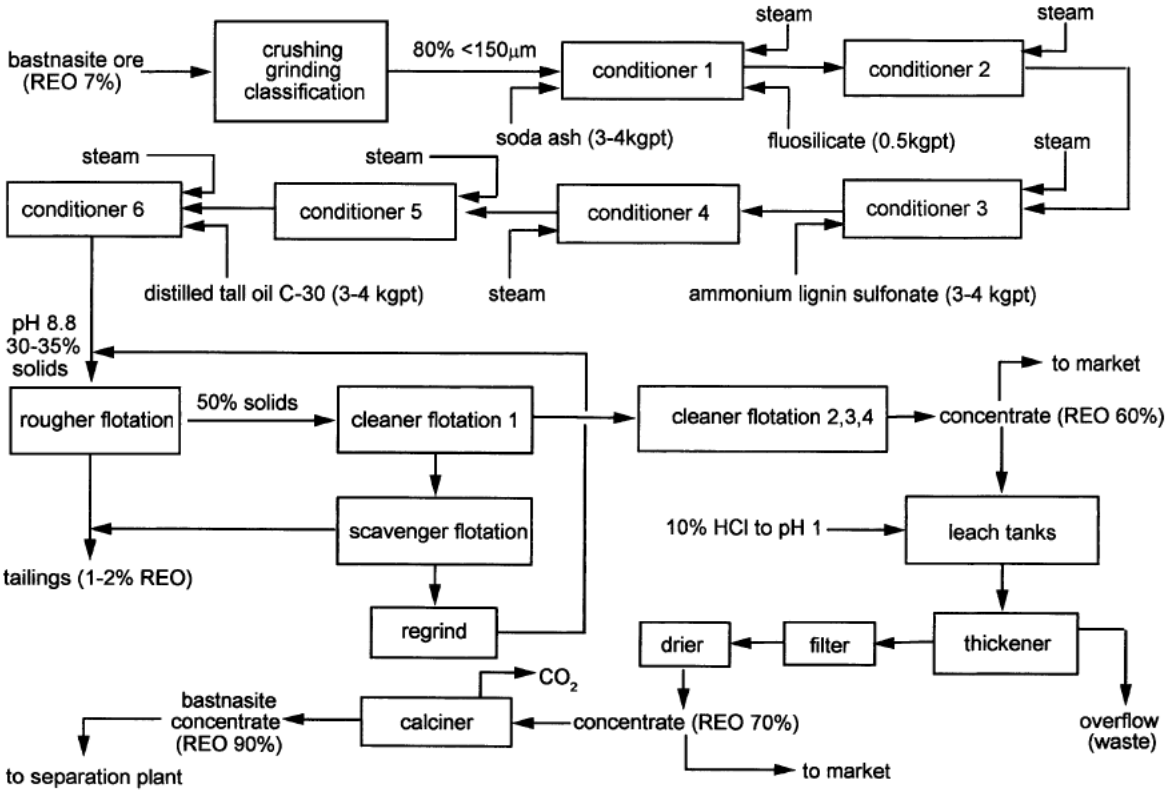

Figure 2.3: Historic Molycorp process for physical beneficiation and roasting to produce a cerium-depleted rare earth concentrate for separations [9].

Alternately, more aggressive cracking may be undertaken (as was practiced at Mountain Pass upon restart in the 2010 era) to solubilize cerium and enable its downstream recovery in purified form. The process utilized a concentrated HCl leach step, with the remaining residue undergoing metathesis with sodium hydroxide at elevated temperatures to produce a solid rare earth hydroxide cake upon filtration. The liquor produced from concentrated HCl leaching was combined with the rare earth hydroxide cake to re-dissolve the rare earths, producing a mixed rare earth chloride solution as a feed to the solvent extraction plant. A metathesis concentrate process is shown in Figure 2.4 [9].

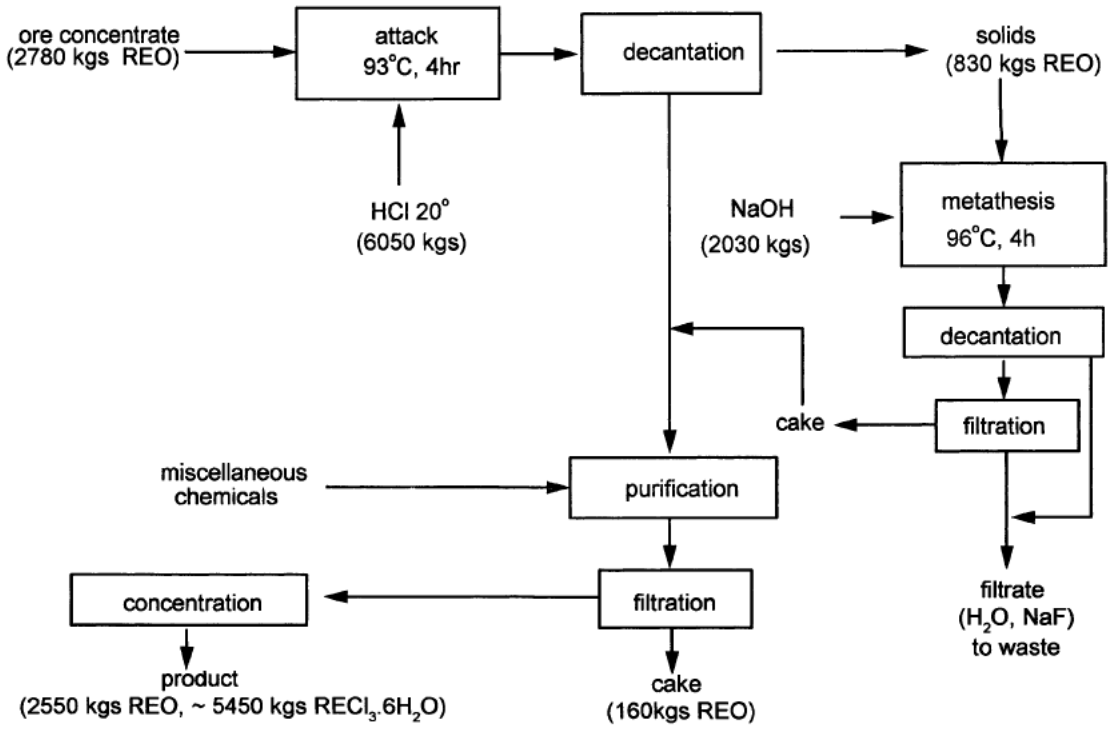

Figure 2.4: Leach-metathesis hydrometallurgy process to produce aqueous rare earth chlorides [9].

Domestic bastnäsite processing has traditionally removed significant portions of cerium using the historic roast/leach process, or through a patented process to selectively precipitate tetravalent cerium away from trivalent lanthanide chlorides in aqueous solution. Removal of bulk cerium simplifies downstream separation requirements for the production of didymium, as the high concentration of cerium, when left with the other rare earths requires significantly more stages to make a clean separation between cerium and praseodymium. Regardless of how cerium is handled in the process, a mixed rare earth chloride feed is produced from leaching and carries impurities such as calcium, potassium, iron, lead, and uranium at an acid normality amendable to separations via solvent extraction [9]. It is also important to note that domestic REO production almost exclusively utilizes hydrochloric acid as the primary mineral acid for dissolution and separations, citing its low cost, ease of disposal, and reduced regulatory burden as compared to other mineral acids.

Separation of Rare Earth Elements Using Solvent Extraction

Solvent extraction functions on the principle of partitioning solutes between two immiscible liquid phases of differing density. Solutes in an aqueous phase may be extracted into an organic phase solvent via intense mixing to facilitate mass transfer across the phases, followed by phase separation through means of gravitational or centrifugal force. Multiple contacts between the aqueous and organic phase may be implemented in a continuous counter-current cascade, thereby allowing high degrees of both recovery and purity [19, 20]. Solvent extraction has seen successful applications in the nuclear industry for uranium extraction and nuclear fuel reprocessing, as well as a vast array of applications in the mining industry to produce purified metals such as copper, cobalt, nickel, molybdenum, rare earth elements, and many more.

A detailed review of solvent extraction fundamentals, theory of counter-current solvent extraction, solvent extraction equipment, and lanthanide chemistry is described previously [21]. However, key aspects of this unique group of elements' solvent extraction chemistry shall be discussed herein to provide context and rationale for the experimental approach to rare earth separations using TODGA in subsequent chapters.

The chemistry of the rare earths is predominantly ionic and is determined by the size of the metal ion [22]. The lanthanides primarily exist as Ln(III) ion due to the valence [Xe] noble gas core electron configuration that is achieved in this oxidation state, as the 4f orbital electrons are inner-shell electrons. For example, the electron configuration of elemental Gd is $[Xe]4f^{7}5d^{1}6s^{2}$; Gd(III) is the only observed cation in aqueous solution due to the stability of the full valence electron shell [Xe] configuration. There are notable exceptions to the Ln(III) oxidation state due to the special stability associated with empty, half-filled, or filled f-shell electrons. For example, Ce(IV) maintains an empty f-shell configuration and Eu(II) maintains a half-filled f-shell configuration. Not surprisingly, traditional industrial separation techniques for Ce and Eu have exploited the stability of these alternate oxidation states [9].

Separation of individual trivalent rare earths is extremely difficult due to this inherent chemical similarity across the series. The 4f orbital electrons do not directly participate in bonding. Fortunately, as inner shell electrons, they do have a unique influence on the

properties of each element. As atomic number increases across the lanthanide series, the atomic radius actually decreases, an effect known as the Lanthanide Contraction (published REE ionic radii may be found in Appendix A). This effect is caused by imperfect shielding of one electron by another in the same subshell. Nuclear charge increases with increasing atomic number, and electron shielding causes the effective nuclear charge to increase for f-shell electrons. Consequently, the ionization energy increases with increasing atomic number. Lanthanide ions in aqueous solution act as Lewis acids and therefore exhibit a decrease in basicity across the series. Lanthanide ions of the smallest ionic radius (i.e. "heavy" atomic weight lanthanides) will form the strongest ligand complexes, allowing a means to exploit their chemical behavior for separation processes [22].

Various extractants have been used for industrial separation of REEs using solvent extraction, typically phosphoryl-based molecules, carboxylic acids, or amines. Well-established examples include bis (2-ethylhexyl) phosphoric acid (HDEHP), n-tributyl phosphate (TBP), versatic acid, versatic 10, and Aliquat 336 [19]. However, modern rare earth solvent extraction separation processes are almost exclusively performed with 2-ethylhexylphosphonic acid mono-(2-ethylhexyl) ester, also known under the common trade names of EHEHPA, PC88A, P-507, Ionquest 801, or DS-100 (from here on it shall be referred to as PC88A, shown in Figure 2.5).

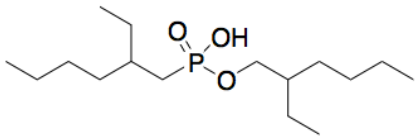

Figure 2.5: 2-ethylhexylphosphonic acid mono-(2-ethylhexyl) ester (PC88A).

PC88A is a phosphonic acid ligand with extraction behavior that characterizes it as a liquid cation exchanger according to the following equilibrium reaction [23]:

$$[RE^{3+}]_{aq} + [3(HA)_2]_{org} \leftrightarrow [RE(HA_2)_3]_{org} + 3[H^+]_{aq} \quad \text{(Eq. 1)}$$

In Equation 1, HA designates the acidic extractant molecule PC88A, with "H" representing the hydroxyl group proton bonded to the phosphorus atom. The extractant forms a dimer due to hydrogen bonding that occurs with the hydroxyl and double bonded oxygen groups. Lanthanides are extracted into the organic phase at a ratio of 3 moles of extractant dimer to

one mole of trivalent lanthanide. Extraction of one mole of trivalent lanthanide into the organic phase liberates three moles of proton to the aqueous phase, maintaining overall charge balance in the system. The extent to which component *i* is extracted into the organic phase is typically expressed using the distribution ratio:

$$D_i = \frac{y_i}{x_i} \quad \text{(Eq. 2)}$$

Where y_i and x_i represent the equilibrium organic and aqueous phase concentrations of component *i*, respectively. Typically, a high distribution ratio (> 1) implies a large extent of extraction, while a low distribution ratio (< 1) indicates that limited extraction occurs, retaining the component in the aqueous phase. This may not always be the case if the ratio of organic to aqueous phase volumes (O/A) deviate from unity in the solvent extraction contact. For example, consider a generic single solvent extraction contact to extract component *i*. A mass balance may be written assuming component *i* is initially only present in the aqueous phase:

$$V_A x_{F,i} = V_O y_i + V_A x_i \quad \text{(Eq. 3)}$$

Where

- V_O and V_A = Volumes of organic and aqueous phases, respectively [L]
- $x_{F,i}$ = Initial aqueous phase concentration of component *i* [mol/L]
- y_i = Equilibrium organic phase concentration of component *i* [mol/L]
- x_i = Equilibrium aqueous phase concentration of component *i* [mol/L]
- $\frac{O}{A} = V_O/V_A$

Percent extraction of component *i* is calculated as follows:

$$\%\, Extraction = \left(\frac{V_O y_i}{V_A x_{F,i}}\right) \times 100\% \quad \text{(Eq. 4)}$$

Combining Equations 3 and 2, $x_{F,i}$ may be expressed as:

$$x_{F,i} = x_i \left(\frac{O}{A} D_i + 1\right) \quad \text{(Eq. 5)}$$

Lastly, percent extraction may be calculated using only the O/A ratio and the distribution ratio by combining Equations 2, 4, and 5:

$$\% \, Extraction = \left(\frac{\frac{O}{A} D_i}{\frac{O}{A} D_i + 1} \right) \times 100\% \qquad \text{(Eq. 6)}$$

If D_i = 0.2 and O/A = 1, the calculated percent extraction is only 16.7%. However, if D_i = 0.2 and O/A = 10, the calculated percent extraction is 66.7%. As such, care must be given interpreting equilibrium distribution ratios within the context of the extraction conditions. The ratio of the distribution ratios between two extracting species A and B is defined as the separation factor:

$$\beta_{A/B} = \frac{D_A}{D_B} \qquad \text{(Eq. 7)}$$

The separation factor provides a measure of the relative selectivity the ligand has for extracting one species over another. High separation factors indicate a higher degree of separation between the two species. PC88A separation factors across the lanthanide series are well documented in literature, exhibiting an average adjacent lanthanide separation factor across the entire series of 1.57. Published separation factors for PC88A are shown in Table 2.2:

Table 2.2: Published separation factors (β) for PC88A, $\beta_{A/B} = D_A/D_B$. Extraction from 0.1 M HCl with 0.2 M PC88A in kerosene [9].

B	A												
	Ce	Pr	Nd	Sm	Eu	Gd	Tb	Dy	Ho	Er	Tm	Yb	Lu
La	1.30	1.42	1.67	3.33	6.52	9.52	22.5	36.4	93.9	117	156	175	199
Ce		1.09	1.28	2.57	5.02	7.36	17.3	28.0	72.3	90.5	120	135	152
Pr			1.17	2.35	4.59	6.72	15.8	64.2	66.0	82.7	110	123	140
Nd				2.00	3.94	5.74	13.5	21.8	56.3	70.5	93.7	105	119
Sm					1.96	2.87	6.74	10.9	28.2	35.3	46.8	52.6	59.5
Eu						1.46	3.45	6.39	14.4	18.0	24.0	26.9	30.4
Gd							2.35	3.81	9.82	12.3	16.3	18.3	20.7
Tb								1.62	4.18	5.23	6.95	7.81	8.83
Dy									2.58	3.23	4.29	4.82	5.45
Ho										1.25	1.66	1.87	2.11
Er											1.33	1.49	1.69
Tm												1.12	1.26
Yb													1.13

The selectivity trend across the lanthanide series indicates that PC88A has a higher extraction affinity for heavier atomic weight REEs than it does for light atomic weight REEs. This agrees well with the expected trend in ligand complexation strength across the series due to Lanthanide Contraction effects [22]. The equilibrium constant for the reversible reaction depicted in Equation 1 may be expressed as:

$$K_{eq} = \frac{[RE(HA_2)_3]_{org}[H^+]_{aq}{}^3}{[RE^{3+}]_{aq}[(HA)_2]_{org}{}^3} = D_{RE}\frac{[H^+]_{aq}{}^3}{[(HA)_2]_{org}{}^3} \quad \text{(Eq. 8)}$$

Inspection of Equation 8 indicates that this reaction is strongly dependent on the aqueous phase acid concentration. Although the third-power dependency exists for the ligand concentration, counter-current extraction cascades are almost always operated at very high O/A ratios to prevent solubility issues and third phase formation and thus the change in free ligand concentration does not have an appreciable effect as compared to the aqueous phase acid concentration. In fact, empirical equilibrium models to predict PC88A-REE distribution ratios have been published in literature for counter-current cascade process design that are only a function of initial rare earth concentration and initial acid concentration [19]. For PC88A, the distribution ratio increases for low acid concentrations (high pH) and decreases for high acid concentrations (low pH). PC88A's extraction dependence on acid concentration is the basis for counter-current cascade operation. A typical PC88A counter-current rare earth solvent extraction cascade is shown in Figure 2.6.

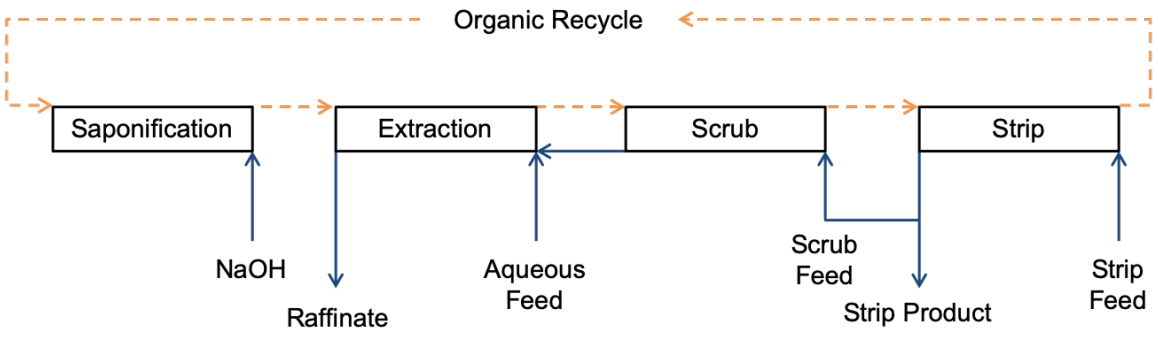

Figure 2.6: Typical PC88A counter-current rare earth solvent extraction cascade.

The majority of PC88A rare earth solvent extraction cascades consist of four major sections: saponification, extraction, scrub, and strip. Each section consists of one or more counter-current equilibrium stages. The saponification section pre-neutralizes a certain fraction of PC88A in the organic phase. Common bases utilized in industry for this purpose include NH_4OH, NH_4HCO_3, or NaOH [13]. The saponification reaction replaces PC88A's hydroxyl group proton with the respective cation (NH_4^+, Na^+, etc.), which readily extracts lanthanides with no net change in aqueous phase acid concentration [24]. Saponification is required to achieve high degrees of purity and recovery; without this step the acid liberated to the

aqueous phase during metal extraction would adversely shift the extraction equilibrium shown in Equation 1 in accordance with Le Chatelier's Principle, establishing an equilibrium pH at which REE distribution ratios do not favor extraction.

The aqueous feed solution containing the mixture of REEs is fed to the extraction section. As its name implies, the extraction section provides bulk extraction of the desired REEs into the organic phase from the aqueous phase. As previously mentioned, REE extraction is favored at low feed acidities. The spent aqueous phase, referred to as the raffinate, exits the extraction section. The organic phase containing extracted REE shall be referred to as loaded organic (LO). As indicated by the relatively low adjacent separation factors shown in Table 2.2, the loaded organic will contain significant fractions of co-extracted neighboring REEs if complete recovery of the desired REE(s) is to be obtained. Loading of REEs into the organic phase occurs with minimal separation [25].

The scrub section is responsible for the actual purification of REEs by selectively removing co-extracted REEs from the loaded organic phase. Rare earth separation cascades use a unique process to accomplish selective scrubbing by refluxing a portion of the purified product solution as the aqueous scrub feed, as shown in Figure 2.6. Under appropriate equilibrium pH conditions and reflux ratio, PC88A will selectively exchange one rare earth for another based on REE extraction affinity. Using Nd and Pr as an example, Equation 9 shows the observed net effect of metal-metal exchange selective scrubbing:

$$[Nd^{3+}]_{aq} + [Pr(HA_2)_3]_{org} \leftrightarrow [Nd(HA_2)_3]_{org} + [Pr^{3+}]_{aq} \quad \text{(Eq. 9)}$$

PC88A exhibits a higher extraction affinity for Nd over Pr. Consequently, the organic phase will selectively displace Pr and become purified in Nd, provided an aqueous phase source of Nd is available via reflux of the purified Nd product solution. The organic phase, now purified in Nd, is referred to as the scrubbed loaded organic. This selective scrubbing reflux technique minimizes dilution of the rare earths in the solvent extraction cascade and minimizes the number of equilibrium stages required to achieve an effective separation [23]. Again, this reflux technique is essential to achieve high degrees of purity and recovery in a reasonable number of stages because the extraction and stripping behavior of adjacent lanthanides is so similar.

The final section of the counter-current cascade is the strip section. REEs are removed from the organic phase by shifting the reaction equilibrium in Equation 1 to the left by means of a highly acidic aqueous strip feed solution. REEs in the organic phase are transferred to the aqueous phase, with the purified REE solution leaving the strip section being referred to as the strip product. Product data sheets for phosphonic acids indicate acid concentrations as high as 3.6 M HCl are required to strip heavy atomic weight REEs such as erbium from PC88A [26]. The stripped solvent (referred to as barren organic), now depleted in REEs, is continuously recycled in the solvent extraction cascade.

The acid and base consumptions required to operate PC88A solvent extraction circuits contribute to the high operating costs of a separations plant and also generate significant volumes of wastewater effluents. For example, conventional Chinese processing estimates from 2014 suggest that REE dissolution, separations, and precipitation consume 11 tons of hydrochloric acid, 2.4 tons of sodium hydroxide, and 120 tons of water per ton of REO produced, translating to over 20 million gallons of wastewater and 800,000 tons of salt discharge annually [27].

Industrial rare earth separation plants almost exclusively use mixer-settlers and therefore this equipment will be the sole equipment choice utilized for this research. Mixer-settlers are chosen in the rare earth industry for several reasons: they are simple to operate, reliable, easily scalable, provide long residence times to achieve stage equilibrium, and can be re-started rapidly in the event of a process upset. Primary disadvantages for mixer-settlers include large holdup volumes, rare earth inventory holdup, floor space requirements, and a long approach to steady state [20].

The counter-current cascade shown in Figure 2.6 only represents a single REE separation process; multiple cascades are required to completely separate individual purified REEs. As previously discussed, REE concentrates produced from bastnäsite primarily contain Ce, La, Nd, and Pr, with a significantly smaller fraction of the higher atomic weight REEs. REEs are first separated into groups based on atomic weight, followed by further downstream processing to make separations between adjacent REEs, eventually obtaining pure individual REEs. Each separation step requires a solvent extraction cascade complete with saponification, extraction, scrubbing, and stripping to achieve the desired separation [25].

Figure 2.7 illustrates the separations typically performed for bastnäsite ores targeting didymium oxide production, with the minimum required solvent extraction circuits circled:

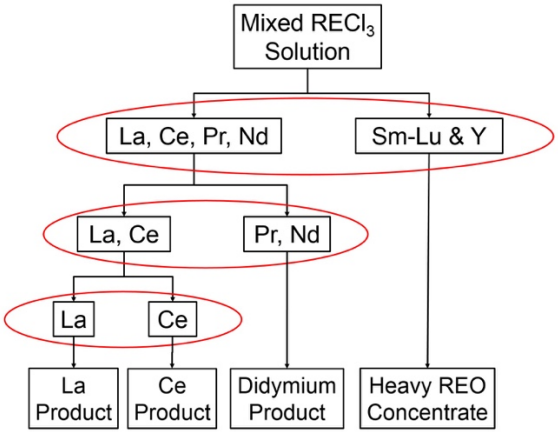

Figure 2.7: Target separations for a mixed rare earth chloride solution derived from bastnäsite ore processing.

Many miners of light rare earths simply produce a heavy REO concentrate containing Sm-Lu + Y for sale to producers overseas, as the significantly lower concentration of these species often precludes the possibility of economic separation of individual heavy REE. It becomes evident that a separations facility producing pure REE products could potentially consist of hundreds of stages of solvent extraction stages with a large number of complex, connected circuits that are highly susceptible to process transients and deviations in feed composition. For example, Solvay's La Rochelle rare earth processing plant utilized 18 solvent extraction circuits comprising over 1,100 mixer-settlers to separate and purify all of the individual REE [28]. Due to the economic competitive nature of the mining and metals industries, the actual details of plant design and operation are typically closely guarded secrets. While industry state-of-the-art phosphonic acid solvent extraction processes are an effective method for separating the rare earths, there are significant drawbacks to the process chemistry including poor selectivity, chemical reagent consumption, and environmental impacts. Alternative REE separation extractants that exhibit higher selectivity and eliminate chemical processing steps may offer reductions in capital and operating costs. Hence the research on the electroneutral solvating extractant TODGA, as described in the following chapters, aims to develop counter-current solvent extraction processes with improved REE separation factors and elimination of saponification.

CHAPTER 3: TODGA CHEMISTRY AND ITS APPLICATIONS[1]

Introduction

Solvent extraction of trivalent lanthanides using electroneutral solvating ligands has been a focus in separations science for over 50 years, albeit for different applications and goals. Specific to the rare earth industry, n-tributyl phosphate (TBP) has been used industrially for the separation of light rare earth nitrates at both Rhône-Poulenc in France and Thorium Ltd. in the United Kingdom [29, 23, 9]. Rhône-Poulenc's process was historically regarded as the industry standard for rare earth processing, using a combination of solvent extraction, ion exchange, and a variety of extractants to facilitate the separation and purification of all of the individual rare earths [9]. Thorium Ltd.'s process was unique in that the mixer-settler cascade was operated batchwise under 100% reflux, followed by draining of select mixer-settler stages to recover the desired purified solutes once steady state was obtained [23, 29]. Equilibrium data for the extraction of chloride and nitrate salts of Pr and Nd with TBP at various metal concentrations, acid concentrations, and Nd:Pr mole ratios are available in literature [30]. Gray reported Nd:Pr separation factors ranging from 1.07 to 1.67 in nitrate media, with distribution ratios for both species generally ranging from 0.15 to 0.7. Chloride media Nd:Pr separation factors ranged from 0.9-1.0, with extremely low distribution ratios for both species ranging from 0.006-0.01. Consequently, TBP's low affinity for lanthanide extraction from HCl has precluded its use in chloride-based industrial applications. Despite historic industrial applications of TBP for rare earth nitrate separations, the chemistry was displaced with the advent of cation exchange ligands that readily extract REEs from HCl media such as HDEHP and PC88A. The PC88A-Ln(III)-HCl solvent system offers improved separation factors as compared to the TBP-Ln(III)-HNO_3 system as well as reduced operating costs associated with the migration from HNO_3 to HCl. The use of electroneutral solvating extractants in industry has thus far been limited to lanthanide

[1] *Work referenced in the TODGA Extraction Chemistry section of this chapter has been published by team members on CMI's rare earth separations research program. The program is led by Idaho National Laboratory in collaboration with Oak Ridge National Laboratory and Colorado School of Mines. ORNL authors have kindly shared their extraction data for analysis and interpretation in the context of the work conducted in this dissertation.*

separations in nitric acid, with lower separation factors and consequently less efficient process configurations than current state of the art separations facilities.

Diglycolamide Ligands

N, N, N', N' Tetraoctyl Diglycolamide (TODGA) has been studied extensively in various liquid-liquid extraction systems, primarily for applications in the nuclear fuel cycle. A simple literature search for TODGA reveals a seemingly endless plethora of research aimed at 4f and 5f element extraction using solvent extraction, extraction chromatography, membrane solvent extraction, and others. For example, TODGA and other DGA derivatives have been evaluated for the separation of trivalent lanthanides from trivalent actinides in high level acidic waste, such as the Actinide Lanthanide Separation (ALSEP) process [31]. Similarly, European researchers have utilized TODGA in the innovative SANEX (Selective Actinide Extraction) process to co-extract and separate actinides and lanthanides from PUREX (Plutonium Uranium Reduction Extraction) raffinate solutions [32]. Membrane solvent extraction systems utilizing TODGA have demonstrated the separation of rare earths from recycled magnets for the recovery of critical materials such as Nd and Pr [33]. TODGA's chemical structure is shown in Figure 3.1.

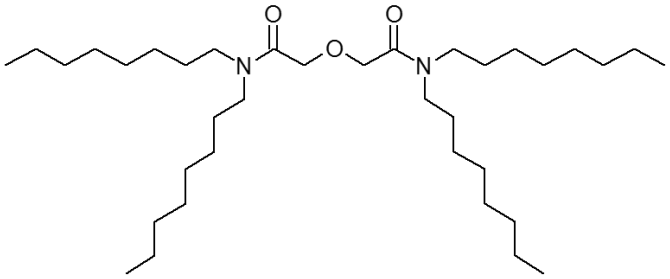

Figure 3.1: N, N, N', N' Tetraoctyl Diglycolamide (TODGA).

Despite the vast quantity of available literature, the majority of applications utilize TODGA as a group lanthanide extractant, i.e. the primary purpose is the co-extraction and recovery of all trivalent lanthanides present in an acidic aqueous solution. Some studies have attempted to separate individual lanthanides using TODGA extraction chromatography resins but arrived at the conclusion that the lanthanides cannot be mutually separated from one another unless they are on diverging ends of the 4f series, e.g. separation of lanthanum from lutetium [34].

Recent literature published by CMI researchers suggests that TODGA may be well suited for light rare earth separations due to the "anion swing" behavior of neutral diglycolamide (DGA) extractants, potentially eliminating the need for acid-base chemistry and the associated secondary wastes produced with traditional phosphonic acid chemistries utilized in the rare earth industry [11]. TODGA's extraction behavior also demonstrated improved separation factors among light adjacent lanthanides, averaging 2.6 for lanthanum through neodymium [11]. This represents more than a two-fold increase in separation factors published for PC88A [9], suggesting that REE separations using TODGA could be achieved in a reduced number of solvent extraction stages. High HCl concentrations in the aqueous phase yield appreciable extraction of lanthanides using DGAs [35]. Extraction data for the TODGA-Ln(III)-HCl system discussed in this chapter indicates significant improvements in REE distribution ratios across the lanthanide series when compared to the TBP-Ln(III)-HCl extraction system, marking a significant advance in the extraction of REEs from acidic HCl solutions using electroneutral solvating extractants.

TODGA Extraction Chemistry

TODGA and DGA derivatives extract trivalent lanthanide ions and the corresponding counter-anions from aqueous solutions as an electroneutral ligand:metal complex. Brigham et. al. reported complementary experimental results using liquid-liquid extraction, X-ray absorption spectroscopy (XAFS), density functional theory (DFT) simulations, and classical molecular dynamics simulations to propose insight into the structure, coordination, and stoichiometry of DGA-Ln(III) extraction. Their work revealed that DGAs coordinate to trivalent lanthanides in a tridentate fashion, accommodating three counter-anions in the outer-coordination sphere as shown in Figure 3.2 [36]:

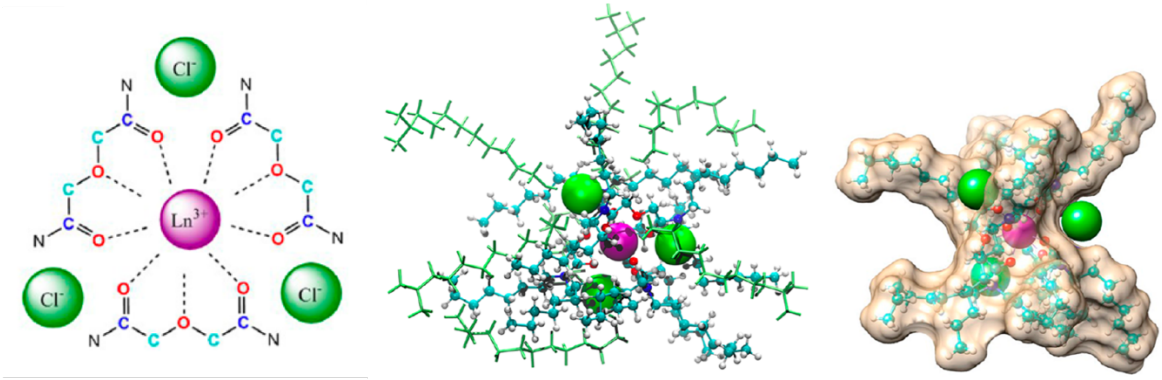

Figure 3.2: $[Nd(TODGA)_3]^{3+}(Cl^-)_3$ tridentate structure (left), classical molecular dynamics simulation of the $[Nd(TODGA)_3]^{3+}(Cl^-)_3$ complex with phase modifier molecules (center), and Solvent-accessible surface representation of $[Nd(TODGA)_3]^{3+}(Cl^-)_3$ [36].

Classical molecular dynamics simulations from this study proposed that the three TODGA molecules provide "clefts" to accommodate the anions, maximizing electrostatic attraction to the cation while minimizing repulsive interactions from the chloride anions. The overall proposed reversible extraction mechanism and stoichiometry for this solvent system is given as:

$$[Ln^{3+}]_{Aq} + 3[Cl^-]_{Aq} + 3[TODGA]_{Org} \leftrightarrow [LnCl_3 \cdot 3TODGA]_{Org} \qquad \text{(Eq. 10)}$$

According to Le Chatelier's Principle, Equation 10 indicates that TODGA will favor the extraction of trivalent lanthanides into the organic phase under high ionic strength conditions (i.e. high aqueous phase chloride concentrations), and extracted lanthanides are stripped from the organic phase by contacting it with a low ionic strength aqueous phase such as dilute HCl. Manipulation of TODGA's "anion swing" behavior provides control over extraction and stripping conditions similar to the pH swing behavior utilized for the extraction and stripping of lanthanides using phosphonic acids. As previously described, phosphonic acids liberate protons to the aqueous phase during extraction of trivalent lanthanides via a cation exchange mechanism, adversely impacting recovery without the use of saponification as a pre-neutralization step for the ligand. Given sufficient ionic strength, TODGA will not self-limit extraction equilibrium because the overall charge balance is satisfied by the extraction of an electroneutral complex into the organic phase. The equilibrium constant for this reversible reaction may be expressed as:

$$K_{eq} = \frac{[LnCl_3 \cdot 3TODGA]_{Org}}{[Ln^{3+}]_{Aq}[Cl^-]^3_{Aq}[TODGA]^3_{Org}} \quad \text{(Eq. 11)}$$

Upon inspection of Equation 11, the equilibrium organic and aqueous phase lanthanide concentrations are contained in the numerator and denominator, respectively. Incorporating the definition of the distribution ratio from Chapter 2 into Equation 11 yields:

$$D_{Ln} = K_{eq}[Cl^-]^3_{Aq}[TODGA]^3_{Org} \quad \text{(Eq. 12)}$$

The distribution ratio therefore has a third power dependence on the aqueous phase chloride concentration at equilibrium and a third power dependence on the organic phase TODGA concentration at equilibrium. Ellis et. al. conducted TODGA extraction studies at varying HCl feed concentrations to determine selectivity trends across the lanthanide series; their results are shown in Figure 3.3:

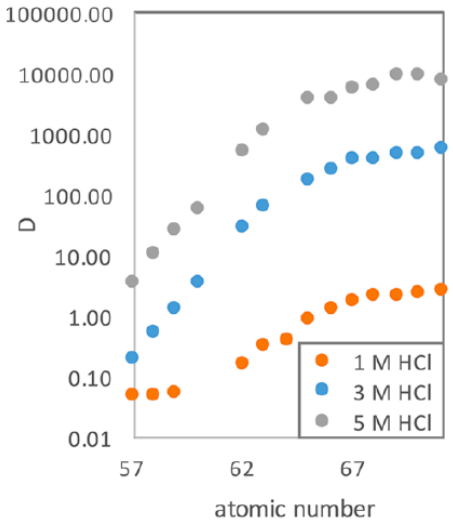

Figure 3.3: 0.1 M TODGA extraction trends across the lanthanide series (La-Lu) at varying HCl feed concentrations. Aqueous feed contained 0.1 mM of each Ln(III) [11].

The slope of the extraction curve is indicative of the adjacent lanthanide separation factor. Their work exhibited a non-linear extraction trend across the series, with an average adjacent lanthanide separation factor of 2.6 for the light atomic weight rare earths La-Nd and an average adjacent lanthanide separation factor of 1.2 for the heavy atomic weight rare earths Er-Lu. Using a combination of liquid-liquid extraction experiments, XAFS, and DFT calculations the authors concluded that the $[Ln(TODGA)_3]^{3+}(Cl^-)_3$ complex is the dominant

extracted species in the organic phase for all lanthanides across the series under the extraction conditions tested. Furthermore, the nonlinear trend in extraction was rationalized as a balance between steric effects and coordination energies [11]. Ultimately, there are two conclusions that can be drawn about the industrial applicability of TODGA for rare earth separations. First, TODGA exhibits the highest extraction affinity for heavy rare earths but demonstrates poor adjacent heavy lanthanide separation factors, therefore offering no significant advantage over state of the art phosphonic acids as an extractant to produce individual purified heavy rare earths. However, while less selective for light lanthanides, TODGA's adjacent light lanthanide separation factors are significantly higher than those published for PC88A. Consider Table 3.1 comparing light separation factors of interest to the processing of bastnäsite ore:

Table 3.1: Published separation factors (β), $\beta_{A/B} = D_A/D_B$ for TODGA [11] and PC88A [9]. TODGA extraction from 3 M HCl with 0.1 M TODGA, PC88A extraction from 0.1 M HCl with 0.2 M PC88A.

TODGA				
B	A			
	Ce	Pr	Nd	Sm
La	3.0	7.3	19.2	159.1
Ce		2.4	6.4	19.2
Pr			2.6	21.9
Nd				8.3

PC88A				
B	A			
	Ce	Pr	Nd	Sm
La	1.3	1.4	1.7	3.3
Ce		1.1	1.3	2.6
Pr			1.2	2.4
Nd				2.0

Furthermore, extraction trends at 3 M HCl and 5 M HCl shown in Figure 3.3 suggest that control of the chloride concentration in the aqueous phase will enable selective extraction of lanthanides to facilitate the required separations relevant to bastnäsite ore processing described in Chapter 2. Extraction at 1 M HCl yields D values less than 1 for all lanthanides below Dy, with a maximum D value of 2.63 for Lu. The slope of the extraction curve decreases across the series at lower acidity, suggesting that TODGA is less selective at low chloride concentrations not suitable for extraction. This implies that the rare earths will exhibit similar stripping behavior upon recovery from the solvent in a counter-current cascade using dilute HCl.

Despite the potential benefits of TODGA's extraction chemistry suggested in literature, separation of neighboring adjacent light lanthanides that simultaneously achieves both high recovery and high purity has not been demonstrated for the TODGA-Ln(III)-HCl solvent system. The process conditions to facilitate such a separation using a counter-current solvent

extraction cascade are unknown, and it is also unknown if recovery must be sacrificed in order to obtain high purity. The following chapters provide a basis for the deliberate design approach and operation of a solvent extraction cascade for rare earth separations using TODGA.

CHAPTER 4: MATERIALS AND METHODS

Chemical Reagents and Solution Preparation

Hydrochloric acid is used almost exclusively in the rare earth industry for solvent extraction separations due to its low cost, ease of disposal, and reduced environmental and regulatory burden. Therefore, HCl was chosen as the aqueous phase acid medium for all solvent extraction experiments. Reagent grade 37% HCl was purchased from GFS Chemical (Columbus, OH) and used directly without further purification. REE-bearing aqueous feeds were prepared from 99.9% purity rare earth oxides (La_2O_3, Pr_6O_{11}, Nd_2O_3, and Sm_2O_3, GFS Chemical, Columbus, OH) and 99.9% purity anhydrous rare earth chloride salts ($CeCl_3$, Sigma-Aldrich, St. Louis, MO). Didymium oxide (79.5% Nd_2O_3, 20.5% Pr_6O_{11} by mass) was graciously provided by Molycorp LLC (Mountain Pass, CA) and utilized for selective scrubbing experiments described in Chapter 6. Aqueous solutions were prepared by dissolving rare earth oxides in excess 37% HCl and 18 MΩ nanopure water. The resulting solutions were cooled to ambient laboratory temperature (average 22 °C, experiments were not conducted in a temperature-controlled atmosphere). Anhydrous $CeCl_3$ was added for feeds containing cerium after cooling to prevent oxidation and subsequent precipitation of tetravalent cerium. $CeCl_3$ was utilized because purified ceric oxide, CeO_2, does not dissolve readily in concentrated HCl solutions. Once all rare earths were in solution, feeds were diluted to final desired volumes using 18 MΩ nanopure water.

Purified TODGA, technical grade TODGA, N,N'-dimethyl-N,N'-dioctyl diglycolamide (DMDODGA), and N,N,N′,N′-tetra-2-ethylhexyl diglycolamide (T2EHDGA) were obtained from Marshallton Research Laboratories, Inc. (King, NC). DMDODGA and T2EHDGA were utilized for comparison and evaluation of dispersion number measurements in Chapter 8. Purified TODGA was utilized for fundamental experiments described in Chapter 6 to explore and understand the extraction and scrubbing behavior of DGA chemistry. Technical grade TODGA was utilized for experiments and counter-current solvent extraction experiments described in Chapter 7 due to the large volumes required to operate mixer-settlers. Extraction experiments performed with both purified TODGA and technical grade TODGA indicate that the ligand's selectivity and strength are not impacted by the presence of impurities. While impure, technical grade TODGA was pursued for mixer-settler

experiments to ensure relevant industrial process economics. TODGA is traditionally purified using costly silica gel columns; large plant solvent inventories required by mixer-settlers would make purified solvent economically impractical. Technical grade TODGA contains approximately 92 wt% TODGA with an undetermined balance of remaining synthesis reagent impurities, of which are shown in the synthesis reaction described in Figure 4.1 [37]:

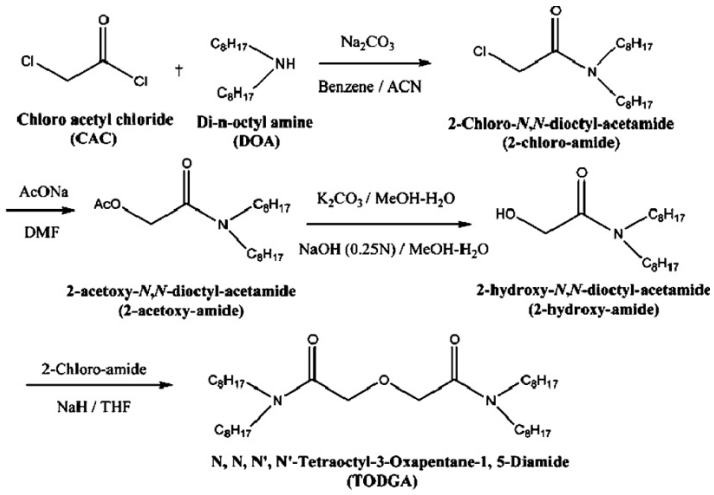

Figure 4.1: Synthesis of TODGA using chloro-acetyl chloride and di-n-octyl amine [37].

Exxal-13 was purchased from chemical distributor Univar (Salt Lake City, UT) and used without further purification. Exxal-13, produced by Exxon Mobile, is a branched aliphatic alcohol primarily consisting of isotridecyl alcohol. Preliminary solvent extraction experiments revealed that the TODGA-Ln(III)-HCl system would form precipitates and/or third phase formation; Exxal-13 was added as a phase modifier to achieve a stable organic phase. Exxal-13 was added at a ratio of 30% by volume for solvent preparation unless otherwise noted.

Isopar-L was purchased from chemical distributor Univar (Salt Lake City, UT) and used without further purification. Isopar-L acts as a diluent to improve the hydrodynamic properties of the organic phase such that it is fit for use in solvent extraction equipment. Isopar-L, produced by Exxon Mobile, is an aliphatic isoparaffinic hydrocarbon solvent consisting of C11-C13 isoalkanes. Isopar-L has an aqueous phase solubility that is below measurable detection limits, has a low vapor pressure (0.3 mm Hg), and contains less than 1 ppm aromatic hydrocarbons, making it a suitable diluent for laboratory scale solvent

extraction processes. Industrial applications typically use a similar low-grade diluent (contains appreciable impurity aromatic and sulfur compounds) due to the increased costs associated with high purity diluents such as Isopar-L [21].

Organic phase solvents were prepared by weighing the required mass of TODGA in a volumetric flask. Exxal-13 was pipetted into the flask, and the solvent was brought to the desired final volume using Isopar-L diluent. The solvent was mixed thoroughly on a vortex orbital mixer until all components were fully solubilized and uniformly mixed.

Due to limited availability from the manufacturer, various Exxal products were used for batch equilibrium experiments in this work. The three products utilized were Exxal-13, Exxal-12, and Exxal-10 and their use is specifically denoted for all solvent extraction experiments. The primary difference between these solvents is the average number of carbons present in the branched aliphatic chain [38]. Complimentary work conducted at ORNL indicated that these phase modifiers could be used interchangeably with minimal impact to the solvent system; however, Exxal-13 was chosen as the primary modifier as experiments progressed toward mixer-settler testing due to its commercial availability.

Batch Solvent Extraction Experiments

Batch solvent extraction experiments were conducted by pipetting the desired volumes of aqueous and organic phases into capped culture tubes, conical bottom centrifuge tubes, or separatory funnels as dictated by the desired O/A ratio and total experiment volume. The phases were intimately mixed to ensure equilibrium was achieved (3 minutes on vortex orbital mixer, five minutes vigorous shaking by hand, or 1 hour on a rotary wheel mixer, as dictated by the size of the contacting experiment). After mixing, the phases were separated using a centrifuge operated at 7000 RPM for three minutes (or settling overnight, approximately 12 hours, for larger separatory funnel shakeouts). The phases were then separated using Pasteur pipettes and sampled for analysis.

Various extraction data were obtained for both individual metal species and mixed metal feeds throughout this work. Data were obtained as a function of HCl feed concentration, metal concentration, and O/A ratio. Scrubbing and stripping data were obtained by contacting an organic phase containing the metal species of interest with an aqueous phase of varying acidity or metal concentration. Scrubbing contacts were aimed at producing an

organic phase rich in the target REE from an organic feed that contains a mixture of REE (REE composition and concentration dependent upon specific separation). Strip data were obtained for Nd and Pr because the stripping process is the final recovery step in a counter-current solvent extraction process where it is expected to have high purity metal concentrations.

Counter-Current Mixer-Settler Tests

Counter-current mixer-settler experiments were conducted using a laboratory scale 32-stage mixer-settler system. The mixer-settlers were manufactured by MEAB Metallextraktion AB based in Sweden. The units are compact, portable, easily reconfigurable, have a low holdup volume, and are constructed of materials that have superior chemical compatibility to allow a versatile testing environment for solvent extraction testing. The system's low solvent inventory is crucial for custom-synthesized ligands that are not commercially available in large quantities, such as TODGA. The 32-stage system is shown in Figure 4.2.

Figure 4.2: INL's 32 stage MEAB mixer-settler system.

The mixer-settlers are constructed of polyvinylidene difluoride (PVDF) for all wetted parts and PVDF or polytetrafluoroethylene (PTFE) connections and tubing were used in the operation of the system. Mixer motor speed was adjusted using a manual control knob. Aqueous and organic feeds to the mixer-settlers are delivered by FMI pumps from Fluid Metering, Inc. Model RHV pumps were chosen for this application because they can deliver

highly accurate flow rates at the low process throughputs required by the mixer-settlers. Table 4.1 lists the mixer-settler specifications provided by the manufacturer.

Table 4.1: MEAB mixer-settler properties.

Mixing chamber volume	120 mL
Settling chamber volume	480 mL
Loading surface area	0.006 m^2
Maximum total throughput (combined Org+ Aq+ Aq recycle)	10 L/hr

The loading surface area describes the total surface area of the settling section in the mixer-settler unit. The loading surface area is typically used to scale up solvent extraction processes- increased loading surface area allows higher throughputs. Scale-up works very well for solvent extraction processes because the process chemistry is unaltered, assuming phase ratios, relative flow rates and adequate mixing are maintained.

Proper operation requires a balance of mixing speed and throughput in order to obtain stage equilibrium and still provide adequate time for phase disengagement. Previous work identified suitable operating conditions for the MEAB mixer-settlers [21]. All counter-current solvent extraction experiments conducted in this work used a maximum throughput of 40 mL/min (organic plus aqueous flow) to ensure a minimum three-minute residence time in the mixing chamber. Mixer motor speeds were maintained at 950±50 RPM as read on a portable tachometer. Mixer speeds below 900 RPM adversely affected phase dispersion and stage equilibrium due to poor mixing. Excessive mixer speeds created emulsions that caused excessive carryover of the aqueous phase in the organic outlet.

Analytical Procedures

Aqueous phase acid titrations were performed using an automated Mettler Toledo DL70 titrator. The titrant is 0.1 M sodium hydroxide and the titrator automatically determines the equivalence point of the acid-base titration to determine the sample's acid concentration. One issue that requires mitigation during titration is the presence of metal ions in acidic aqueous solution. Hydrated metal ions in solution can act as a Bronsted acid, causing hydrolysis and lowering the pH of an aqueous solution. The observed pH of the solution will be lower than the pH that would be observed solely from the contribution of mineral acid. This phenomenon, known as metal hydrolysis, is easily mitigated by adding 5 mL of 1 M

potassium oxalate to complex any metal ions in the sample solution. Addition of potassium oxalate forms an insoluble metal precipitate, allowing an accurate measurement of the solution pH. Typically oxalate precipitation is only necessary for extremely high metal concentrations, but this method was used for all titrated samples to eliminate any uncertainty due to hydrolysis effects.

Metal concentrations were determined for organic and aqueous phases by inductively coupled plasma-optical emission spectroscopy (ICP-OES, Thermo iCAP 6500). ICP-OES analysis services were performed through off-site analytical chemistry laboratories. Aqueous phase samples can be analyzed directly using ICP-OES, but organic-phase samples cannot be analyzed directly due to instrument limitations. Any loaded metal must be stripped from the organic phase into aqueous solution for ICP analysis. This was accomplished by performing a batch contact with the organic phase sample of interest with excess dilute hydrochloric acid. Stripped organic samples are prepared as follows:

- 500 μL of desired organic sample, 5 mL of 0.1 M HCl
- O/A phase ratio of 0.1
- 3-minute mixing time on vortex orbital mixer
- Centrifuge for 3 minutes at 7000 RPM for phase disengagement
- Separate clean aqueous phase for analysis

This method has been confirmed in the laboratory to quantitatively remove extracted metals from the organic phase sample. The low O/A phase ratio dilutes the samples by an order of 10, which must be accounted for after determining the metal concentrations using ICP. Error can be introduced using this technique if the phase volumes are not accurately measured to account for dilution effects, but typically mass balances are ±5% using this method. The mass balance is determined by taking a known feed solution, performing an extraction batch contact, and analyzing each phase's metal content in relation to the feed solution.

Many experiments conducted in this work were resource-intensive or sufficiently complex such that duplication of experiments for validation and uncertainty quantification were not logistically feasible. Consequently, ICP-OES analyses included rigorous quality control standards to provide confidence in analytical data. All samples were analyzed in radial plasma view. All wavelengths for each analyte were used during the analysis, but the

reported wavelength concentration was chosen by looking at the quality control data, sensitivity and minimum spectral interference with each run. The calibration curves were generated each analysis day using NIST traceable standards from Inorganic Ventures. The calibration curve was developed using a blank and 5 concentrations ranging from 10 µg/L to 100,000 µg/L and required a linear correlation of at least 0.995. All samples were diluted 2-500X with 1% HNO_3 to ensure the concentration of each analyte was within the analyzed calibration range. Each matrix type was spiked with a known concentration of analyte and recoveries were calculated and used to determine if there was any interference due to the matrix. There were no matrix interference issues with any of the samples. Duplicates were analyzed at a rate of 10%. A laboratory control standard (LCS) was analyzed prior to sample analysis to verify that the generated calibration curve was valid. The LCS was analyzed every 10 samples to ensure there was no instrument drift. A blank of the 1% HNO_3 used for sample dilution was analyzed every 10 samples to verify there was no contamination. The calibration standards were analyzed as samples at a rate of every 30 samples to also ensure there was no instrument drift [21]. Analytical results determined by ICP-OES are reported at the 95% confidence interval. For simplicity, error bars are omitted from data plots to clearly portray correlation trends. Corresponding errors do not exceed 15% at 2-sigma.

Modeling and Simulation Methods

Counter-current solvent extraction process design requires the coupling of equilibrium solvent extraction data with a mass balance model. Detailed governing equations and processes are discussed in detail in Chapter 5. MATLAB/Simulink R2019b was utilized for all of the process modeling, simulation, and design in the present work. Material balances and ideal cascade design calculations were performed with Microsoft® Excel.

CHAPTER 5: MODELING AND SIMULATION FOR COUNTER-CURRENT SOLVENT EXTRACTION PROCESS DESIGN

Previously published work outlined an empirical method to couple equilibrium solvent extraction data for phosphonic acid chemistries with a governing mass balance model for the purpose of counter-current solvent extraction process design [39, 21]. The REE extraction model treats each stage as a well-mixed volume, solving time-dependent mass balances using MATLAB/Simulink R2019b software to calculate stage-to-stage organic and aqueous effluent concentrations in a counter-current cascade. The previously derived model incorporated a time-dependent acid concentration mass balance, which was determined to be the key driving force that governed extraction equilibria in phosphonic acid solvent systems. Given that the present work focuses on the use of an electroneutral solvating extractant, a more generic mass balance modeling approach may be used. Consider the counter-current cascade shown in Figure 5.1:

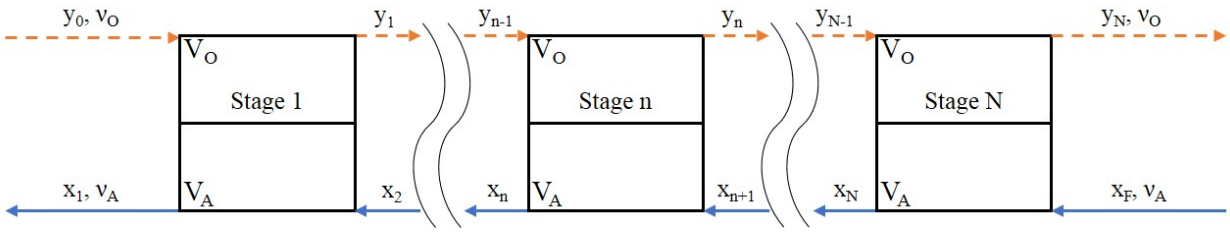

Figure 5.1: Counter-current solvent extraction cascade.

Where:

- V_O and V_A = holdup volume of organic and aqueous phases, respectively [L]
- v_O and v_A = organic and aqueous flow rates, respectively [L/min]
- y_n = organic phase concentration of REE leaving stage *n* [mol/L]
- x_n = aqueous phase concentration of REE leaving stage *n* [mol/L]
- y_0 = feed organic phase concentration of REE [mol/L]
- x_F = feed aqueous phase concentration of REE [mol/L]

A time-dependent mass balance ordinary differential equation (ODE) for component *i* in stage *n* is shown in Equation 13:

$$\frac{d(V_O y_{i,n} + V_A x_{i,n})}{dt} = v_O y_{i,n-1} + v_A x_{i,n+1} - v_O y_{i,n} - v_A x_{i,n} \qquad \text{(Eq. 13)}$$

The organic and aqueous phase concentrations of component *i* are related through the distribution ratio as defined in Equation 2 from Chapter 2. Substitution of Equation 2 into Equation 13 yields the ODE and boundary condition shown in Equation 14:

$$\frac{dx_{i,n}}{dt} = \frac{v_O D_{i,n-1} x_{i,n-1} + (-v_O D_{i,n} - v_A) x_{i,n} + v_A x_{i,n+1}}{V_O D_{i,n} + V_A}, \qquad x_{i,n}(0) = 0 \qquad \text{(Eq. 14)}$$

Equation 14 assumes the distribution ratio is independent of time. This assumption is reasonable for mixer-settlers where the holdup volume is much larger than the volumetric flow rate, i.e. small integration time steps have negligibly small changes in REE concentration [40]. Multicomponent systems may be modeled as a large system of nonlinear ODEs, with one ODE per component per stage.

One weakness identified in this modeling approach is the significant error between calculated and measured stage effluent concentrations during the approach to steady state, especially as applied to mixer-settlers. The mathematical model described in Equation 13 treats each stage as an ideal, homogeneous mixed volume, assuming completely immiscible phases with 100% stage efficiency. In reality, the two phases are mixed into an emulsion in a mixing chamber followed by subsequent phase separation in a settling chamber. Mixer-settlers rely on gravitational forces for coalescence and phase separation based on the density difference and immiscibility of the aqueous and organic phases. Consequently, the settling chamber typically has a holdup volume that is significantly larger than the mixing chamber to allow adequate residence time for phase disengagement prior to exiting the stage at the outlet weirs. When determining steady state equilibrium, these effluent aqueous and organic phase weirs are commonly the reference point for sample measurement. During the approach to steady state, the settling chamber acts as a large dilution volume after extraction has occurred in the mixing chamber, which will yield an actual concentration leaving the stage that is lower than the concentration predicted by assuming the entire stage is uniformly mixed. This dilution issue can be addressed by representing each phase in the settler as a series of well mixed volumes [39, 41]. A representation of this concept is shown in Figure 5.2.

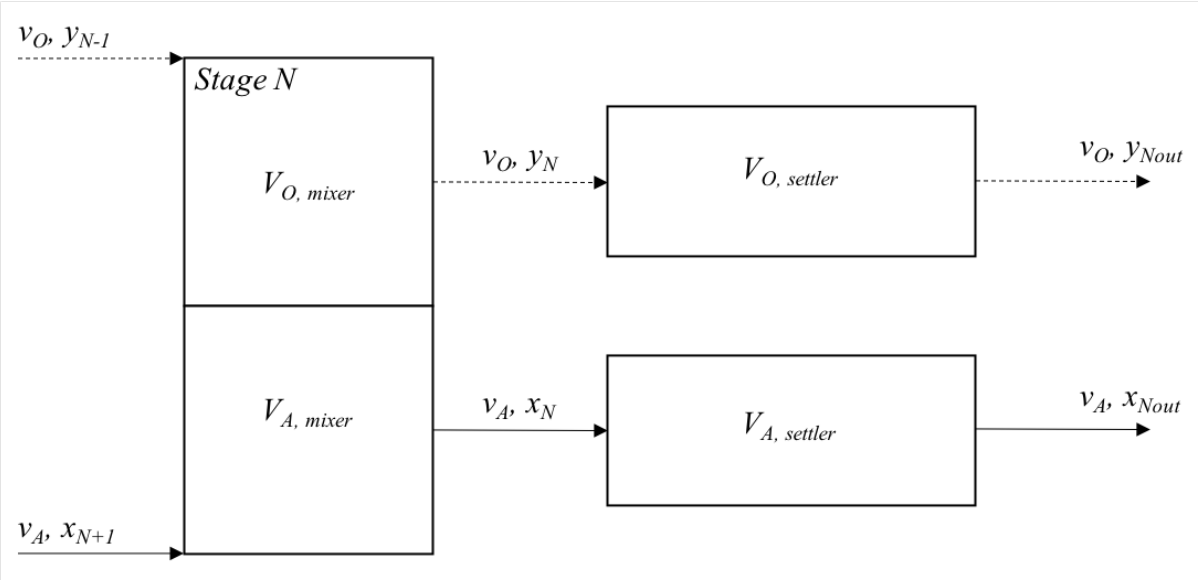

Figure 5.2: Single stage mixer-settler model. The mixer is treated as a homogeneous mixed volume with complete equilibrium phase transfer. Each phase in the settling chamber is treated as a well-mixed tank with no reaction [39].

Using a classic mass balance model for a continuous stirred tank reactor (CSTR) [42], the aqueous and organic phase settling volumes may be expressed as:

$$\frac{dy_{N_{out}}}{dt} = \frac{1}{\tau_{org}}\left(y_N - y_{N_{out}}\right) \qquad y_{N_{out}}(0) = 0 \tag{Eq. 15}$$

$$\frac{dx_{N_{out}}}{dt} = \frac{1}{\tau_{aq}}\left(x_N - x_{N_{out}}\right) \qquad x_{N_{out}}(0) = 0 \tag{Eq. 16}$$

Where the organic and aqueous phase residence time is defined as:

$$\tau_{org} = \frac{V_{org,settler}}{v_{org}} \tag{Eq. 17}$$

$$\tau_{Aq} = \frac{V_{Aq,settler}}{v_{Aq}} \tag{Eq. 18}$$

Improved agreement between observed and calculated transient stage effluent concentrations using this dilution model may be further improved by breaking the settling chamber into a series of CSTRs, approaching plug-flow behavior [41].

The primary modeling objective for the present work is to predict the steady state performance as indicated by solute recovery and purity in a counter-current solvent

extraction cascade. While the time-dependent model may still be utilized for this purpose, rigorous approaches have been identified in literature that may be used to determine organic and aqueous phase steady state concentrations [43, 44]. At steady state, the differential operator cancels out and yields a simplified material balance around stage *n* for component *i*:

$$v_O y_{i,n-1} + v_A x_{i,n+1} = v_O y_{i,n} + v_A x_{i,n} \quad \text{(Eq. 19)}$$

Similarly, combination of the distribution ratio as defined in Equation 2 with Equation 14 followed by simplification by moving all terms to the left-hand side of the equation yields the following:

$$[v_O] y_{i,n-1} + \left[-v_O - \frac{v_A}{D_{i,n}}\right] y_{i,n} + [v_A] x_{i,n+1} = 0 \quad \text{(Eq. 20)}$$

Stage *n+1* aqueous equilibrium concentration may be eliminated from the equation through the use of the calculated distribution ratio from stage *n+1*:

$$[v_O] y_{i,n-1} + \left[-v_O - \frac{v_A}{D_{i,n}}\right] y_{i,n} + \left[\frac{v_A}{D_{i,n+1}}\right] y_{i,n+1} = 0 \quad \text{(Eq. 21)}$$

A mass balance around the extraction feed stage *N* for component *i* yields the following:

$$v_O y_{i,N-1} + v_A x_{i,F} = v_O y_{i,N} + v_A x_{i,N} \quad \text{(Eq. 22)}$$

In this instance, x_F represents the incoming solute-bearing aqueous feed and is assumed to be known. Again, using the distribution ratio for stage *N* and re-arranging yields:

$$[v_O] y_{i,n-1} + \left[-v_O - \frac{v_A}{D_{i,N}}\right] y_{i,n} = v_A x_{i,F} \quad \text{(Eq. 23)}$$

Upon further inspection, conducting a material balance around any given stage will yield a mass balance equation that may be written in the general form:

$$a_i y_{i-1} + b_i y_i + c_i y_{i+1} = d_i \quad \text{(Eq. 24)}$$

The generic mass balance format specified in Equation 24 may be implemented in the form of a tridiagonal matrix. Steady state solvent extraction models have made use of tridiagonal matrices and the Thomas Algorithm forward sweep technique to solve large systems of mass balance equations [43]. Equation 25 shows a tridiagonal matrix representation of a system of equations containing *n* number of stage mass balances:

$$\begin{bmatrix} b_1 & c_1 & 0 & 0 & 0 \\ a_2 & b_2 & c_2 & 0 & 0 \\ 0 & a_3 & b_3 & \ddots & 0 \\ 0 & 0 & \ddots & \ddots & c_{n-1} \\ 0 & 0 & 0 & a_n & b_n \end{bmatrix} \begin{bmatrix} y_1 \\ y_2 \\ y_3 \\ \vdots \\ y_n \end{bmatrix} = \begin{bmatrix} d_1 \\ d_2 \\ d_3 \\ \vdots \\ d_n \end{bmatrix} \quad \text{(Eq. 25)}$$

Equation 25 assumes that $y_0 = 0$, e.g. the incoming organic solvent is solute-free. Using the Thomas Algorithm forward sweep method [45], new coefficients c_i' and d_i' are defined as:

$$c_i' = f(x) = \begin{cases} \frac{c_i}{b_i}, & i = 1 \\ \frac{c_i}{b_i - a_i c_{i-1}'}, & i = 2, 3, \dots, n-1 \end{cases} \quad \text{(Eq. 26)}$$

$$d_i' = f(x) = \begin{cases} \frac{d_i}{b_i}, & i = 1 \\ \frac{d_i - a_i d_{i-1}'}{b_i - a_i c_{i-1}'}, & i = 2, 3, \dots, n \end{cases} \quad \text{(Eq. 27)}$$

The solution to the system of equations is then obtained via back-substitution:

$$y_n = d_n' \quad \text{(Eq. 28)}$$

$$y_i = d_i' - c_i' y_{i+1} \quad ; \quad i = n-1, n-2, \dots, 1 \quad \text{(Eq. 29)}$$

Equations 26-29 represent the governing steady state mass balance model that may be utilized to conduct counter-current cascade calculations. For simplified scenarios, constant distribution ratios may be utilized for rough order of magnitude estimates and general performance trends. However, rigorous calculations that yield high purity, high recovery, and more accurate predictive capabilities require the use of variable distribution ratios through an iterative solving method. The final piece of information required to complete this system of equations is the calculation of distribution ratios for the TODGA-Ln(III)-HCL solvent system as a function of total chloride and free TODGA concentrations at equilibrium in each stage. Recall from Chapter 3 that Ln(III) extraction by TODGA suggests that the distribution ratio has a third power dependence on both the total chloride concentration in the aqueous phase and the free TODGA concertation in the organic phase at equilibrium. In the context of the mass balance model, this may be calculated as:

$$D_{i,n} = K_{i,n}[x_{Cl^-}]^3[y_{DGA}]^3 \quad \text{(Eq. 30)}$$

Using a similar technique described in Benedict, Pigford, and Levi for uranium and plutonium extraction with n-tributyl phosphate [46], the free TODGA concentration at equilibrium may be calculated by:

$$y_{DGA} = y_{DGA_0} - \sum_i y_i \xi_{yi} \quad \text{(Eq. 31)}$$

Where

- y_{DGA} = Free TODGA concentration at equilibrium, mol/L
- y_{DGA_0} = Total TODGA concentration in the organic phase, mol/L
- y_i = Organic phase rare earth concentration for species *i*, mol/L
- ξ_{yi} = Stoichiometric coefficient for extracted solutes (ξ = 3 for all trivalent lanthanides)

Similarly, the total aqueous phase chloride concentration at equilibrium may be calculated by:

$$x_{Cl^-} = x_{HCl} + x_{NaCl} + \sum_i x_i \xi_{xi} \quad \text{(Eq. 32)}$$

Where

- x_{Cl^-} = Total aqueous phase chloride concentration at equilibrium, mol/L
- x_{HCl} = Aqueous phase hydrochloric acid concentration, mol/L
- x_{NaCl} = Aqueous phase sodium chloride concentration (if used for salting), mol/L
- x_i = Aqueous phase rare earth concentration for species *i*, mol/L
- ξ_{xi} = Stoichiometric coefficient for counter anions (ξ = 3 for all trivalent lanthanides)

TODGA does not readily extract hydrochloric acid or sodium chloride, as such their contributions to total chloride concentration are treated as constant in Equation 32 for simplicity (although their extraction stoichiometry and equilibrium concentrations could easily be included in the summation term for completeness).

With a flexible modeling framework approach now specified for conducting multi-stage counter-current calculations in a counter-current extract-scrub-strip solvent extraction cascade, the following chapters focus on determining the required TODGA loading conditions, selective scrubbing mechanisms, and equilibrium data required for REE separation process design.

CHAPTER 6: SELECTIVE SCRUBBING OF TETRAOCTYL DIGLYCOLAMIDE FOR INTRA-LANTHANIDE SEPARATIONS USING COUNTER-CURRENT SOLVENT EXTRACTION

Introduction

TODGA's extraction chemistry and selectivity trends across the lanthanide series, as discussed in Chapter 3, suggested that light rare earth separation factors may potentially be improved nearly twofold as compared to the industry standard phosphonic acid, PC88A. However, it must be noted that TODGA's overall separation factors are still quite low for a direct separation scheme through selective extraction alone. For example, consider a theoretical 10-stage counter-current cascade scenario utilizing constant distribution ratios to selectively extract Nd from a mixed feed of Nd and Pr:

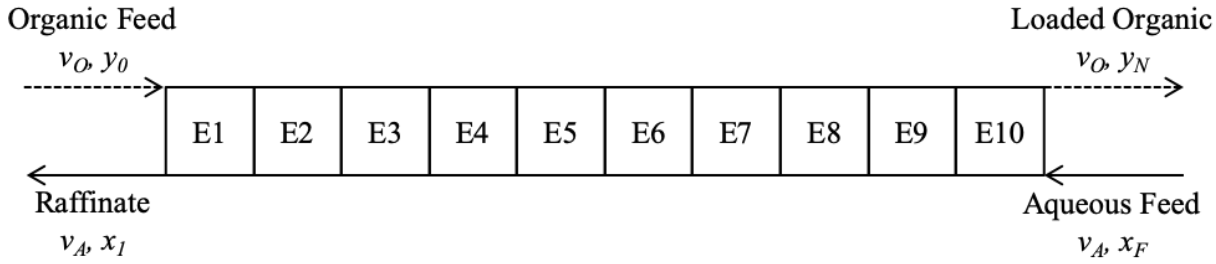

Figure 6.1: 10-stage counter-current extraction bank.

Using multi-stage mass balances for the case of constant distribution ratios, the loaded organic composition of a counter-current cascade containing *N* number of stages can be calculated using a form of the Kremser equation [46]:

$$y_N = \frac{\beta^N - 1}{\beta - 1}(Dx_1 - y_0) + y_0 \qquad \text{(Eq. 33)}$$

Where

y_N = Loaded organic concentration leaving stage N

β = Extraction factor, $\beta \equiv D(v_O/v_A)$

D = Distribution ratio

v_O = Organic phase flow rate

v_A = Aqueous phase flow rate

N = Total number of stages in cascade

x_1 = Aqueous raffinate composition leaving stage 1

y_0 = Organic feed concentration entering stage 1

This form of the Kremser equation contains two unknown variables, the loaded organic concentration y_N and the aqueous raffinate concentration x_1. An overall material balance around the cascade may be represented as:

$$v_O y_0 + v_A x_F = v_O y_N + v_A x_1 \quad \text{(Eq. 34)}$$

Combining Equations 33 and 34 yields the following [46]:

$$\frac{y_N - y_0}{D x_F - y_0} = \frac{\beta^N - 1}{\beta^{N+1} - 1} \quad \text{(Eq. 35)}$$

Since the cascade assumes fresh, metal-free organic solvent is used as the organic feed, y_0= 0. Using an arbitrary aqueous feed concentration of 52 mM Nd and 18 mM Pr with a phase ratio O/A = 1, the loaded organic (LO) composition may be calculated using Equation 35. Calculated percent extraction (% EXT) and LO percent composition of Nd and Pr for this theoretical 10-stage cascade are presented in Table 6.1 for variations in distribution ratios and separation factors for Pr and Nd.

Table 6.1: Calculated extraction results for 10 counter-current stages of Nd and Pr extraction using constant distribution ratios and separation factors.

$ß_{Nd/Pr}$	D_{Nd}	D_{Pr}	% Nd EXT	% Pr EXT	LO % Nd	LO % Pr	LO Nd/Pr Ratio
1.5	10	6.67	100%	100%	75%	25%	3.0
1.5	1.1	0.73	95%	72%	80%	20%	3.9
1.5	0.1	0.07	10%	7%	82%	18%	4.5
2.5	10	4.00	100%	100%	75%	25%	3.0
2.5	1.1	0.44	95%	44%	87%	13%	6.5
2.5	0.1	0.04	10%	4%	88%	12%	7.5

These calculations, covering a range of D_{Nd} and D_{Pr} values, indicate that selective extraction alone will never adequately separate adjacent lanthanides with low separation factors without severely impacting recovery, despite TODGA's selectivity improvements over the current industry standard PC88A. While "anion swing" salting strength may be used to manipulate

the extraction chemistry for loading and stripping conditions as shown in the forthcoming results in this chapter, the chemistries of Nd and Pr are so similar that they will always contaminate one another in the product streams. Therefore, selective scrubbing is required to achieve high degrees of purity and recovery in a counter-current solvent extraction cascade. The hypothesis of this chapter is that under proper loading conditions, selective scrubbing utilizing reflux of the strip product solution (an industrial rare earth separation technique described in Chapter 2) will facilitate separation of adjacent lanthanides. Review of the literature indicates that such a technique has never been demonstrated using an electroneutral extractant in HCl media, let alone an extractant that exhibits a near twofold increase in average adjacent light lanthanide separation factors. Consequently, the experimental work described herein is aimed at 1) determining the organic phase loading conditions required for selective scrubbing to occur, and 2) determine if it is feasible to selectively scrub adjacent lanthanides in a continuous counter-current solvent extraction circuit using the electroneutral TODGA-HCl solvent system. Due to the relevance to domestic production of critical rare earths, this chapter will focus strictly on Pr and Nd for proof-of-concept selective scrubbing studies.

Batch Equilibrium Experiments

Extraction and Organic Phase Loading

Work conducted by Ellis et. al. suggested that TODGA's light atomic weight REE separation factors remain consistent and robust across a wide range of ionic strengths, which can be used to control extraction and stripping in a solvent extraction cascade [11]. However, robust and consistent separation factors across a wide range of extraction conditions further strengthens the argument presented above that co-extraction alone will not yield any appreciable separation without significant sacrifices in recovery. Selective scrubbing techniques are utilized in industry to overcome this limitation by controlling the organic phase loading. Counter-current cascades utilizing PC88A cannot exceed 30% of theoretical stoichiometric loading to prevent gelling [26], therefore the organic phase loading is controlled based on equilibrium pH and the O/A phase ratio. Phosphonic acids will extract metals until the increase in aqueous phase acid concentration due to liberated proton from the extractant prohibits further extraction. The extract-scrub cascade will operate at this

equilibrium pH and maintain organic phase loading. The strip product reflux technique previously discussed in Chapter 2 is implemented to selectively load higher affinity lanthanide(s) and scrub out the lower affinity lanthanide(s). This raises the question: what loading conditions are required to facilitate a similar selective scrubbing mechanism with an electroneutral solvating extractant? Trivalent lanthanides are extracted along with the accompanying three chloride counter-anions in the outer coordination sphere, yielding no net change in HCl concentration [36]. Prior to evaluation of TODGA metal loading conditions, batch extraction experiments were conducted to evaluate the extent of HCl extraction and its potential effect on REE loading in the organic phase. Batch experiments were conducted utilizing a 5 M HCl aqueous feed with no REE, 2.3 mM didymium, and 50 mM didymium (measured ratio of 20.5% Pr, 79.5% Nd by mass). The organic phase TODGA concentration was varied from 0.1 to 0.25 M to determine the extent of acid extraction. All acid extraction experiments were conducted using 30% by volume Exxal-12 in Isopar-L diluent at an O/A ratio of 1. Results are shown in Table 6.2:

Table 6.2: HCl extraction dependence as a function of TODGA concentration and didymium concentration.

TODGA (M)	Feed HCl (M)	Feed Didymium (mM)	D_{HCl}	HCl % Extraction
0.1	4.88	N/A	0.012	1.2%
0.15	4.88	N/A	0.017	1.6%
0.2	4.88	N/A	0.023	2.3%
0.25	4.88	N/A	0.027	2.6%
0.1	4.84	2.33	0.014	1.4%
0.15	4.84	2.33	0.017	1.6%
0.2	4.84	2.33	0.020	2.0%
0.25	4.84	2.33	0.022	2.2%
0.1	4.82	50	0.012	1.2%
0.15	4.82	50	0.015	1.5%
0.2	4.82	50	0.018	1.7%
0.25	4.82	50	0.019	1.9%

These results reveal that TODGA has a very low affinity for acid extraction, averaging 1.8% extraction across all conditions tested. The presence of extractable trivalent lanthanides does not have an appreciable impact on acid extraction, regardless of whether the molar ratio of

total REE to TODGA is low or high. While acid extraction nearly doubles as TODGA concentration is increased from 0.1 to 0.25 M, these results still indicate that it is a reasonable assumption to treat HCl as a non-extractable species and it is not expected to have any significant impact on organic phase loading conditions.

A series of extraction experiments were conducted using varying organic phase TODGA concentrations and aqueous feed didymium (Di) concentrations to determine the extraction system's behavior under various loading conditions. Equilibrium distribution data for Pr and Nd are shown in Figure 6.2.

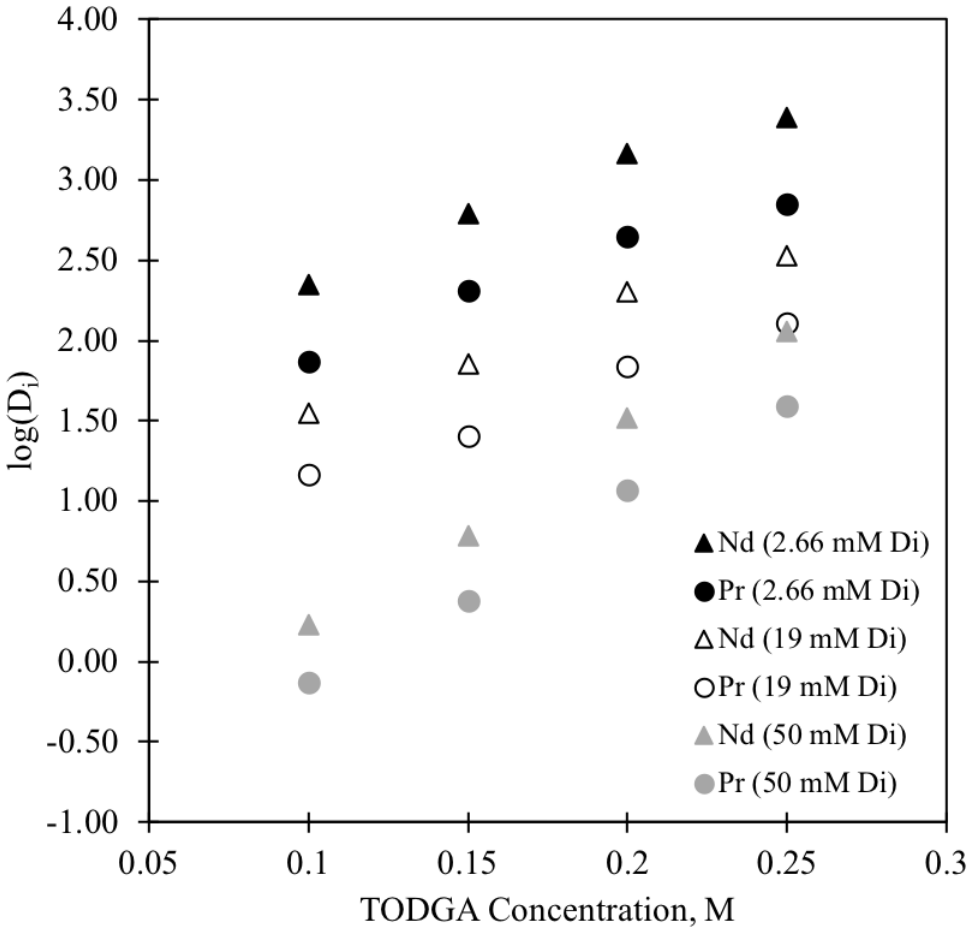

Figure 6.2: Log D vs. organic phase TODGA concentration for Pr and Nd extraction from 5 M HCl at various didymium (Di) feed concentrations. 30% v/v Exxal-12 phase modifier in Isopar-L diluent. All contacts performed at O/A = 1 at ambient temperature, 22 °C.

As expected, Pr and Nd behaved very similarly under all extraction conditions tested. Increasing TODGA concentration increases the distribution ratio due to the reaction

mechanism's third power dependence on TODGA concentration. Increasing the aqueous feed didymium concentration depressed the distribution ratio values, which at first appears somewhat counter-intuitive because an elevated amount of reactant should shift the reaction equilibrium further towards completion as dictated by Le Chatelier's Principle. These results reveal an interesting point that while useful, evaluation of distribution ratios alone can be misleading and lead to false conclusions about the solvent system's performance. The TODGA separation factor for Nd and Pr is markedly improved from the published value of 1.2 for PC88A, and Figure 6.2 indicates a trend of decreasing distribution ratios with increasing REE feed concentration. Additional insight is gained through calculation of percent extraction, loaded organic composition, and theoretical TODGA loading for the same set of experiments. Results are summarized in Table 6.3.

Table 6.3: Percent extraction, loaded organic composition, and theoretical TODGA loading (assuming 3:1 ligand:metal ratio).

TODGA, M	Feed Didymium, mM	$\beta_{Nd/Pr}$	% Pr EXT	% Nd EXT	LO % Pr	LO % Nd	TODGA % Loading
0.1	2.66	3.04	99%	100%	20%	80%	8%
0.1	19.00	2.40	94%	97%	20%	80%	55%
0.1	50.00	2.27	43%	63%	15%	85%	88%
0.15	2.66	3.02	100%	100%	20%	80%	5%
0.15	19.00	2.81	96%	99%	20%	80%	37%
0.15	50.00	2.50	71%	86%	18%	82%	83%
0.2	2.66	3.25	100%	99%	21%	79%	4%
0.2	19.00	2.90	99%	94%	21%	79%	27%
0.2	50.00	2.80	92%	97%	20%	80%	72%
0.25	2.66	3.44	100%	100%	20%	80%	3%
0.25	19.00	2.62	99%	100%	20%	80%	23%
0.25	50.00	2.94	97%	99%	20%	80%	59%

These results yield a few interesting points for discussion. First, quantitative extraction of both Pr and Nd occurs for the 2.66 mM didymium feed under all TODGA concentrations tested. For a constant TODGA concentration, increasing the didymium feed concentration leads to a suppression in percent extraction as the organic phase approaches its theoretical loading capacity. The theoretical loading capacity was calculated assuming a 3:1 stoichiometry for ligand:metal complex formation in accordance with results published in

literature [11]. Most interesting is the loaded organic composition for this set of extraction experiments. The ratio of Nd to Pr is exactly the same for all practical purposes in the loaded organic phase as it is in the didymium aqueous feed, indicating that the metals are co-extracted with no selectivity. The calculated separation factor therefore is somewhat an artifact of the ratios present in the feed; quantitative co-extraction is not separation whatsoever despite the fact that the calculated separation factor is higher for the TODGA system as compared to PC88A. The only two instances where the organic phase composition changes and enriches in Nd is when the theoretical organic phase loading capacity exceeds 80% (these rows are highlighted gray in Table 6.3 for clarity). This suggests that at theoretical loading capacities exceeding 80%, the solvent is reaching saturation with as much metal as it can take up and preferential Nd extraction begins to occur, presumably due to a crowding effect or selective metal-metal exchange due to TODGA's slightly higher affinity for Nd over Pr. The proposed overall reaction mechanism may be expressed as:

$$[PrCl_3 \cdot 3TODGA]_{Org} + [Nd^{3+}]_{Aq} \leftrightarrow [NdCl_3 \cdot 3TODGA]_{Org} + [Pr^{3+}]_{Aq} \qquad \text{(Eq. 36)}$$

However, single extraction contacts alone are not sufficient to determine if preferential loading will occur to purify Nd and maintain high recoveries of both species. Selective scrubbing experiments were conducted to determine the effect on organic phase loading and composition using reduced HCl concentration scrub feeds, as well as Nd-bearing scrub feeds. These experiments were conducted by first preparing a loaded organic phase by contacting freshly prepared 0.25 M TODGA/30% Exxal-12/Isopar-L organic phase solvent with a 50 mM didymium feed in 5 M HCl at O/A = 1. The loaded organic phase from this contact served as the organic feed for the selective scrubbing experiments shown in Table 6.4.

Table 6.4: Batch equilibrium experiments for scrubbing of Pr from a mixed Nd/Pr loaded organic feed, 0.25 M TODGA/30% Exxal-12/Isopar-L. Initial loaded organic phase concentration of 10.4 mM Pr, 39.9 mM Nd(20.5% Pr, 79.5% Nd). All contacts performed at O/A = 1 at ambient temperature, 22 °C.

Scrub HCl, M	Scrub Nd, mM	LO % Δ Pr	LO % Δ Nd	$\beta_{Nd/Pr}$	Scrubbed LO % Pr	Scrubbed LO % Nd
0.05	-	-98%	-98%	0.69	26.6%	73.4%
0.1	-	-99%	-100%	0.58	30.4%	69.6%
0.5	-	-99%	-96%	3.11	7.7%	92.3%
1	-	-86%	-75%	2.02	12.6%	87.4%
5	10	-4%	24%	2.79	16.4%	83.6%
5	25	-12%	56%	2.67	12.6%	87.4%

Results in the first four rows of Table 6.4 suggest that Pr and Nd in the organic phase behave very similarly when contacted with scrub acids of varying concentration, with low acid molarities effectively stripping both metals from the organic phase. This further validates the hypothesis that the two metals cannot be separated from one another via selective acid stripping and simultaneously obtain both high recovery and high purity. Rows 5 and 6, however, indicate a reduction in the loaded organic praseodymium concentration and an increase in the organic phase neodymium concentration. These contacts were performed at 5 M HCl (same as the initial loading extraction) to retain metals in the organic phase. Calculation of the theoretical organic phase loading capacity reveals that the initial loaded organic phase had a 60% loading, the 10 mM Nd scrub contact achieved 72% loading, and the 25 mM Nd scrub contact achieved 86% loading. Again, the organic phase began to enrich in Nd once the theoretical loading capacity approaches and exceeds 80%.

A final set of scrubbing experiments were conducted using 0.05 M TODGA to ensure complete loading of the solvent prior to conducting the scrubbing contact. Similar to the results presented in Table 6.4, an initial loaded organic phase was prepared by contacting 0.05 M TODGA/30% Exxal-10/Isopar-L with a 50 mM didymium aqueous feed in 5 M HCl. The initial loaded organic phase contained 2.2 mM praseodymium and 14.2 mM neodymium (13% Pr, 87% Nd), yielding a theoretical loading capacity of 98.4%. As expected, some degree of Nd purification occurred in the initial preparation of the loaded organic because the solvent was saturated with metal. This fully loaded organic phase was then contacted with 5 M HCl scrub solutions containing varying concentrations of Nd at O/A = 1. The results are

shown in Figure 6.3. The composition of the loaded organic phase (percent Nd) is plotted as a function of the aqueous scrub feed Nd concentration on the primary axis; the percent of Pr selectively scrubbed from the loaded organic phase is plotted as a function of the aqueous scrub feed Nd concentration on the secondary axis.

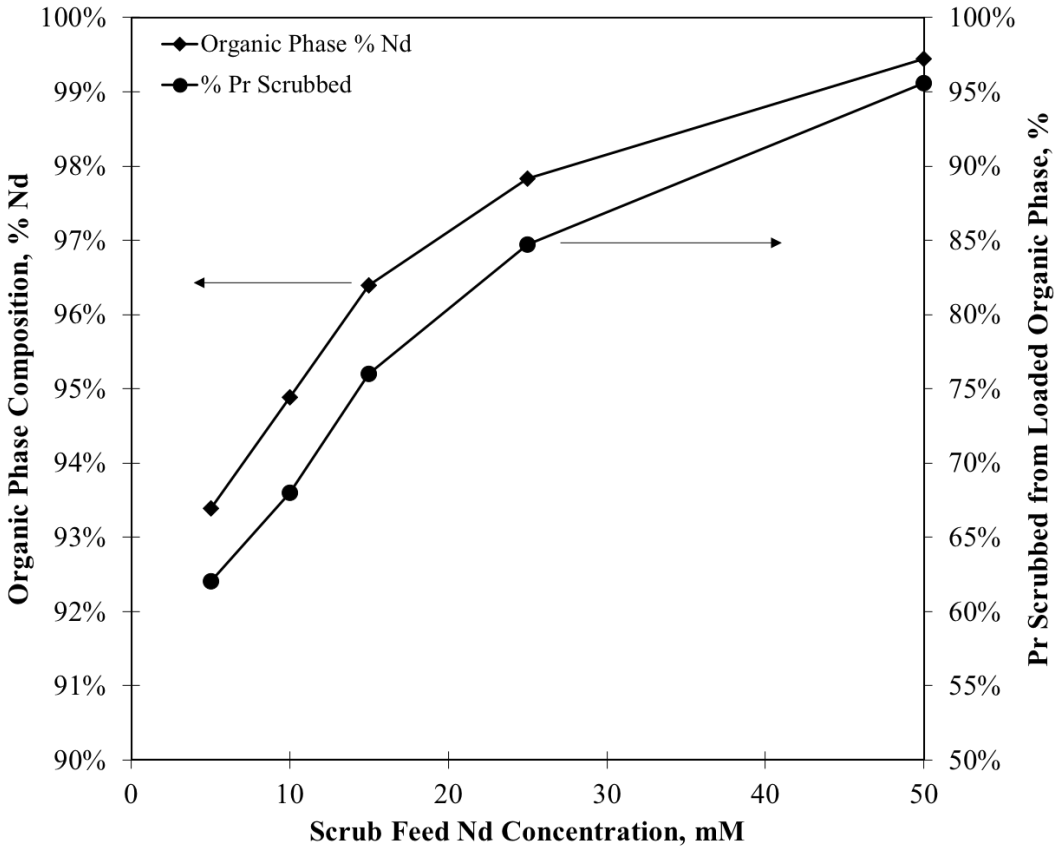

Figure 6.3: Scrubbing of 0.05 M TODGA-30% v/v Exxal-10-Isopar-L loaded organic phase containing Pr and Nd using 5 M HCl Nd-bearing scrub feed solutions.

The presence of Nd in the scrub feed significantly alters the final loaded organic composition, preferentially removing Pr from the organic phase and replacing it with Nd due to TODGA's affinity for the heavier metal. The original loaded organic phase prepared for these experiments had a calculated theoretical loading of 98%; the calculated loading capacity for the 5 mM Nd scrub feed contact reduced to 75% presumably due to the low concentration of rare earths in the feed stream. Again, as demonstrated through Le Chatelier's Principle, low concentrations of aqueous phase rare earths drive the reaction backwards, stripping some of the metal from the organic phase into the aqueous phase. The

single-contact scrubbing experiments suggest that reflux of the purified Nd product stream can facilitate efficient scrubbing in a reduced number of stages due to TODGA's higher separation factors for light rare earths.

The final set of batch equilibrium experiments required for counter-current cascade design is identification of suitable stripping conditions. Ideally, the strip solution minimizes chemical reagent consumption, efficiently strips all REEs from the organic phase in a minimum number of stages, and strips sufficiently well such that O/A ratios can be utilized to concentrate the rare earths in the strip product solution. Producing a concentrated strip product solution alleviates downstream processing requirements for precipitation and calcination to purified oxide products, notably improved efficiency and minimizing effluent process water generation. Preliminary experiments revealed that TODGA is readily stripped with water or very dilute pH 2-3 HCl. However, contacting the solvent with water or extremely dilute acid caused significant entrainment in both phases, and in some instances created an emulsion or gel which would not perform well in solvent extraction equipment. Therefore, strip solutions with intermediate ionic strength were explored to determine stripping conditions that strike a compromise between proper phase disengagement and minimizing reagent consumption. Results are presented in Table 6.5.

Table 6.5: Stripping performance of Nd and Pr from 0.1 M TODGA/30% Exxal-12/Isopar-L as a function of strip HCl concentration. Initial loaded organic phase contained 3.3 mM Pr and 23.6 mM Nd. All contacts performed at O/A = 1 at ambient temperature, 22 °C.

Strip HCl, M	% Pr Stripped	% Nd Stripped	D_{Pr}	D_{Nd}
0.1	99%	98%	0.002	0.004
0.25	97%	95%	0.005	0.009
0.5	96%	93%	0.007	0.013
0.75	96%	91%	0.009	0.019
1	93%	85%	0.014	0.032
1.5	87%	72%	0.031	0.074

Each of the strip conditions tested in Table 6.5 demonstrate excellent single-contact removal of Pr and Nd from the organic phase. All of the shakeout tests coalesced well and did not exhibit signs of phase entrainment. Therefore, pH 1 HCl was selected as the strip feed due to its near-quantitative stripping of the organic phase. Additionally, selection of this fairly dilute acid concentration minimizes acid consumption in the circuit while still providing

excellent stripping and suitable hydrodynamic behavior for use in solvent extraction equipment.

Selective Scrubbing Counter-Current Mixer-Settler Configuration and Modeling

Single batch shakeout experiments provided useful insight into the loading conditions required to facilitate selective scrubbing and indicated that Nd can preferentially load onto the organic phase by replacing Pr in the ligand:metal complex with no net change in ionic strength or free ligand concentration. However, variations in the equilibrium distribution ratios are anticipated as concentrations change from stage to stage in a counter-current cascade. Therefore, single batch shakeout experiments are not indicative of the performance that can be expected in a counter-current solvent extraction cascade.

The objective of selective scrub counter-current mixer-settler testing was to determine the feasibility of separating adjacent lanthanides through selective scrubbing techniques, therefore a less traditional cascade design was selected to simplify the experiment and reduce the number of uncertainties that would impact the outcome of the selective scrubbing test. The intent of the cascade design was to prepare a mixed Nd/Pr fully loaded organic phase in the extraction section, which is subsequently fed to another counter-current bank that is fed a pure Nd aqueous scrub solution at the same acidity as the extraction section. Using batch shakeout experimental results as a basis, the loaded organic phase TODGA will be at complete theoretical loading, at which point the Nd scrub feed solution displaces Pr in the organic phase due to TODGA's higher affinity toward the heavier rare earth species. After selective scrubbing, the organic phase is stripped using dilute hydrochloric acid such that the organic phase may be recycled back to the extraction section. The purpose of this cascade is *not* to achieve a high degree of purity and recovery of each respective rare earth, but rather to determine the feasibility of the selective scrubbing mechanism for rare earth separations in a counter-current cascade. The overall cascade arrangement is shown in Figure 6.4.

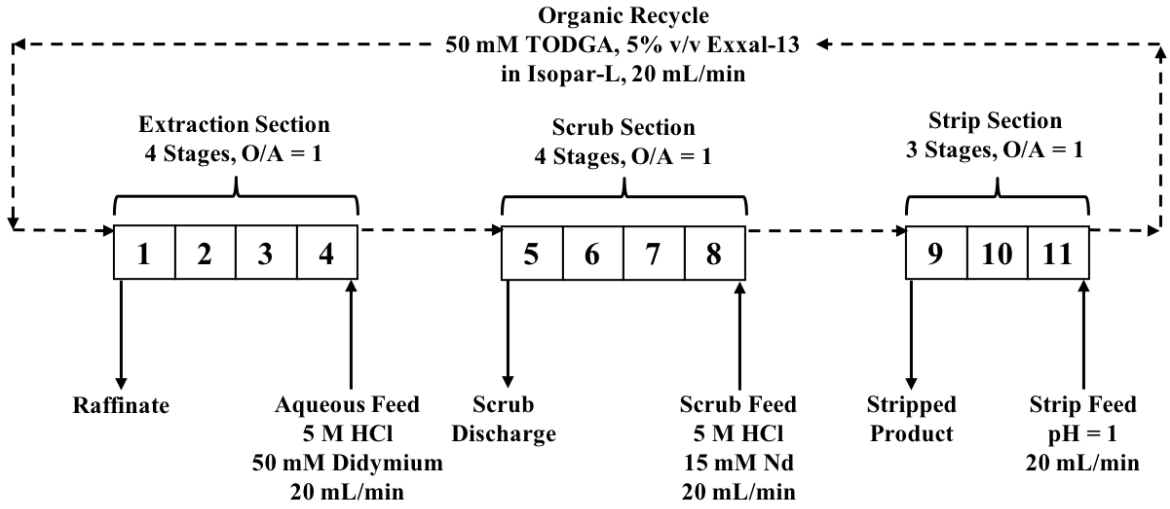

Figure 6.4: 11-stage counter-current mixer-settler cascade to demonstrate selective scrubbing of an Nd/Pr loaded organic phase using a pure Nd scrub solution.

Several design aspects of this cascade were simplified to focus on the selective scrubbing objective. First, a high chloride concentration of 5 M HCl was chosen to remain consistent with batch equilibrium experiments, but also to maintain favorable extraction conditions in the scrub section to ensure metal-metal exchange may occur and not be impacted by selective stripping that could take place under lower ionic strength conditions. Second, an O/A phase ratio of 1 was chosen for all sections and not optimized to perform any degree of concentrating, control of loading conditions for maximum recovery, or waste minimization. Third, an aqueous feed concentration of 50 mM didymium in 5 M HCl was chosen such that the loaded organic would be completely loaded under the chosen extraction conditions to prevent unintended loading effects from partial extraction. Fourth, a scrub feed concentration of 15 mM Nd in 5 M HCl was chosen based upon the selective scrubbing results presented in Figure 6.3. An Nd concentration of 15 mM is sufficiently in excess to facilitate metal-metal exchange with co-extracted Pr in the organic phase. Additionally, the 15 mM Nd batch scrub contact results indicated that the theoretical loading capacity of the solvent had exceeded 80%, at which point the selective scrubbing effect was experimentally observed. Finally, the extraction and scrub sections were four stages each in the MEAB mixer-settler bank configuration. Four stages each of extract-scrub is adequate to conduct the selective scrubbing experiment, while minimizing operating time and the approach to steady state.

The counter-current cascade was modeled using the MATLAB/Simulink ODE mass balance model described in Chapter 5. A simplified approach utilizing constant distribution ratios was utilized due to the limited information obtained from batch equilibrium contacts and uncertainty under saturated loading conditions. Distribution ratios for the model were selected based upon measured 50 mM TODGA laboratory batch contact equilibrium data for extraction, scrub, and strip. Equilibrium distribution ratios utilized in the MATLAB model are shown in Table 6.6.

Table 6.6: Extraction, scrub, and strip equilibrium distribution ratios for Pr and Nd.

Section	D_{Pr}	D_{Nd}
Extraction	0.017	0.031
Scrub	0.041	0.097
Strip	0.002	0.004

The basis for extraction section distribution ratios is the measured distribution ratio for the 50 mM didymium feed/ 50 mM TODGA extraction contacts used to prepare loaded organic feeds for the results presented in Figure 6.3. Similarly, the calculated scrub distribution ratio for a 15 mM Nd scrub feed was utilized in the model based on experimental data presented in Figure 6.3. Modeling predictions for the cascade are presented in Figures 6.5 and 6.6 later in this chapter alongside experimental data for stage-wise organic and aqueous REE concentration profiles.

Selective Scrubbing Mixer-Settler Experiment Results

The MEAB mixer-settlers were initially filled with metal-free HCl solutions (5 M HCl in extraction and scrub, 0.1 M HCl in strip) and fresh organic phase throughout (0.05 M TODGA, 5% v/v Exxal-13, in Isopar-L). The system was run until hydraulic steady state was achieved, i.e. the outlet flow rates from the mixer-settlers as measured with a graduated cylinder and stopwatch were approximately the same as the delivery flow rates from the calibrated FMI pumps. Aqueous phase weir jacklegs were adjusted such that the settling chamber was approximately 50% aqueous and 50% organic phase in each stage. Once hydraulic steady state was reached, the aqueous feed and scrub feed solutions were switched to didymium and neodymium-bearing feed solutions, respectively. The mixer-settlers were operated for a minimum of 12 hours (basis of five turnovers of organic phase inventory in the

system) to reach equilibrium. Once the mixer-settlers achieved steady state operation, the feed pumps and mixers were shut off. Final samples of the aqueous and organic phases from each stage were collected for subsequent analysis.

A complete set of steady state aqueous and organic phase concentration data and the associated equilibrium calculations are shown in Table 6.7. The extraction section produced a loaded organic solvent containing 1.78 mM Pr and 12.28 mM Nd, suggesting that the solvent is fully loaded when compared to the loading conditions evaluated via batch contact experiments. Again, the intent of the extraction section was to produce this fully loaded solvent in preparation for selective scrubbing, not to achieve a high degree of Nd recovery nor produce a purified Pr raffinate product.

The scrub section utilized a 15 mM Nd feed. The results indicate that 87% of the Pr was selectively scrubbed from the organic phase, enriching the loaded organic from 87% Nd up to 98% Nd with no net change in the scrub section's calculated theoretical loading capacity. The calculated loading capacity in the scrub section dropped down to 73% as compared to the extraction section's calculated loading capacity of 84%. A Pr material balance around the scrub section reveals that all of the Pr is accounted for within 2.4%, with 90% of the Pr reporting to the scrub aqueous discharge. While these experimental conditions are by no means optimized for efficient cascade operation, the results indicate that continuous counter-current selective scrubbing of TODGA is indeed possible by means of refluxing a purified metal stream. Final tank assays for the aqueous feed, scrub feed, raffinate, scrub discharge, and strip product are presented in Table 6.8. Again, the composite tank assays indicate that any co-extracted Pr in the loaded organic phase leaving the extraction section reported to the aqueous scrub discharge, producing a high purity Nd strip product solution.

Table 6.7: Final steady-state concentration results and calculated equilibrium data for 11-stage proof-of-concept scrubbing mixer-settler experiment.

Section	Stage	Aq Pr (mM)	Aq Nd (mM)	Org Pr (mM)	Org Nd (mM)	D_{Pr}	D_{Nd}	$\beta_{Nd/Pr}$	% Loading	Org % Nd
EXTRACT	1	10.89	24.29	2.03	10.88	0.19	0.45	2.40	77%	84%
	2	12.80	34.91	1.85	11.89	0.15	0.34	2.36	82%	87%
	3	12.57	35.54	1.70	12.23	0.14	0.34	2.55	84%	88%
	4	12.40	36.10	1.78	12.28	0.14	0.34	2.38	84%	87%
SCRUB	5	1.70	14.23	0.61	11.75	0.36	0.83	2.29	74%	95%
	6	0.68	13.71	0.30	11.89	0.43	0.87	2.00	73%	98%
	7	0.30	13.93	0.13	12.06	0.41	0.87	2.10	73%	99%
	8	0.13	14.37	0.24	11.95	1.77	0.83	0.47	73%	98%
STRIP	9	0.09	13.97	0.01	0.52	0.08	0.04	0.46	3%	99%
	10	0.01	1.02	0.00	0.01	0.45	0.01	0.03	0%	80%
	11	0.01	0.20	0.00	0.00	0.00	0.00	-	0%	-

Table 6.8: Feed and effluent tank compositions for 11-stage proof-of-concept scrubbing mixer-settler experiment.

Tank	Pr (mM)	Nd (mM)	% Pr	% Nd
Aqueous Feed	13.12	37.98	25.2%	74.8%
Scrub Feed	0.11	14.53	0.8%	99.2%
Scrub Discharge	1.60	12.04	11.5%	88.5%
Raffinate Tank	9.71	20.60	31.5%	68.5%
Strip Product	0.10	11.95	0.8%	99.2%

The final section of the cascade utilized pH 1 HCl to strip metals from the organic phase back into an aqueous phase stripped product solution, allowing the solvent to recycled continuously back to the extraction section for the duration of the experiment. The final Nd stripped product tank assayed at 99.2% Nd, which is in good agreement with the scrubbed loaded organic solvent leaving the scrub section. Pr and Nd were not detected in the organic phase leaving stage 11, indicating that the solvent was fully stripped prior to recycle.

Results for stage-wise organic and aqueous phase concentration profiles were plotted along with MATLAB/Simulink steady state modeling predictions for comparison. The organic phase profile is shown in Figure 6.5.

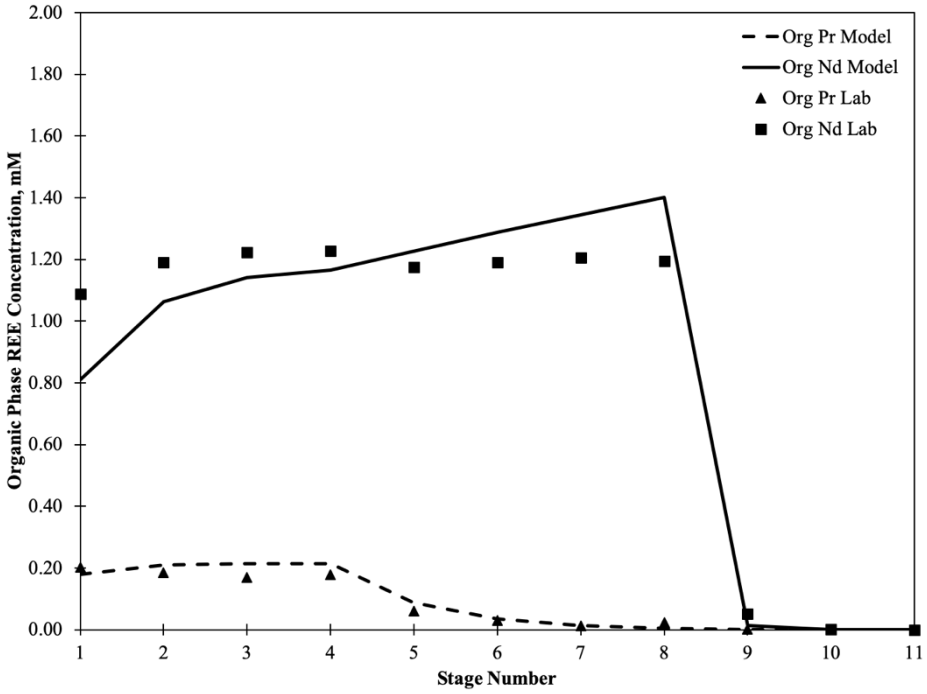

Figure 6.5: Steady state stage-wise organic REE concentration comparison, measured laboratory data and MATLAB/Simulink model.

The steady state organic phase model prediction, while imperfect, provides a reasonable estimation of the scrubbing performance and loading conditions in the organic phase. The primary source of error is likely attributed to the use of constant distribution ratios for the extraction, scrub, and strip sections in the MATLAB model. The Nd concentration increases slightly as it progresses from stage 5 to stage 9, as the Pr is being selectively removed from the organic phase. The model predicted a loaded organic composition of 84.4% Nd and a

scrubbed loaded organic concentration of 99.7% Nd, whereas, the experimental data showed 87% and 98% Nd, respectively. The aqueous phase concentration profiles are shown in Figure 6.6.

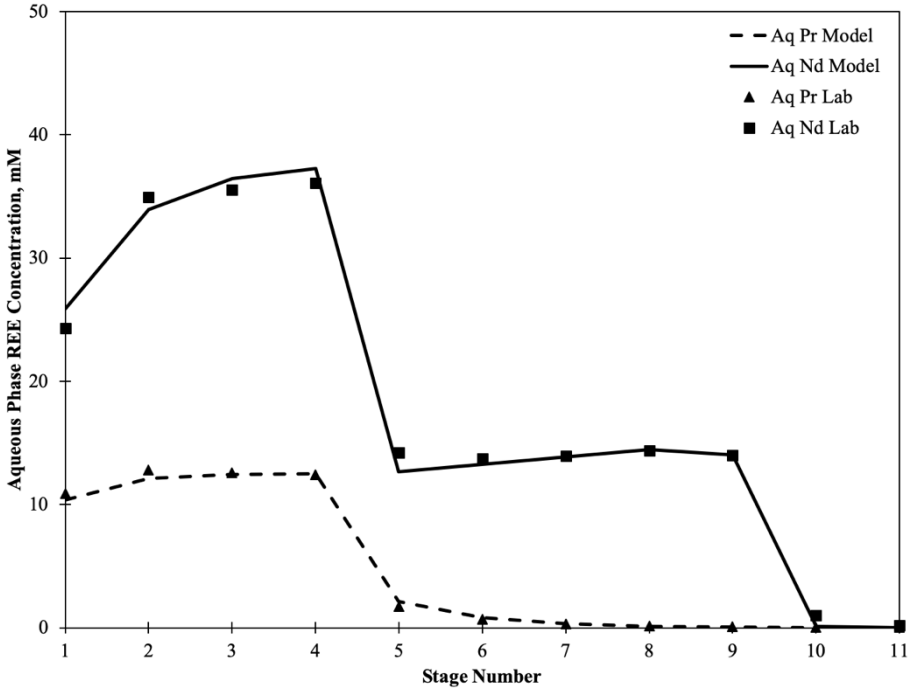

Figure 6.6: Steady state stage-wise aqueous REE concentration comparison, measured laboratory data and MATLAB/Simulink model.

Complementary to the organic phase results, the aqueous phase concentration profile also indicates that Pr is selectively scrubbed from the organic phase under saturated loading conditions. In counter-current flow, the scrub aqueous phase progresses from the feed in stage 9 to the scrub discharge in stage 5. The Pr concentration increases from stage 9 to 5 as it is stripped from the organic phase. The Nd concentration remains relatively unchanged because it is was fed to the cascade in significant excess as compared to the loaded organic Pr concentration entering the scrub section from stage 4. The simplified modeling approach utilized for this cascade demonstrated the observed selective scrubbing trend based on batch equilibrium experimental data. While this approach was adequate for the simplified cascade design, a more rigorous approach will be required for the solvent extraction process design and testing forthcoming in Chapter 7.

Upon inspection of the calculated equilibrium data for this simplified counter-current cascade, several conclusions may be drawn regarding the separation performance. First, an average Nd/Pr separation factor of 2.42 was calculated in the extraction section, which is in reasonable agreement with the published separation factors displayed in Table 3.1. Interestingly, the average Nd/Pr separation factor in the scrub section was calculated to be 1.72. This may be due a seemingly apparent data outlier in stage 8, as the measured Pr concentration in the organic phase unexpectedly increased. There are several potential causes such as instrument error, measurement error, excessive entrainment (although unlikely as entrainment was not appreciable throughout the duration of the experiment), and extraction of Pr contaminant present in the Nd scrub feed (Nd_2O_3 purchased from GFS was 99.9% purity, ICP analysis of the dissolved oxide in the scrub feed contained 99.2% Nd, 0.8% Pr). Regardless, the calculated average Nd/Pr separation factor in the scrub section is 2.13 if the stage 8 data is excluded. This suggests that while the separation factor is improved relative to the industry standard PC88A and will likely accomplish separations in a reduced number of stages, the actual performance in a counter-current cascade may not be as significant as previously suggested in literature.

Strip Product Reflux Requirements

One essential assumption required to facilitate the selective scrubbing counter-current mixer-settler experiment was that the Nd scrub feed solution was at the same acid molarity as the aqueous feed to extraction (5 M HCl). The scrub section equilibrium acid concentration has a strong influence on the organic phase loading; the scrub section will operate at a constant acid concentration and undergo metal-metal exchange under these conditions. Industrial practices for phosphonic acids utilize direct reflux of the strip product solution as the scrub feed, typically a certain percent reflux of the strip product optimized to maximize recovery and purity:

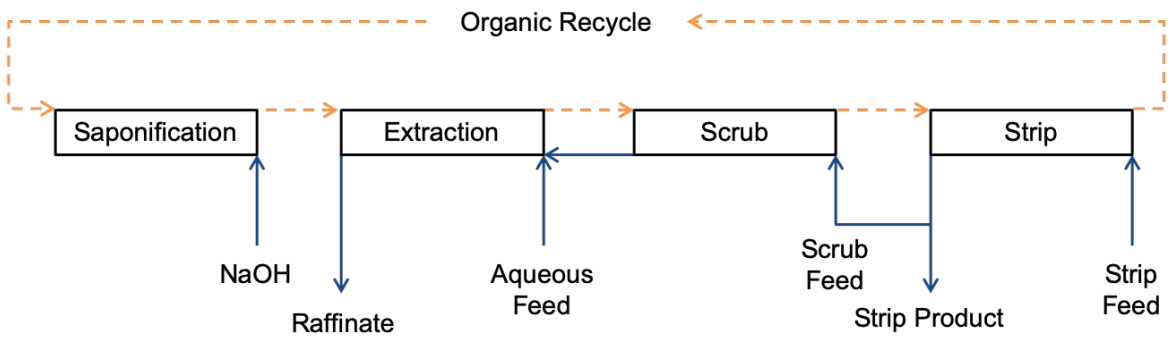

Figure 6.7: Typical phosphonic acid industrial rare earth separation cascade utilizing strip product reflux.

Phosphonic acid circuits operate the extraction and scrub section at a constant pH to control the organic phase loading and facilitate metal-metal exchange. Using extraction, scrub, and strip equilibrium data presented in this chapter as a basis, it is well established that TODGA effectively strips rare earths from the organic phase utilizing dilute HCl solutions. Maintaining REEs in the organic phase requires significantly high concentrations of chloride ion. The strip section of the mixer-settler experiment operated using pH 1 HCl as the strip feed. Based upon HCl extraction results previously reported, the strip product solution essentially contains recovered Nd and Pr in pH 1 HCl. Based on stripping data alone, it is anticipated that direct reflux of a fraction of the strip product as the scrub feed in a TODGA counter-current cascade would strip all REE from the organic phase and lose all separation functionality. To test this hypothesis, experiments were conducted to determine the impact of organic phase loading as a function of scrub feed ionic strength. First, a fully loaded organic phase was prepared by contacting fresh organic solvent (0.1 M TODGA, 30% by volume Exxal-13, Isopar-L diluent) with a 300 mM didymium solution (measured 62.2 mM Pr, 238.2 mM Nd) at O/A = 1. Composition of the organic phase was not a primary concern; excess REEs were utilized to ensure a fully loaded organic phase. The calculated theoretical loading capacity of this solvent was determined to be 80.6%, which is in good agreement with the loading capacities calculated for selective scrubbing experiments. Next, the loaded organic phase was contacted with the same HCl acid concentrations utilized in Table 6.5 for stripping studies at O/A = 5. An O/A of 5 was selected to determine if stripped rare earths could potentially self-salt aqueous phase ionic strength due to the concentrating effect, thereby limiting the amount of REE stripped. The amount of REE stripped from the organic

phase was calculated using the measured REE concentrations in the organic phase before and after the contact. Results are presented in Figure 6.8.

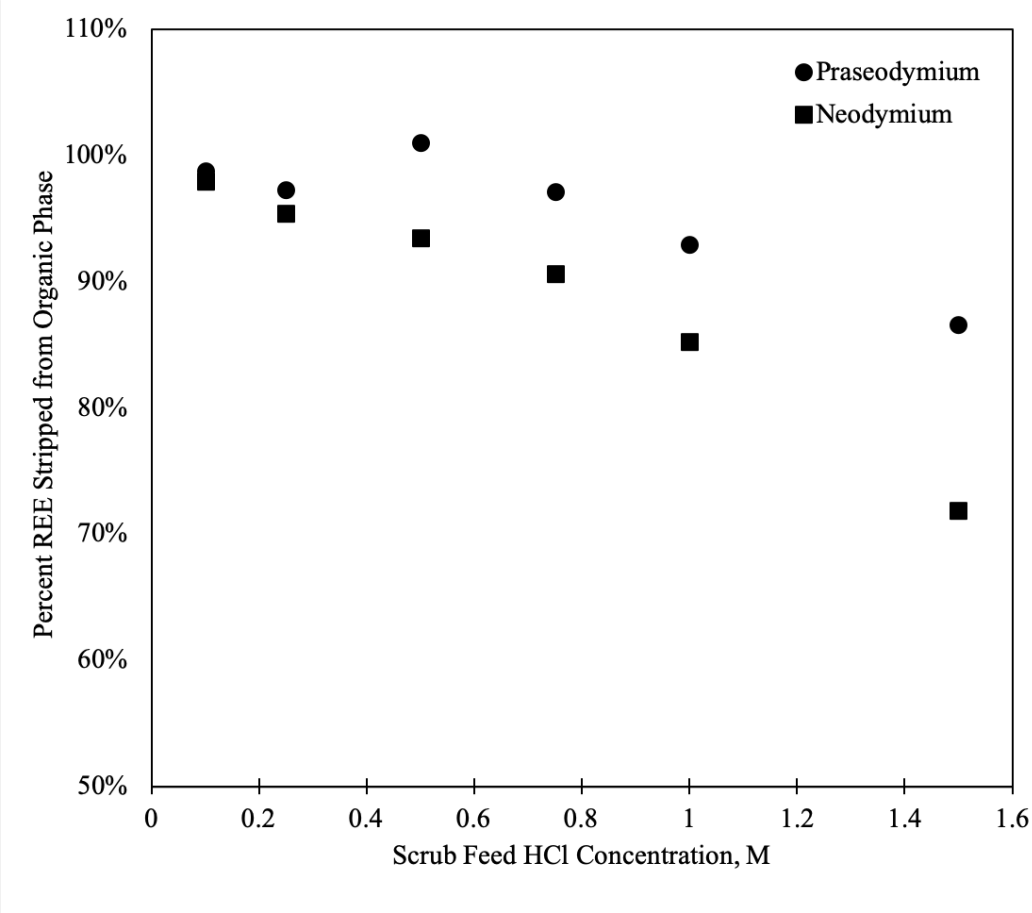

Figure 6.8: REE stripping dependence as a function of scrub feed HCl concentration.

These results indicate that both Nd and Pr would approach near-quantitative stripping from the organic phase using a scrub feed at pH 1, and at an O/A = 5 there would not be sufficient ionic strength from rare earth chlorides to maintain any REEs in the organic phase. Consequently, the "anion swing" extraction and stripping behavior of the rare earths necessitates the need for feed adjustment of the strip product solution prior to reflux as a scrub feed. A representative TODGA REE separation cascade is shown in Figure 6.9 for comparison with the typical phosphonic acid cascade shown in Figure 6.7.

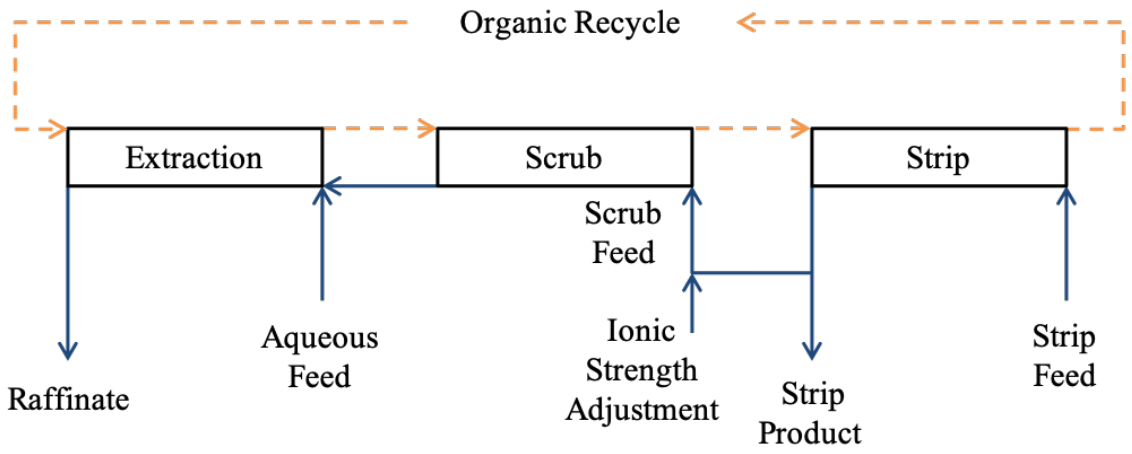

Figure 6.9: TODGA rare earth separation cascade configuration with ionic strength adjustment to scrub feed.

The ionic strength adjustment could be performed by reacidification with HCl or by adding salting strength through the addition of sodium chloride or similar. Regardless, this raises several issues from a practicality standpoint in an operating solvent extraction plant. First, feed adjustment to increase ionic strength significantly dilutes the metal concentration in the refluxed strip product solution. This reduces the driving force for metal-metal exchange, potentially requiring additional scrub stages to achieve a given degree of separation. This could potentially be mitigated by increasing the strip section O/A ratio, thereby further concentrating the strip product solution prior to feed adjustment. However, pushing high O/A ratios in the strip section may require additional stripping stages to allow solvent recycle and may have an upper bound to concentrating ability. Feed adjustment also increases chemical reagent and water consumption in the solvent extraction plant, potentially negating the perceived benefits gained from eliminating the need for saponification. Furthermore, operating an extract-scrub cascade at high ionic strength produces a raffinate stream of significantly higher ionic strength as compared to phosphonic acid separation processes, which has major implications on process and wastewater effluents that may require recycling or treatment. The implications of TODGA selective scrubbing circuits will be discussed in further detail in Chapter 8.

Conclusions

TODGA's enhanced light lanthanide selectivity trends published in literature suggest that improved separation processes may be realized using a reduced number of stages without requiring the use of saponification to achieve high degrees of recovery. In practice, the separation factors between adjacent lanthanides are still sufficiently low that non-selective coextraction occurs. Similarly, selective stripping with acid indicates that adjacent lanthanides will strip from the solvent together, only achieving high purity at the cost of significant loss in recovery. TODGA will continue to extract lanthanides with minimal discrimination until the solvent is fully saturated at a theoretical organic phase loading capacity, calculated to occur at loadings that exceed 80%. Once fully loaded, heavier atomic weight REEs with a higher extraction affinity may displace light atomic weight REEs with a lower affinity via "crowding" manifested as a net metal-metal exchange reaction. This selective scrubbing technique may be exploited in a counter-current cascade by refluxing the heavier REE strip product solution at the same acidity/ionic strength as the extraction section. A proof-of principle selective scrubbing mixer-settler experiment with Pr and Nd revealed that such a scrubbing mechanism can indeed selectively remove impurity lanthanides to achieve high degrees of purity. While not optimized for maximum recovery and purity of both Pr and Nd, these results suggest that selective scrubbing can be utilized in a continuous counter-current solvent extraction cascade for the separation of adjacent lanthanides. Design of such a cascade requires feed adjustment of the refluxed strip product solution prior to introduction to the scrub section, which has implications on the required number of solvent extraction stages, chemical reagent consumption, and process water recycling or treatment requirements.

CHAPTER 7: SOLVENT EXTRACTION PROCESS DESIGN AND TESTING FOR LIGHT RARE EARTH SEPARATIONS

Introduction

Chapter 2 provided an overview of industrial counter-current solvent extraction processes for the separation of rare earth elements, with a particular focus on domestic bastnäsite sources and the separations required to produce rare earth oxide products associated with this light rare earth mineralogy. In particular, processes are designed around the production of high-value critical rare earths utilized for the production of rare earth permanent magnets, notably a combined neodymium-praseodymium product referred to as didymium oxide. The use of TODGA as an alternative extractant for light rare earth separations has several implications for potential process improvements to these separations, notably the elimination of solvent saponification required for phosphonic acids and improved adjacent light rare earth separation factors, potentially allowing the separations to be performed in a reduced number of solvent extraction stages. Thus far, the present work has established that separations may be facilitated via targeted acid or salting strength conditions, and manipulating extraction, scrubbing, and stripping conditions via "anion swing" in the aqueous phase. In order to achieve high degrees of recovery and purity in a continuous counter-current solvent extraction cascade, this work now postulates that the TODGA solvent must maintain a saturated organic phase loading capacity to enable metal-metal exchange via a "crowding" scrubbing mechanism by which higher affinity lanthanides selectively replace lower affinity lanthanides in the organic phase metal:ligand complex. This requires feed adjustment to enable the reflux of purified strip product solutions prior to introduction to the scrub section of the cascade.

With a framework laid out for rational cascade design, this chapter aims to test TODGA-based counter-current solvent extraction cascades for the separation and purification of rare earth elements relevant to domestic industrial practices for rare earth concentrates derived from the processing of bastnäsite ore. First, extraction equilibria expressions must be developed to predict partitioning between the aqueous and organic phase, i.e. prediction of distribution ratios under varying chemical conditions anticipated to be encountered within a counter-current cascade. Second, the equilibrium model must be coupled to a mass balance

model to compute stage-wise aqueous and organic equilibrium concentrations in a counter-current cascade. While this procedure generically applies to any lanthanide separation process with TODGA, the main focus will be on the separation of Pr and Nd as a mixed didymium product from a mixture of La, Ce, Pr, and Nd. Domestically, this is the most challenging separation to produce high value didymium oxide because the feed contains a significant amount of undesired Ce relative to the adjacent Pr concentration in the feed.

This chapter explores and applies established techniques in the literature to model extraction equilibrium behavior for the TODGA-HCl system. This predictive capability, coupled with industrial rare earth separation techniques, enables for the first time the rational design and testing of continuous counter-current rare earth separation processes utilizing an electroneutral solvating extractant in hydrochloric acid media.

Basis for Solvent Extraction Aqueous Feed Concentrations

Physical beneficiation and leaching operations yield an aqueous mixed rare earth chloride feed stream to the separations plant. The elemental distribution of this pregnant liquor solution reflects the distribution found in the ore, comprising mostly light lanthanides with a very small fraction of heavy lanthanides. Published process data indicate that the total leach liquor REE concentration is 1.5 mol/L and the solvent extraction cascades utilize PC88A in kerosene diluent; PC88A concentrations range anywhere from 1-1.5 mol/L [45]. As depicted in Figure 2.7, bastnäsite ore is processed domestically by first making a light-heavy REE split between Nd and Sm, followed by a downstream light rare earth separation making a split between Ce and Pr to produce the high-value didymium oxide product.

Determining a relevant REE feed concentration basis for the separation and purification of didymium from a mixture of La-Nd is essential to guide experimental efforts and evaluate the performance of the TODGA solvent extraction cascade. However, detailed industrial processes and operating parameters are often closely guarded trade secrets with limited information published in open literature to provide such a basis. There are a wide variety of unit operations that can be utilized for the processing of bastnäsite ore, notably containing various upstream techniques for cerium removal. The rare earth concentrations are also manipulated through O/A phase ratios in upstream solvent extraction circuits in an effort to maximize solvent loading, REO recovery and purity, and minimize waste effluent generation

and downstream processing [21]. Consequently, a feed basis of 180 mM total REE was chosen for light rare earth separations containing 52% La, 23% Ce, 6% Pr, and 19% Nd (molar basis). This basis was chosen due to its compatibility with the 0.1 M TODGA solvent system organic phase loading capacity, while still containing appreciable amounts of La and Ce to demonstrate a relevant separation cut between Ce and Pr. This basis also assumes a reduced Ce content as compared to the initial leach liquor, as bulk Ce is typically removed upstream to reduce stage requirements when making the cut between Ce and Pr [23].

The actual feeds utilized in solvent extraction experiments all have an inherent degree of variation from the basis feed concentrations specified above due to errors in measurement in feed recipe preparations from oxides and concentrated HCl. Consequently, each feed was analyzed for HCl concentration and REE composition to develop extraction trends using varying acid and REE concentrations.

Batch Shakeout Equilibrium Data

Techniques and procedures for modeling solvent extraction and metal complexation reactions are well established in the literature. For example, experimental extraction studies may be used to determine equilibrium parameters. Slope analysis techniques have been demonstrated to be a viable method to elucidate reactant stoichiometries and equilibrium constants from experimental data [47]. For the present work, consider the proposed equilibrium constant expression for TODGA in Chapter 3. Equation 11 assumes that an aqueous phase trivalent lanthanide ion and its accompanying three counter-anions are extracted into the organic phase, coordinated by three tridentate TODGA molecules. However, multiple adducts may form between a metal salt and the extractant with multiple extractable solvated species present, yielding a significantly more complex expression for the distribution ratio [47]:

$$D_M = \frac{[ML_iB]_{org}+[ML_iB_2]_{org}+[ML_iB_3]_{org}+\cdots}{[M]_{aq}+[ML_1]_{aq}+[ML_2]_{aq}+[ML_3]_{aq}+\cdots} \quad \text{(Eq. 37)}$$

Where *M* represents a generic metal cation, *L* represents the corresponding anion, *i* represents the anion stoichiometry in the extracted adduct, and *B* represents the extractant. TODGA has been experimentally validated to demonstrate variable reaction stoichiometries in nitric acid systems relevant to separation applications in the nuclear fuel cycle, notably

with the formation of tetramer polar core reverse micelles [48], a topic that will be further explored in Chapter 8. Therefore, such rigorous metal complexation reactions in a large multicomponent system are not only likely to be invalid across varying organic phase loading conditions, but difficult to elucidate in a practical manner for predicting equilibrium distribution data. As a simplified approach, the equilibrium constant expression may be rewritten in a generic form to calculate distribution ratios for unknown or varying metal complexation stoichiometries:

$$D_i = K_i[x_{Cl^-}]^{\alpha_1}[y_{DGA}]^{\alpha_2} \quad \text{(Eq. 38)}$$

Where

- D_i = Distirbution ratio of component *i*
- K_i = Equilibrium constant for component *i*
- x_{Cl^-} = Total aqueous phase chloride concentration at equilibrium, M
- y_{DGA} = Free DGA concentration at equilibrium, M
- α_1 = Equilibrium stoichiometry coefficient for x_{Cl^-}
- α_2 = Equilibrium stoichiometry coefficient for y_{DGA}

Taking the common logarithm of both sides of Equation 38 yields:

$$\log(D_i) = \log(K_i) + \alpha_1 \log(x_{Cl^-}) + \alpha_2 \log(y_{DGA}) \quad \text{(Eq. 39)}$$

Plotting the logarithm of the distribution ratio versus the logarithm of reactants enables determination of the dominant solvation stoichiometries and equilibrium constant via slope analysis of the data. These unknown parameters may be obtained using Equation 39 by varying the concentration of one reactant while holding the other constant. However, this procedure is only valid under the following conditions [47]:

1. The system behaves ideally, i.e. activity coefficients are assumed to be unity.
2. The extracted metal is present at trace concentrations, i.e. $M_{total} << Extractant_{total}$.
3. The reactant concentrations are low in both phases (REE, DGA, and Cl^- in this instance)

Industrial solvent extraction practices typically maximize use of expensive extractants by saturation of the organic phase, significantly reducing free ligand concentrations within the system [49]. This often corresponds with high aqueous feed metal concentrations to 1) reduce the volume of raffinate streams that require additional treatment prior to recycle or disposal, and 2) reduce chemical reagent consumption. Furthermore, it is anticipated that activity coefficients would deviate significantly from unity because TODGA requires very high ionic strengths in HCl media to facilitate lanthanide extraction. Any apparent calculation of the equilibrium constant would be a lumped term that reflects contributions from activity coefficients. Again, elucidation of rigorous activity coefficients and corresponding equilibrium constants for such a large multicomponent system is not only a significant undertaking, it is also beyond the scope of the present work.

Batch equilibrium experiments were conducted for the individual rare earth species of interest (La, Ce, Pr, Nd, and Sm) at various feed HCl concentrations and feed metal concentrations in an effort to establish mathematical expressions that predict equilibrium distribution ratios, and by extension predict equilibrium effluent concentrations from solvent extraction equipment. Therefore, experiments were limited to relevant chemical conditions anticipated to be encountered for applied separation processes. Empirical fitting of experimental data is only valid within the range of experimental validation and should not be extrapolated as a predictive modeling tool. However, the procedure described herein may easily be expanded to include more rigorous equilibrium data sets, providing a larger range of validated experimental conditions in the empirical model.

Ln(III)-TODGA-HCl extraction trends published by Ellis et. al. indicate that selectivity remains relatively unaltered under varying extraction aqueous phase chloride ionic strengths, potentially enabling separations through “anion swing” for extraction and stripping of specific lanthanides [11]. Target feed acidities for TODGA extraction experiments were chosen to capture the point at which each metal would transition from chemical conditions that inhibit extraction to conditions that favor extraction. Aqueous feed metal concentrations were varied to subject the solvent to a variety of loading conditions, with relative ratios representative of those anticipated within the context of bastnäsite separations. All experiments were conducted at O/A = 1 at ambient temperature using methods described in

Chapter 4. The organic phase composition was 0.1 M TODGA, 30% v/v Exxal-13 in Isopar-L diluent for all single metal extraction experiments. Table 7.1 provides a summary of the extraction conditions tested; a complete set of equilibrium data and slope analysis plots are provided in Appendix B. Slope analysis plots include distribution ratios as a function of equilibrium aqueous phase chloride concentration and organic phase free TODGA concentration, and logarithmic plots of the said parameters for each REE. Linear fit equations are provided on logarithmic plots for evaluation in the context of the slope analysis methods described above.

Table 7.1: Summary of single metal extraction experiment conditions.

Element	Target HCl Feed (M)	Target Metal Feed (mM)
La	5, 4, 3	240, 120, 60
Ce	5, 4, 3	220, 110, 55
Pr	4, 3, 2	18, 9, 3
Nd	4, 3, 2	60, 30, 15
Sm	3, 2, 1	8, 4, 2

Several conclusions may be drawn from the single metal extraction data. First, distribution ratios are highly nonlinear, demonstrating an apparent exponential increase in distribution ratio with increasing chloride concentration. Theoretical organic phase loading calculations were conducted for all extraction experiments assuming a 3:1 ligand:metal stoichiometry; the highest metal concentrations for La, Ce, and Nd fully saturated the solvent according to the experimental observations demonstrated in Chapter 6. Log-log plots demonstrated reasonable linear fits in nearly all cases, but slopes for *log(D)* versus *log(Cl^-)* and *log(D)* versus *log(DGA)* were highly variable for a given single metal extraction data set. It is hypothesized that non-ideality coupled with potential changes in metal complexation and coordination chemistry occur in the saturated solvent system as indicated by variations in the calculated slopes for each plot. Pr and Sm are present at significantly lower concentrations in bastnäsite leachates, as such the organic phase loading capacities did not exceed 37% and 18% for the two metals, respectively. Interestingly, Pr and Sm plots for *log(D)* versus *log(Cl^-)* converged at these low loading conditions, with slopes that were in much closer agreement than the variable loadings calculated for the other metals. However, reactant stoichiometries cannot be reliably extracted from this data set through slope analysis techniques derived from Equation 39 due to the high degree of variability observed for each single metal data set.

Simplified calculation of equilibrium constants using Equation 11 yields results that vary over two orders of magnitude within a single metal, a nonsensical result considering the equilibrium constant as defined should be a constant regardless of reactant and product concentrations in the system. The overarching conclusion from interpretation of this data set is that nonideality and complex speciation are likely making a significant contribution to the observed deviations when attempting to extract equilibrium parameters using slope analysis. Consequently, an empirical multivariable surface fitting of the data was selected as an applied empirical approach to predict distribution ratios within the constraints of the experimental conditions evaluated.

MATLAB's curve fitting application was utilized to map data in three-dimensional space to generate a surface plot of the logarithm of the distribution ratio D_i (z-axis) versus the logarithm of equilibrium chloride concentration x_{Cl^-} (x-axis) and the logarithm of equilibrium free TODGA concentration y_{DGA} (y-axis). Linear and polynomial fits were explored for empirical data fitting, and while higher polynomial degrees for x and y significantly improved the data's fit to the model of regression, the mapped polynomial surfaces would result in non-real results when extrapolating between data sets. For example, consider logarithmic surface plots for Nd extraction data, shown in Figure 7.1.

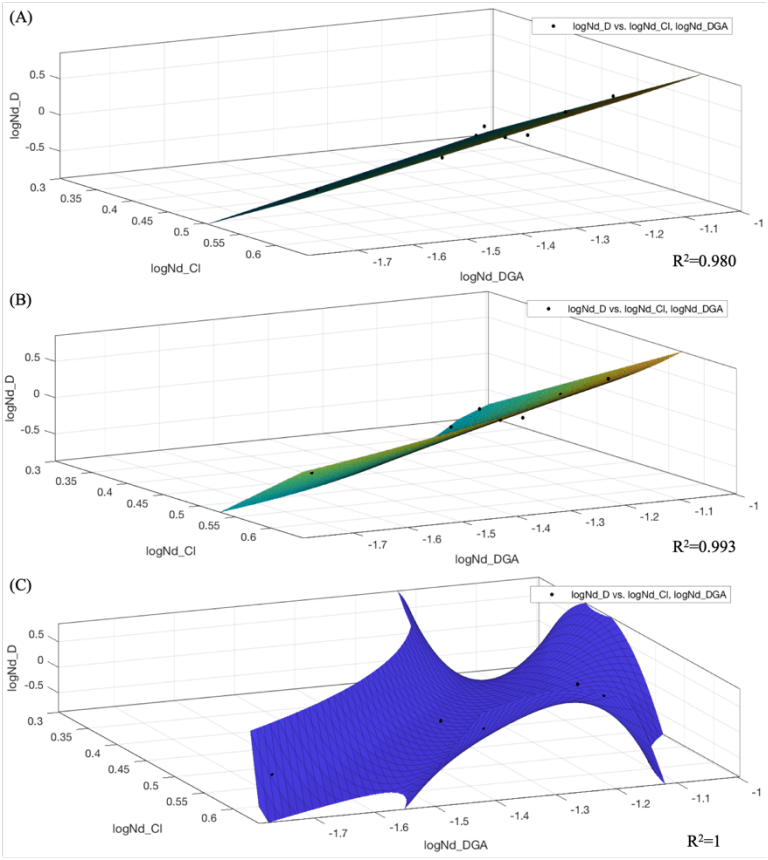

Figure 7.1: MATLAB surface fits for neodymium extraction data.

Higher order polynomial fits with increasing independent variable degrees provide an exceptional surface mapping fit of the experimental data, but do not have any basis in reality. The polynomial fit in Figure 7.1(C) has two degrees in *log(Cl^-)* and three degrees in *log(DGA)* with an excellent regression fit, but visual inspection of the surface map reveals that extrapolation in any direction away from the data clusters results in significant deviation that does not make logical sense based on reaction equilibria trends. Linear regression provided reasonable fits for all single metal extraction data sets and provides a reasonable basis for extrapolation between data at known acidities. This assumption is reasonable because the fitting of logarithmic data had reasonable fits for all metals as indicated by the plots shown in Appendix B. MATLAB linear surface equations were derived from the curve fitting application for each REE species La-Sm, with all equations being of the form:

$$f(x,y) = p00 + p10x + p01y \qquad \text{(Eq. 40)}$$

Upon inspection, Equation 40 is the same form as Equation 39, with $p00 = log(K_i)$, $p10 = \alpha_1$, and $p01 = \alpha_2$. Table 7.2 shows the coefficients derived from MATLAB curve fitting of the extraction data for each lanthanide, with a derived empirical expression to calculate distribution ratios. The coefficient K_i was calculated by taking the antilog of $log(K_i)$ for inclusion in the distribution ratio correlation.

Table 7.2: Coefficients from MATLAB curve fitting of experimental extraction data and corresponding empirical distribution ratio expressions.

Element	log(K_i)	α_1	α_2	D_i Expression
La	-2.56	5.32	1.02	$D_{La} = (2.77\text{E}-03)[x_{Cl^-}]^{5.32}[y_{DGA}]^{1.02}$
Ce	-2.43	5.20	0.87	$D_{Ce} = (3.72\text{E}-03)[x_{Cl^-}]^{5.20}[y_{DGA}]^{0.87}$
Pr	-0.52	5.50	2.20	$D_{Pr} = (3.02\text{E}-01)[x_{Cl^-}]^{5.50}[y_{DGA}]^{2.20}$
Nd	-0.99	5.73	1.55	$D_{Nd} = (1.03\text{E}-01)[x_{Cl^-}]^{5.73}[y_{DGA}]^{1.55}$
Sm	1.93	4.33	2.99	$D_{Sm} = (8.57\text{E}+01)[x_{Cl^-}]^{4.33}[y_{DGA}]^{2.99}$

Experimentally determined distribution ratios from the single metal extraction experiments were plotted versus distribution ratios calculated using the empirical expressions from Table 7.2. Many distribution ratios from the data set were less than one, presumably due to low acidity for favorable extraction or conversely saturation of the organic phase under said conditions. Figure 7.2 contains two plots comparing experimental and calculated distribution ratios, one with all data in its entirety and another for distribution ratios less than two. A y = x line is plotted as a visual aid of model deviation from experiment.

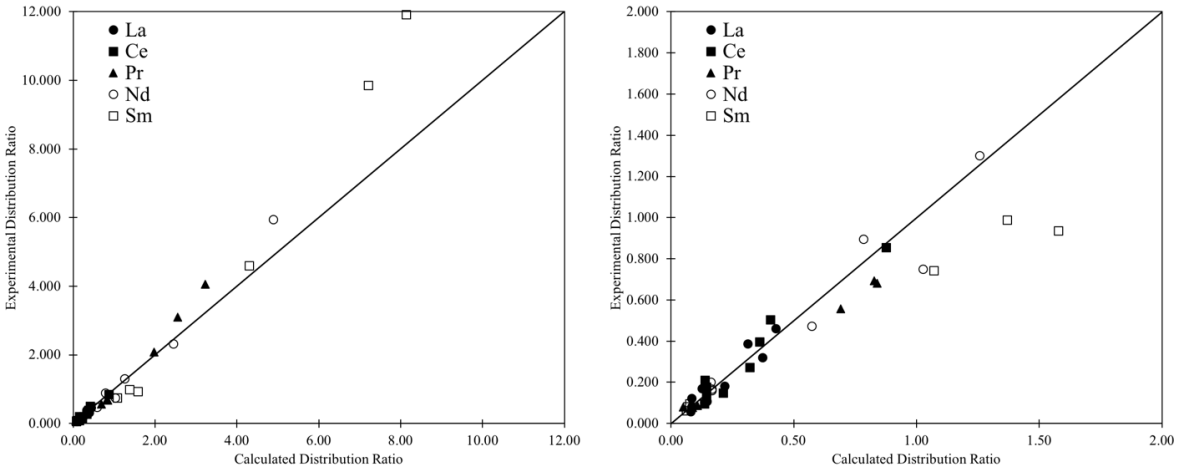

Figure 7.2: Comparison of experimental distribution ratios and calculated distribution ratios from empirical correlations using single metal extraction data. The left figure represents the entirety of the extraction data set; the right figure is magnified to show distribution ratios less than 2.

Generally speaking, the error associated with distribution ratio predictions increases as the distribution ratio increases. In particular, data fitting for Sm exhibited significant error at the highest extraction acidities. Qualitatively, the error observed for high distribution ratios is not that significant (a distribution ratio of 12 corresponds to 92.3% extraction at O/A = 1, as compared to 88.9% extraction with a distribution ratio of 8 at O/A = 1). Samarium's deviation at low acid concentrations is likely due to the drop in TODGA selectivity as the acid concentration is reduced to 1 M HCl. While TODGA selectivity remains robust across the lanthanide series at high ionic strengths, it tapers off when the ionic strength is sufficiently low as indicated by extraction trends shown in Figure 3.3. The proposed empirical model provides a reasonable means of predicting equilibrium partitioning of lanthanides between the aqueous and organic phases using TODGA.

Ideal Cascade Design for Light Rare Earth Separations

Prior to performing detailed stage-wise calculations for counter-current process design, limiting conditions for operation must be identified by means of an ideal cascade design. An ideal cascade utilizes mass balances with the assumption of complete recovery and 100% purity in conjunction with theoretical organic phase loading limitations to specify the minimum O/A ratios and relative flow rates in the system. These calculations are performed independent of stage numbers and ionic strength conditions required for extraction,

scrubbing, and stripping. Due to the fact that experimental data indicates TODGA will extract REEs non-selectively until it is saturated, the actual cascade design should operate at conditions as close as reasonably achievable to the ideal cascade as to limit unnecessary co-extraction of impurity lanthanides, thus minimizing overall stage requirements. Ideal cascade design calculations involve multiple steps and assumptions that rely on REE concentrations and flow rates of the aqueous and organic phases in extraction scrubbing and stripping; a design process flow diagram for the ideal cascade is shown in Appendix C.

Two constraints were placed on the selection of flow rates for the mixer-settlers. First, the MEAB mixer-settlers have an advertised throughput of 10 L/hr, or 166 mL/min. Total combined aqueous and organic flow cannot exceed the total throughput to ensure flooding does not occur. Second, and more constrictive, is the required residence time in the mixing and settling chambers. A target residence time of 3 minutes in the mixing chamber was targeted as a conservative approach to ensure the stages achieve chemical equilibrium for the mixing conditions achieved in the mixer. This equates to a total combined aqueous and organic flow rate of 40 mL/min. DGA extraction and stripping kinetics previously evaluated suggest that equilibrium is achieved well below this threshold. Using this approach, the lowest O/A ratio among extraction, scrub, and strip dictates the organic phase flow rate in the system.

With a throughput basis determined, calculations and mass balances for an ideal separation cascade were performed to estimate the loaded organic phase composition and required scrub feed conditions to facilitate selective scrubbing for complete recovery and 100% purity. Starting with the extraction section, the aqueous feed composition and aqueous phase flow rate were specified. Next, an assumption was made based on experimental observation for the degree of lanthanum and cerium co-extraction into the organic phase, assigning 22% and 49% co-extraction of La and Ce from the feed stream, respectively. Assuming 100% recovery of Pr and Nd in addition to the La and Ce co-extraction assumptions, the organic phase flow rate was specified to maintain 100% theoretical TODGA loading capacity. With specified concentration assumptions for the loaded organic phase leaving the extraction section, the flow rates were then scaled such that extraction section mixer residence times were 3 minutes.

Next, a mass balance was conducted around the entire cascade, assuming all of the Pr and Nd report to the strip product and all of the La and Ce report to the raffinate. This specified the molar flow rates of La, Ce, Pr, and Nd in each of their final product streams. The strip feed flow rate was selected to maintain an O/A of 5, achieving a five-fold concentrating factor of the PrNd product. The scrubbed loaded organic was assumed to be completely La and Ce free with 100% recovery of the Pr and Nd. A mass balance around the strip section was utilized to calculate the stripped product composition.

Minimum ideal reflux was calculated assuming perfect separation in the scrub section, i.e. the total moles of PrNd fed to the scrub section was equivalent to the total moles of LaCe in the loaded organic phase leaving the extraction section. For the assumptions specified, this corresponded to 55% reflux of the strip product solution. The reflux assumption set the scrub feed flow rate and composition conditions. A simulant 3 M HCl PrNd scrub feed solution was utilized for mixer-settler testing, which does not take the feed adjustment dilution into account that is required to raise the ionic strength of the refluxed strip product. Finally, the scrub discharge concentration was calculated by performing a mass balance around the scrub section of the cascade. The scrub discharge aqueous solution is typically recombined with the aqueous feed to the extraction section to ensure complete recovery of PrNd, and as such must be accounted for in the total throughput and O/A ratio in the extraction section. This reduced the extraction section mixer residence time to 2.8 minutes but is reasonably close to the target 3-minute residence time and well within the throughput capabilities of the mixer settler equipment.

A final mass balance check was conducted around each section of the ideal cascade to ensure accuracy of the calculations incorporating all assumptions and constraints. A summary of ideal cascade parameters is shown in Table 7.3.

Table 7.3: Process parameters for an ideal light rare earth separation cascade using TODGA.

	Extraction Section	Scrub Section	Extraction Section	Organic Feed	Aqueous Feed	Scrub Feed	Strip Feed	Loaded Organic	Scrubbed Loaded Organic
Throughput (mL/min)	43.3	33.3	36						
O/A	2.3	9.1	5.0						
τ_{mixer} (min)	2.8	3.6	3.3						
$\tau_{settler}$ (min)	11.1	14.4	13.3						
Flow Rate (mL/min)				30	10	3.3	6	30	30
TODGA (M)				0.1				0.1	0.1
HCl (M)					3	3	0.5		
La (mM)					96.7	0		7.1	
Ce (mM)					39.3	0		6.4	
Pr (mM)					11.0	40.7		5.0	8.1
Nd (mM)					33.4	123.8		14.9	24.8

A baseline counter-current cascade configuration was developed using the ideal cascade calculations. The simulated strip product reflux as a scrub feed does not account for any dilution effects as a result of feed adjustment to reduce uncertainty and ensure successful evaluation of experimentally determined steady state equilibrium data. The ideal cascade design is shown in Figure 7.3.

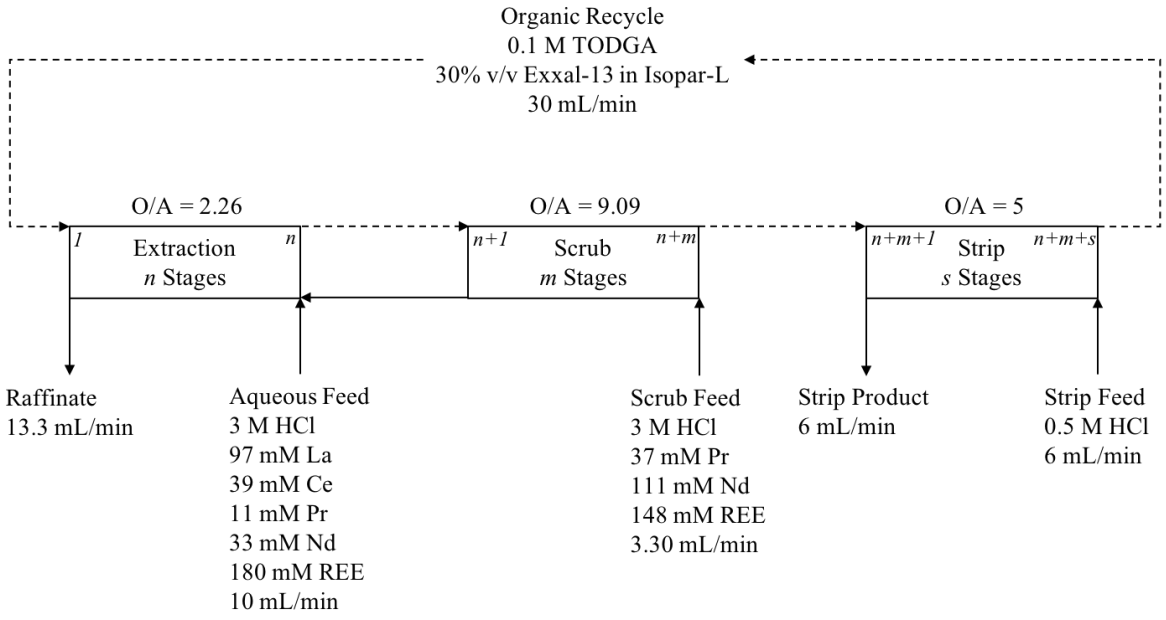

Figure 7.3: Ideal cascade design for light rare earth separations using TODGA.

The first stage of the cascade, depicted on the left side of the extraction section, is fed fresh recycled solvent which will come into contact with an aqueous phase depleted in Pr and Nd.

The loaded organic leaving the extraction section at stage *n* contains Pr, Nd, and co-extracted La and Ce impurities. The scrub loaded organic leaving the scrub section at stage *n+m* has been purified in Pr and Nd, coming into contact with fresh scrub feed containing Pr and Nd. The aqueous scrub discharge leaving the scrub section at stage *n+1* contains La and Ce that have been selectively scrubbed from the organic phase, as well as some Pr and Nd. The scrub discharge is combined with the extraction feed to stage *n* to recover any residual Pr and Nd. Finally, the purified PrNd strip product solution leaves the strip section at stage *n+m+1*. The stripped organic phase, now free of REEs, leaves the strip section at stage *n+m+s* and is continuously recycled back to the extraction section. Industrial solvent extraction cascades typically have a solvent makeup and/or regeneration step prior to recycling back to extraction, this is not included in the ideal cascade design.

The above qualitative conditions described were utilized in conjunction with concentrations calculated from the ideal cascade mass balance model to conduct a series of equilibrium extraction and scrub experiments to validate predicted distribution ratios prior to counter-current mixer-settler testing.

Batch Counter-Current Simulation Experiment Procedure

Calculating rigorous equilibrium data and the required number of stages to achieve a separation is extremely difficult for multicomponent systems. Classic chemical engineering approaches have been developed to determine the separation performance of a counter-current cascade using a series of batch shakeout experiments. This is particularly useful for cascades that utilize reflux [50], as is the case for the proposed TODGA counter-current cascade configurations. Using this technique, organic and aqueous phases are thoroughly mixed at the desired O/A ratio to achieve equilibrium and the phases are allowed to disengage completely. The phases are carefully separated, with special care taken to completely recover each phase with minimum contamination in one another. The recovered loaded organic phase is subsequently contacted with fresh aqueous solution, and the recovered aqueous raffinate is contacted with fresh organic solvent. Depending on the number of counter-current stages being simulated, a network of batch shakeouts is carried out, transferring the recovered phases in a counter-current fashion. After approximately five iterations producing a counter-current raffinate and loaded organic phase, the final set of

samples approaches the observed effect for a counter-current cascade. This technique saves both time and cost prior to scaling up to testing in solvent extraction equipment such as mixer-settlers. An example of a five-stage batch counter-current cascade simulation constructed from available procedures is shown in Figure 7.4 [50]:

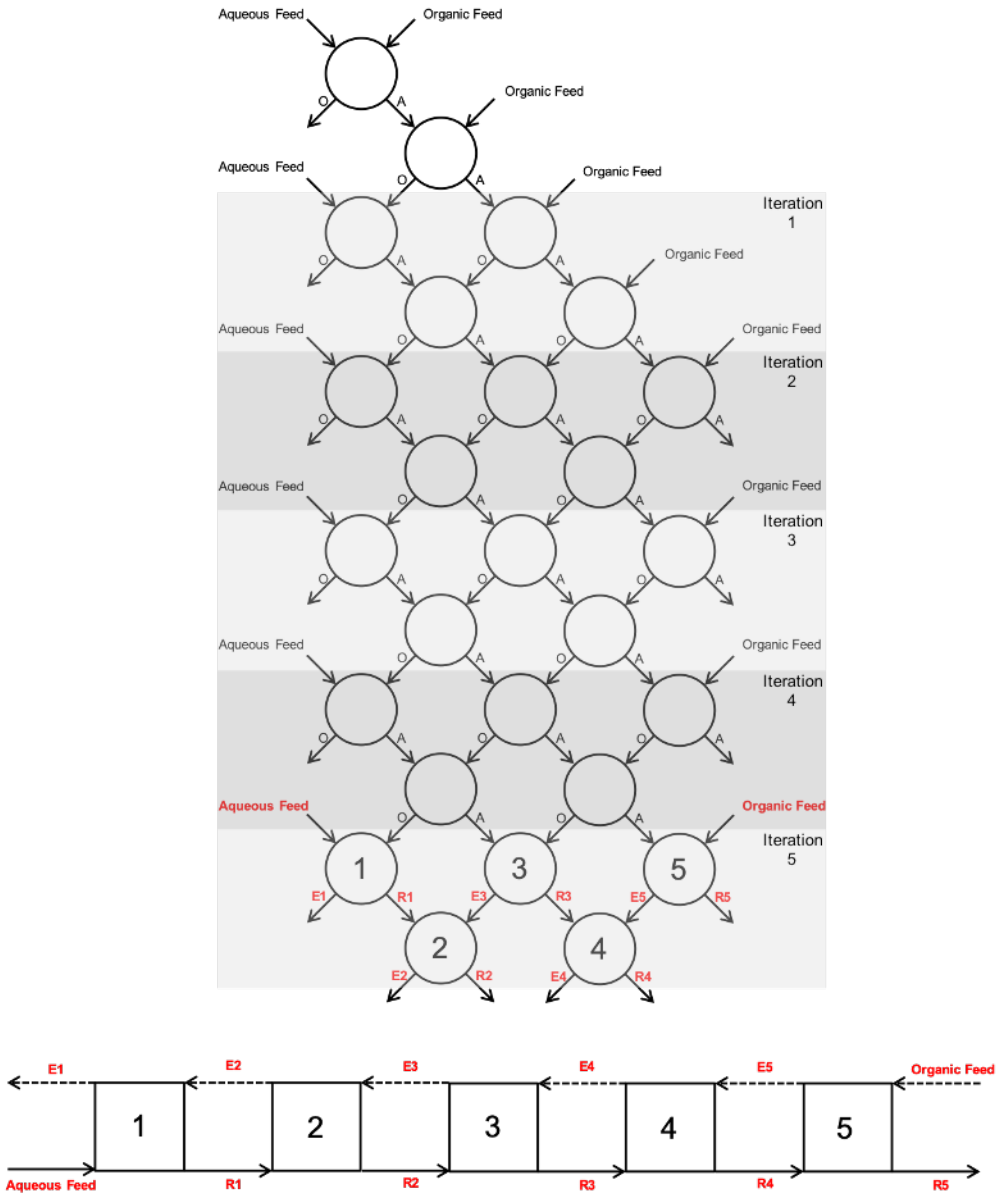

Figure 7.4: 5 stage batch shakeout experiment to simulate counter-current solvent extraction.

Each gray box represents an iteration of batch equilibrium contacts that approaches the anticipated steady-state effect in a counter-current cascade. The red text in Figure 7.4 represents the corresponding organic and aqueous equilibrium concentrations leaving each

stage for a batch counter-current shakeout simulation as compared to an actual counter-current cascade. The batch shakeout procedure specified in Figure 7.4 was conducted for a simulated light REE separation (cut made at Pr and Ce). Simulated 5-stage circuits were tested for both extraction and scrub sections; each 5-stage simulation required 31 total batch extraction experiments. The results from counter-current simulation experiments not only predict expected separation performance in counter-current solvent extraction equipment, they also provide an effective means to determine the efficacy of the distribution ratio correlation models to predict counter-current solvent extraction behavior.

Light Rare Earth Separation Batch Counter-Current Simulation Experiments

A 180 mM light rare earth chloride solution at 3 M HCl was prepared in accordance with the feed composition specified for the ideal cascade design in Table 7.3 (53.6% La, 21.8% Ce, 6.1% Pr, and 18.5% Nd). This feed was contacted with fresh 0.1 M TODGA/30% Exxal-13/Isopar-L solvent to simulate a 5-stage counter-current cascade. Each contact was performed at O/A = 3 following the shakeout procedure specified in Figure 7.4. The simulated extraction cascade is shown in Figure 7.5.

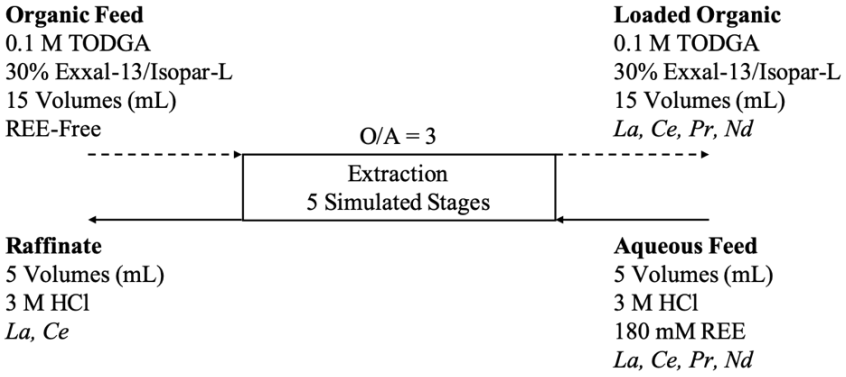

Figure 7.5: 5-stage batch counter-current extraction experiment conditions for light rare earth separations.

The same aqueous feed was utilized to prepare a larger volume of loaded organic for use in a 5-stage simulated counter-current scrubbing cascade by contacting 300 mL aqueous with 300 mL fresh 0.1 M TODGA/30% Exxal-13/Isopar-L solvent at O/A = 1. The loaded organic was utilized as the organic feed to the simulated scrub cascade. The scrub feed was also derived from the ideal cascade design, utilizing a 165 mM didymium chloride solution in 3

M HCl (25% Pr, 75% Nd). Contacts were performed at O/A = 9 for the scrubbing experiment. The simulated scrubbing cascade is shown in Figure 7.6.

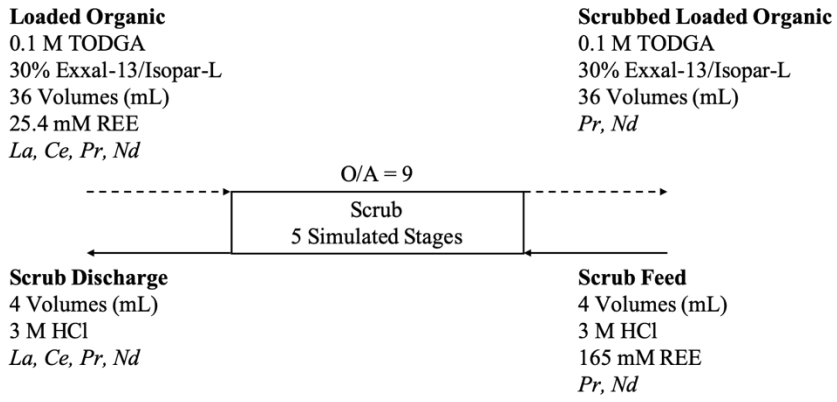

Figure 7.6: 5-stage batch counter-current scrubbing experiment conditions for light rare earth separations.

Actual feed compositions for the simulated extract-scrub cascades are shown in Table 7.4. These feed concentrations were utilized for mass balance purposes as well as inputs to the MATLAB mass balance model described in Chapter 5. A complete set of equilibrium data from these experiments is provided in Appendix D.

Table 7.4: Feed compositions for light rare earth extraction and scrub counter-current simulation experiments.

Feed Stream	La	Ce	Pr	Nd	TOTAL
Aqueous Feed (mM)	80.4	35.9	12.0	28.2	156.5
Scrub Feed (mM)	0	0	35.9	106.7	142.6
Loaded Organic (mM)	5.5	5.1	2.5	12.2	25.4

First, the purpose of the 5-stage experiments is to evaluate extraction and partitioning behavior in a counter-current cascade, as well as providing equilibrium data for further validation of the distribution ratio correlation models prior to their use for counter-current design. These experiments were not designed with the intent of achieving any particular degree of purity or recovery.

Nd and Pr preferentially load into the organic phase in the extraction section with a combined recovery of 94.5% under the specified conditions. The primary loss was Pr to the raffinate. Interestingly, the organic phase loaded to saturation with La and Ce once the Nd and Pr were depleted from the aqueous phase in stages 1 and 2. This is presumably due to the fact that La

and Ce concentrations are significantly higher than Pr and Nd, indicating that TODGA will load essentially non-selectively until it is saturated. Organic phase La loading decreases from stage 3 to 5, indicating preferential exchange to recover Pr and Nd from the aqueous phase. This is similar to the behavior observed in industrial PC88A extraction circuits utilizing saponification as described in Chapter 2. The raffinate leaving the extraction section recovered 57% of LaCe at a purity of 99.1%. Again, the primary contaminant in the raffinate was unextracted Pr. The composition of the loaded organic leaving extraction was 25% La, 24% Ce, 12% Pr, and 40% Nd. While the overall purity of PrNd increased from 26% in the feed to 51% in the loaded organic, a significant amount of La and Ce were co-extracted at the cost of recovering the Pr and Nd. Aqueous and organic phase stage-wise REE concentration profiles across the extraction section are shown in Figure 7.7.

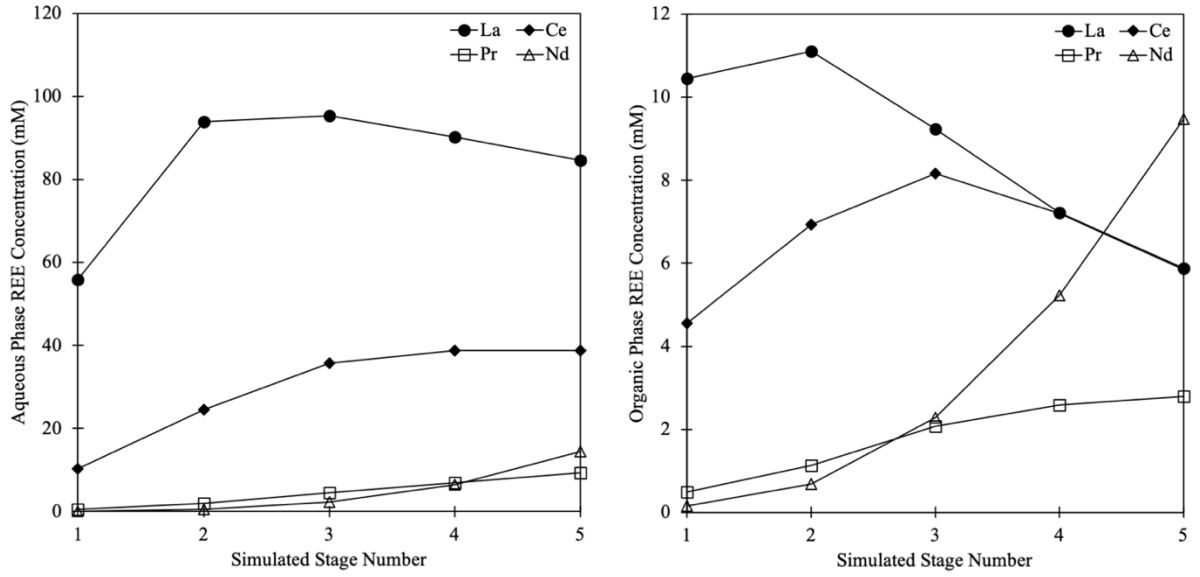

Figure 7.7: Batch counter-current simulation results for light rare earth separation extraction section.

The simulated scrub section utilized a PrNd scrub feed to preferentially scrub La and Ce from the loaded organic phase. Experimental results from Chapter 6 suggest that this exchange only happens if the solvent is saturated with REE. Loading calculations indicate this indeed was the case for this counter-current simulation experiment, with results showing Pr and Nd concentrations increasing in the organic phase with a corresponding decrease in La and Ce concentrations. Aqueous phase results support this observation, as La and Ce

concentrations increase moving from stage 10 toward stage 6. Scrubbing efficiency worked quite well under the specified conditions, removing 91% of the La and Ce. Similar to the extraction section, the major impurity persists from the adjacent lanthanide cut being made with the final PrNd stream containing 3% Ce. Aqueous and organic phase stage-wise REE concentration profiles across the scrub section are shown in Figure 7.8.

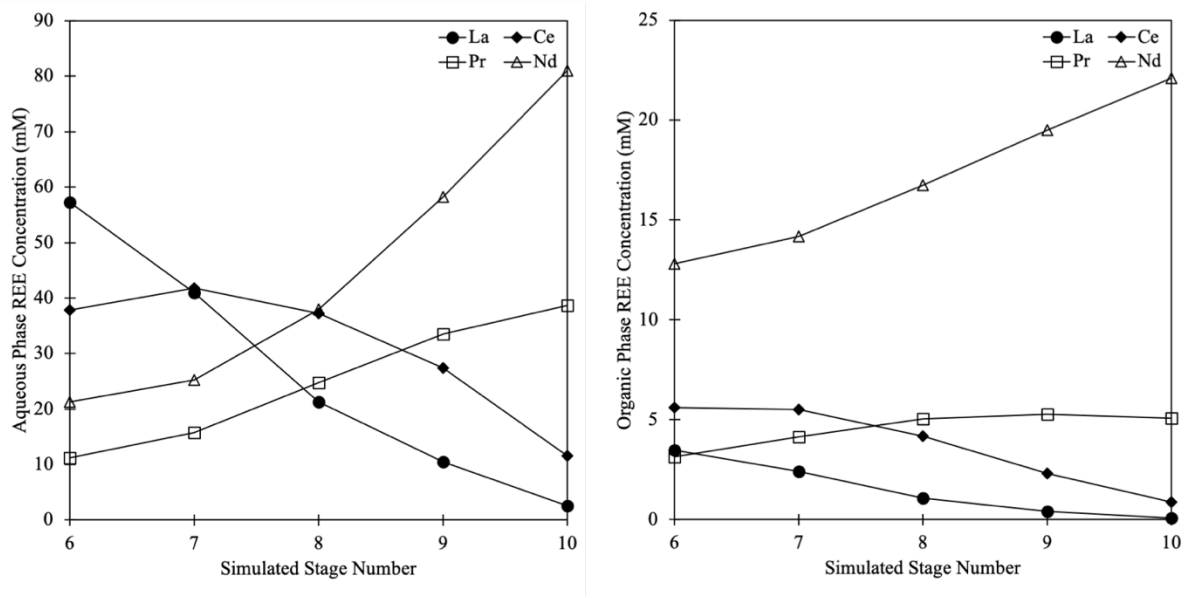

Figure 7.8: Batch counter-current simulation results for light rare earth separation scrub section.

Finally, the results from the batch counter-current simulations experiments were utilized to assess the validity of the empirical distribution ratio model as a predictive tool for separation process design. Total aqueous phase chloride concentrations and organic phase free TODGA concentrations at equilibrium were calculated for each simulated stage. These tabulated values were used to calculate the distribution ratio using expressions provided in Table 7.2. The calculated distribution ratios were used in the MATLAB counter-current mass balance model to calculate stage-wise aqueous and organic phase concentration profiles. Two cases were analyzed: Nd as a representative component that is readily extractable under the specified conditions, and La as a representative component that does not readily extract and primarily reports to the aqueous phase. Figure 7.9 shows a comparison of predicted and experimental concentration profiles for each component's respective phase, with aqueous

phase lanthanum results shown in 32(A) and organic phase neodymium results shown in 32(B).

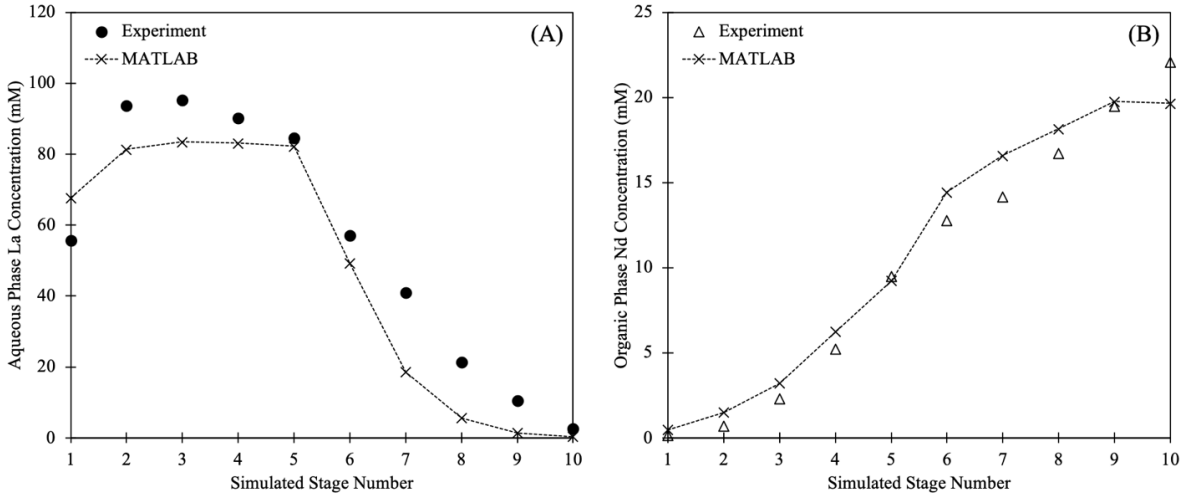

Figure 7.9: Comparison of experimental extract-scrub results with MATLAB model predictions.

The empirical model provides a reasonable fit of the experimental data. Organic phase loading and scrubbing behaviors are modeled well. Notable limitations of the predictive model include the two extreme ends of the extract-scrub cascade. The model under-predicts the loading of La into the organic phase as indicated by the difference in La raffinate concentrations. Similarly, the model under-predicts loading of Nd in the scrub feed stage. This is likely caused by limitations of the empirical model's linear surface fitting of the single metal extraction data set. The ionic strength of the raffinate is appreciably higher than the empirical fit of lanthanum extraction at 3 M HCl due to the presence of other rare earth chloride salts, boosting the extraction efficiency. Similarly, the scrub feed calculated for the ideal cascade design extrapolates Nd extraction data beyond known experimental results. This is anticipated for empirical fitting of the limited data sets for each metal and will be discussed in further detail in Chapter 8.

Light Rare Earth Separations Counter-Current Mixer-Settler Testing

Ideal cascade design coupled with batch counter-current simulation experiments provide valuable insight for stage configurations and operating parameters required to achieve both high degrees of purity and recovery for the separation of PrNd from LaCe. First, counter-

current simulations suggest extraction and scrubbing trends that appeared to be limited by the number of simulated stages. Extraction section trends indicated selective exchange to recover Pr and Nd, while scrubbing section trends indicated selective exchange to remove La and Ce from the organic phase. Consequently, a mixer-settler configuration design containing 10 extraction stages, 10 scrub stages, and 4 strip stages was selected for further evaluation of distribution modeling capabilities. The final counter-current cascade stage configuration is shown in Figure 7.10.

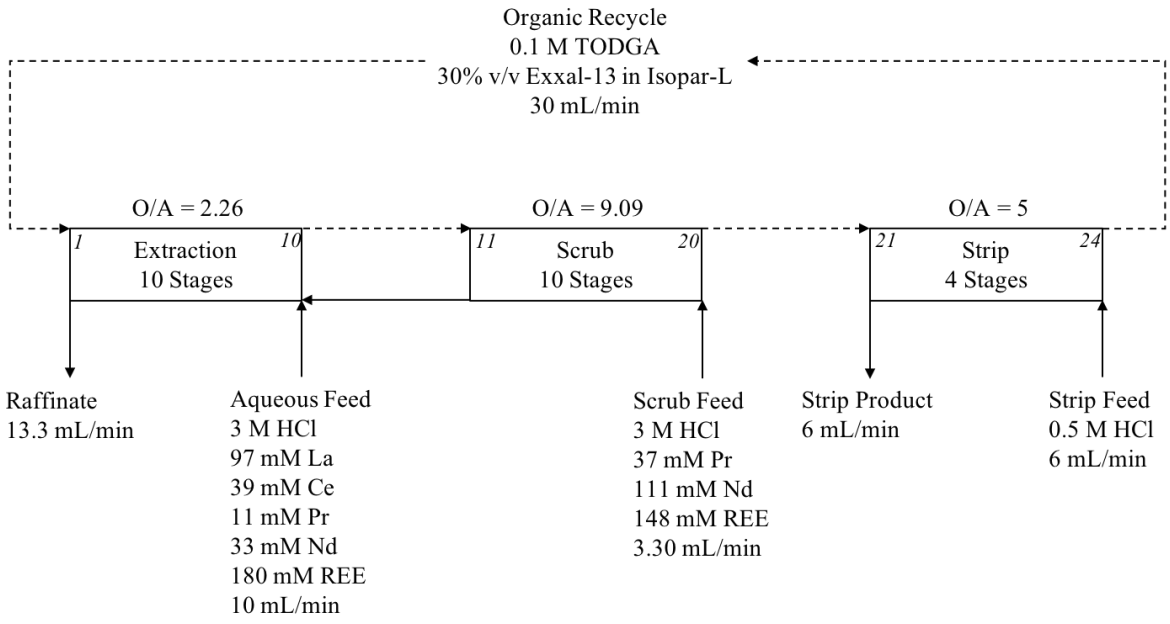

Figure 7.10: Stage configuration for light rare earth separation mixer-settler test.

REE and HCl concentrations, phase ratios, and flow rates are identical to the ideal cascade depicted in Figure 7.3. One limitation not addressed in the proposed counter-current mixer-settler experiment is the feed adjustment requirement for the scrub feed. A continuous counter-current process would utilize a fraction of the PrNd strip product refluxed as the scrub feed. However, results from Chapter 6 indicate direct reflux in a TODGA circuit would strip all REE from the organic phase and therefore must undergo an ionic strength adjustment first. Direct acidification with concentrated HCl would dilute the PrNd metal concentration, thereby reducing the driving force for metal-metal exchange. The alternative would be evaporation followed by acidification but adds significant operating cost and holdup time for preparation of scrub feed solutions. However, as a proof-of-concept counter-

current experiment, an optimum undiluted scrub feed simulant was chosen for the counter-current experiment.

The mixer-settlers were initially filled with freshly prepared technical grade TODGA organic solvent and metal-free hydrochloric acid solutions that corresponded to the operating acidity of the respective section of the cascade. Extraction and scrub sections were filled with 3 M HCl and the strip section was filled with 0.5 M HCl. FMI pumps were calibrated using a stopwatch and graduated cylinder to deliver desired flow rates to the system. Mixer motors were operated at 950 ± 50 RPM as read on a portable tachometer. System startup used metal-free acid feed solutions until hydraulic steady state was reached. Hydraulic steady state was determined when outlet raffinate, stripped product, and stripped organic flow rates exiting the mixer-settlers were measured with a graduated cylinder and stopwatch within 10% of the calibrated pump delivery rate. At time t = 0, the aqueous feed and scrub feed solutions were switched to the respective metal-bearing feed solutions. The mixer-settlers were operated continuously for 75 hours to achieve steady state operating conditions as predicted by the dynamic ODE mass balance model described previously based upon system holdup and throughput. Once steady state was achieved, feed pumps and mixer motors were shut off. Organic and aqueous samples were collected for all 24 stages at the organic and aqueous phase outlet weirs. Organic phase samples were stripped for ICP analysis in accordance with methods described in Chapter 4. Acid-base titrations were performed on all aqueous phase samples to determine the steady state HCl concentration profile across the cascade. Results for the final feed and product effluent concentrations are shown in Table 7.5.

Table 7.5: Product compositions from light REE separation mixer-settler experiment.

Stream	La (mM)	Ce (mM)	Pr (mM)	Nd (mM)	% Purity	% Recovery
Aqueous Feed	93.26	39.38	16.32	28.33	-	-
Scrub Feed	-	0.72	29.00	111.45	99.5 (PrNd)	-
Raffinate	69.57	27.13	8.06	0.00	92.3 (LaCe)	97 (LaCe)
Strip Product	0.00	3.90	22.39	107.32	97.1 (PrNd)	86 (PrNd)

At first glance, it is apparent that the two product streams were significantly enriched in their desired solutes but the raffinate was contaminated with Pr and the strip product was

contaminated with Ce. Pinpointing the exact cause requires a more detailed look at the organic and aqueous phase component concentrations across the cascade. For clarity, Table 7.6 indicates the stage at which feed and effluent streams enter or exit the mixer-settler cascade.

Table 7.6: Inlet and outlet streams from the light REE separation cascade experiment.

Stream	Stage	Flow Direction
Organic Feed	1	In
Aqueous Feed	10	In
Scrub Feed	20	In
Strip Feed	24	In
Raffinate	1	Out
Scrub Discharge	11	Out
Strip Product	21	Out
Stripped Organic	24	Out

Previous extraction experiments indicated that the Ln(III)-TODGA-HCl solvent system is highly dependent on the equilibrium aqueous phase chloride concentration; the steady-state stage-wise aqueous phase hydrochloric acid concentration profile is shown in Figure 7.11 to aid in the interpretation of REE extraction trends across the cascade. The steady state organic phase REE concentration profiles across the cascade are shown in Figure 7.12. The corresponding aqueous phase steady state REE concentration profiles are shown in Figure 7.13.

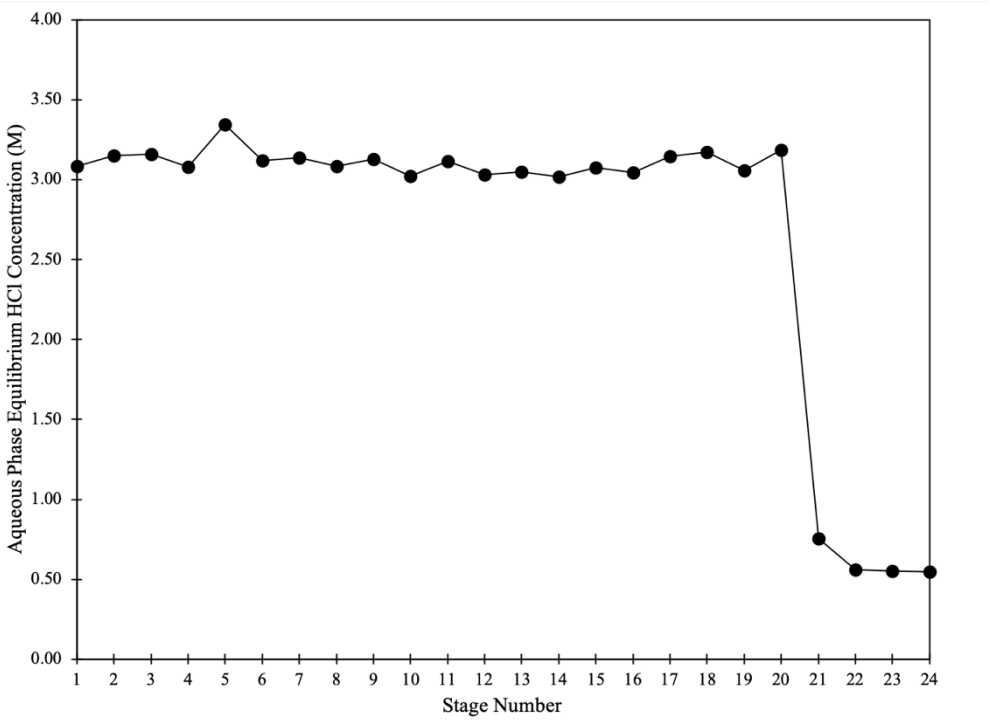

Figure 7.11: Steady state stage-wise aqueous phase hydrochloric acid concentration profile.

First, the extraction and scrub section operated at a constant acid concentration, averaging 3.11 M HCl across the first twenty stages. This is in good agreement with the experimental observation that TODGA does not extract HCl to any appreciable extent. The elevated HCl concentration of 0.75 M measured in the stripped product leaving stage 21 is anticipated based on experimental HCl extraction data presented in Table 6.2. Using a conservative acid extraction distribution ratio of $D_{HCl} = 0.012$ from a 3.11 M HCl solution at O/A = 1, the organic phase HCl concentration is calculated to be 37 mM. Upon stripping with 0.55 M HCl at O/A = 5, the calculated strip product acid concentration is determined to be 0.73 M assuming complete stripping of acid from the solvent. This is due to the concentrating effect of the high O/A phase ratio in the strip section of the cascade. The calculated strip product HCl concentration is in good agreement with the measured concentration.

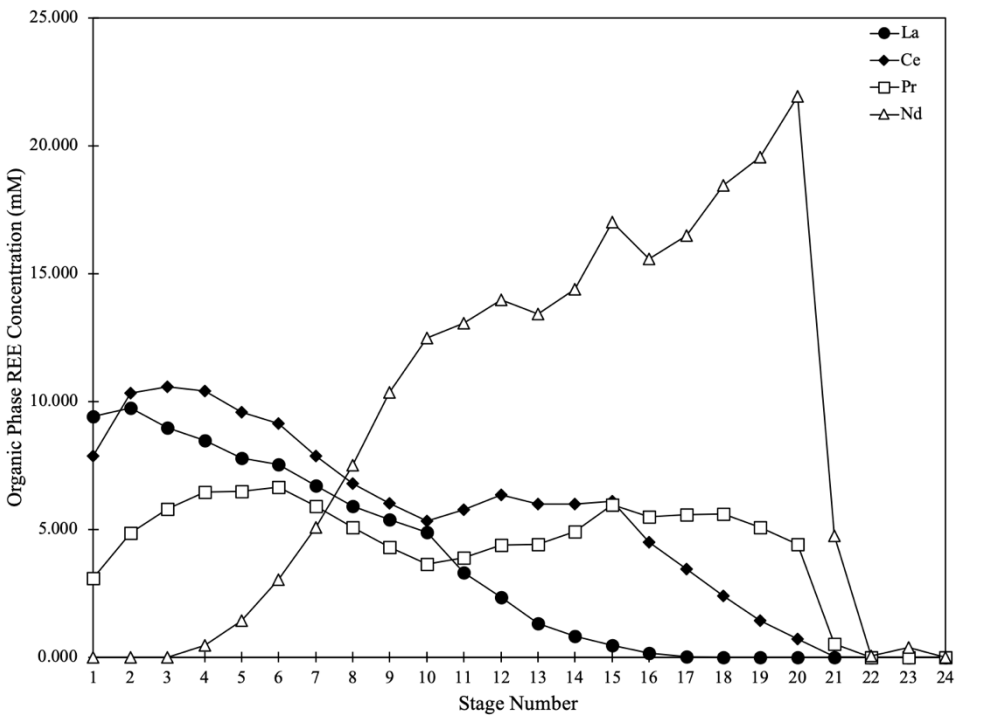

Figure 7.12: Steady state organic phase stage-wise REE concentration profiles for the light REE separation mixer-settler test

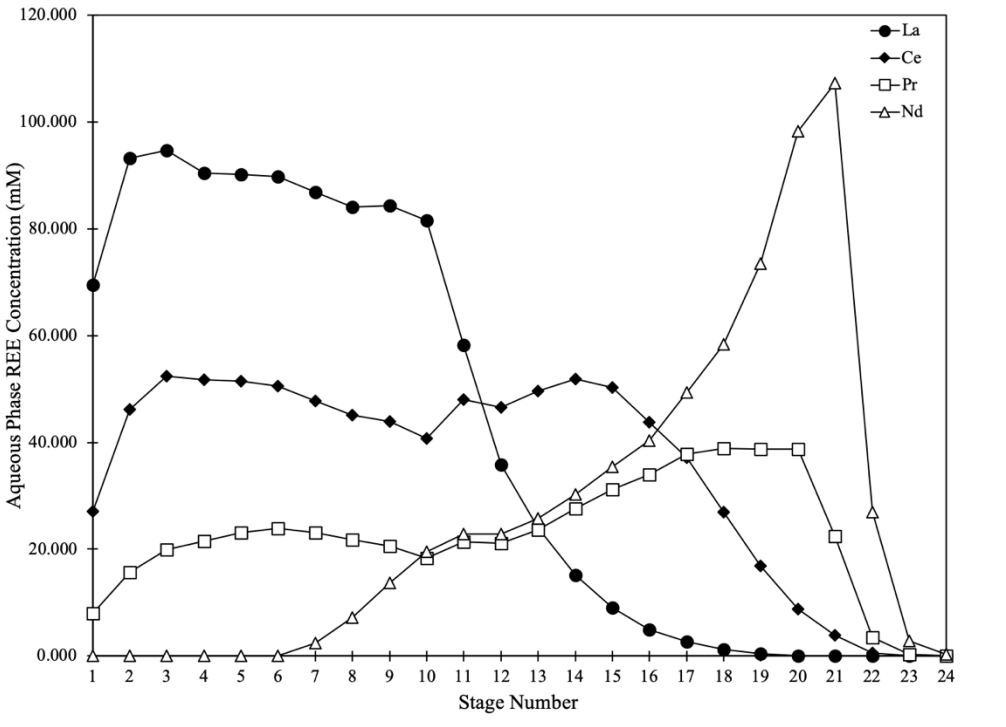

Figure 7.13: Steady state aqueous phase stage-wise REE concentration profiles for the light REE separation mixer-settler test.

Inspection of Figures 7.12 and 7.13 indicate that Nd extracted strongly under these conditions, with essentially all Nd fed to the system being recovered in the strip product solution in stage 21. Nd recovery in the extraction section was achieved in stages 6-10, with no detection of Nd in the raffinate exiting stage 1. The scrub section utilized simulated PrNd reflux to selectively scrub out La and Ce, further loading Nd into the organic phase. Finally, Nd was completely recovered in the strip section, with no detected amounts of Nd in the stripped organic phase solvent exiting stage 24.

Pr behavior in the counter-current cascade was not ideal and its loss to the raffinate was one of the primary deficiencies in the process. Rather than a clean extraction trend as observed with Nd, Pr was essentially retained in the aqueous phase in the extraction section as indicated by Figure 7.13. The incoming recycled solvent quickly loaded with La, Ce, and Pr in the first two extraction stages, after which selective scrubbing occurred to preferentially load Pr over the co-extracted La and Ce. This recovered some of the Pr, but nearly 40% of the total Pr fed to the system ended up reporting to the raffinate. Pr loading in the scrub section did occur as indicated by the increase in organic phase Pr from stages 11-20 with a corresponding decrease in aqueous phase Pr counter-currently from stages 20-11. However, Pr did not selectively load as well as Nd under the ionic strength conditions in the strip section, potentially contributing to the Ce contamination in the final strip product solution.

Conditions were selected to cause Ce to report to the raffinate, thereby performing a clean separation between Ce and Pr. Similar to Pr, the observed extraction behavior did not agree with experimental predictions. Ce largely remained in the aqueous phase, although the fresh incoming organic extracted approximately 38% in stage 1 of the total aqueous phase Ce flowing counter-current from stage 2. The organic phase Ce concentration decreased across the extraction section from stages 2-10 as the organic phase loaded with Pr and Nd. The final loaded organic phase leaving the extraction section contained 40.6% co-extracted Ce from the feed that required removal via selective scrubbing. Organic phase Ce loading in the scrub section remained relatively constant from stages 11-15, dropping off sharply from stages 16-20. Roughly 6% of the total cerium fed to the circuit reported to the strip product as a contaminant. Based on the extraction behavior of Nd in the scrub section, it is likely that the scrub feed Nd was primarily responsible for displacing Ce in the organic phase.

Lanthanum, having the lowest extraction affinity by TODGA across the lanthanide series, behaved as expected at 3 M HCl conditions. La primarily remained in the aqueous phase in the extraction section. The fresh incoming organic solvent extracted 22.8% of the La in stage 1 along with Ce and Pr co-extraction. The organic phase La concentration decreased from stages 2-10 as TODGA selectively loaded Pr (and to a lesser extent possibly some Ce). The final loaded organic phase leaving the extraction section contained 15.7% co-extracted La from the total La fed to the circuit. La concentration in the organic phase dropped off dramatically from stages 11-20 in the scrub section as Pr and Nd preferentially loaded, with La being non-detectable in the organic phase beyond stage 18. All La fed to the circuit reported to the raffinate as anticipated. The estimated extent of La and Ce co-extraction of 22% and 49% respectively in the ideal cascade design was relatively close to the actual observed extent of co-extraction in the extraction section.

With a clear understanding of each species' behavior across the cascade, there are several conclusions that may be drawn regarding the overall separation performance and opportunities for improvement. First, Pr exhibited a reluctance to load unless contacted with saturated TODGA containing significant concentrations of La and Ce. When combined with Ce's tendency to extract and remain in the organic phase in the initial scrub stages indicates that the overall cascade acidity may not have been high enough to facilitate optimized extraction of Pr and Nd. A slight increase in the aqueous feed and scrub feed acidities would promote Pr extraction and its ability to remain in the organic phase. However, while an increase in acid concentration would promote Pr recovery and prevent its loss to the raffinate, it would also promote additional Ce extraction. Higher Ce concentrations in the organic phase entering the scrub section would likely require additional stages to achieve high purity of the PrNd product. It is also unclear how the scrub stage requirements would be impacted, as it was apparent that Pr was not successfully loading into the organic phase under the operating conditions in scrub. Overall mass balances around the cascade on each species closed within 10%, indicating that the mixer-settlers were operating at steady state and well within a reasonable balance given measurement error of process flow rates.

Previous stripping conditions for selective scrubbing investigations utilized pH 1 HCl, but the higher loading conditions of 0.1 M TODGA required the use of 0.5 M HCl to prevent

excessive entrainment in both phases. Furthermore, stripping at an O/A of 5 did not quantitatively strip all metals from the organic phase in a single stage but did achieve complete stripping in 4 stages.

MATLAB Counter-Current Modeling Evaluation

The MATLAB mass balance model described in Chapter 5 was utilized to examine calculated organic and aqueous phase REE concentration profiles across the cascade. Three scenarios were considered. The first used experimentally determined distribution ratios based upon measured organic and aqueous phase equilibrium concentrations for each REE in the cascade. The second approach took an average constant distribution ratio for each species in the extraction, scrub, and strip section. The third approach utilized the distribution ratio correlation expressions described in Table 7.2 to calculate distribution ratios as a function of equilibrium aqueous phase chloride concentration and organic phase free TODGA concentration. Each set of distribution ratios were incorporated as inputs into the MATLAB mass balance model to calculate the corresponding stage-wise aqueous and organic phase REE profiles. Model output in comparison to experimental data for the extractable species Pr and Nd are shown in Figure 7.14. Output comparisons for non-extractable species La and Ce are shown in Figure 7.15.

First, a plot of MATLAB modeling output using experimentally determined distribution ratios provides overall excellent agreement with the measured REE concentration profiles. This provides assurance that the mixer-settlers were operating at steady state and that the calibrated pump flow rates utilized in the experiment delivered consistent target flow rates throughout the system. This also provides confidence that the mass balance equations and corresponding input parameters are correctly transcribed in the modeling framework.

Second, utilizing an average constant distribution ratio for the mass balance model achieved reasonable correlation to experimental data in the latter half of the scrub section, but fails to accurately capture significant changes in concentration when the organic phase is saturated. This is made evident by the extraction section trends for La, Ce, and Pr. Additionally, the use of constant distribution ratios in the scrub section failed to accurately predict the loading in the first half of scrub. This highlights the importance of incorporating a model that can calculate and predict partitioning behavior because the extraction behavior is highly

nonlinear in its dependence on chloride concentration, free TODGA concentration, and organic phase loading.

Finally, a complete breakdown in the accuracy of the calculated distribution ratios using the correlation expressions is observed in the counter-current experiment. Suspected deficiencies must be addressed to improve upon the model's predictive capability for solvent extraction process design. The first issue is tied to the organic phase loading and extraction conditions utilized to generate the empirical data surface fit equations. One limitation is that single-metal experiments were conducted at ranges relevant to the species' actual concentration in bastnäsite ore. This had an adverse consequence on Pr extraction trends (and the same would be expected if modeling Sm) because the theoretical organic phase loading capacity was maintained below 40%.

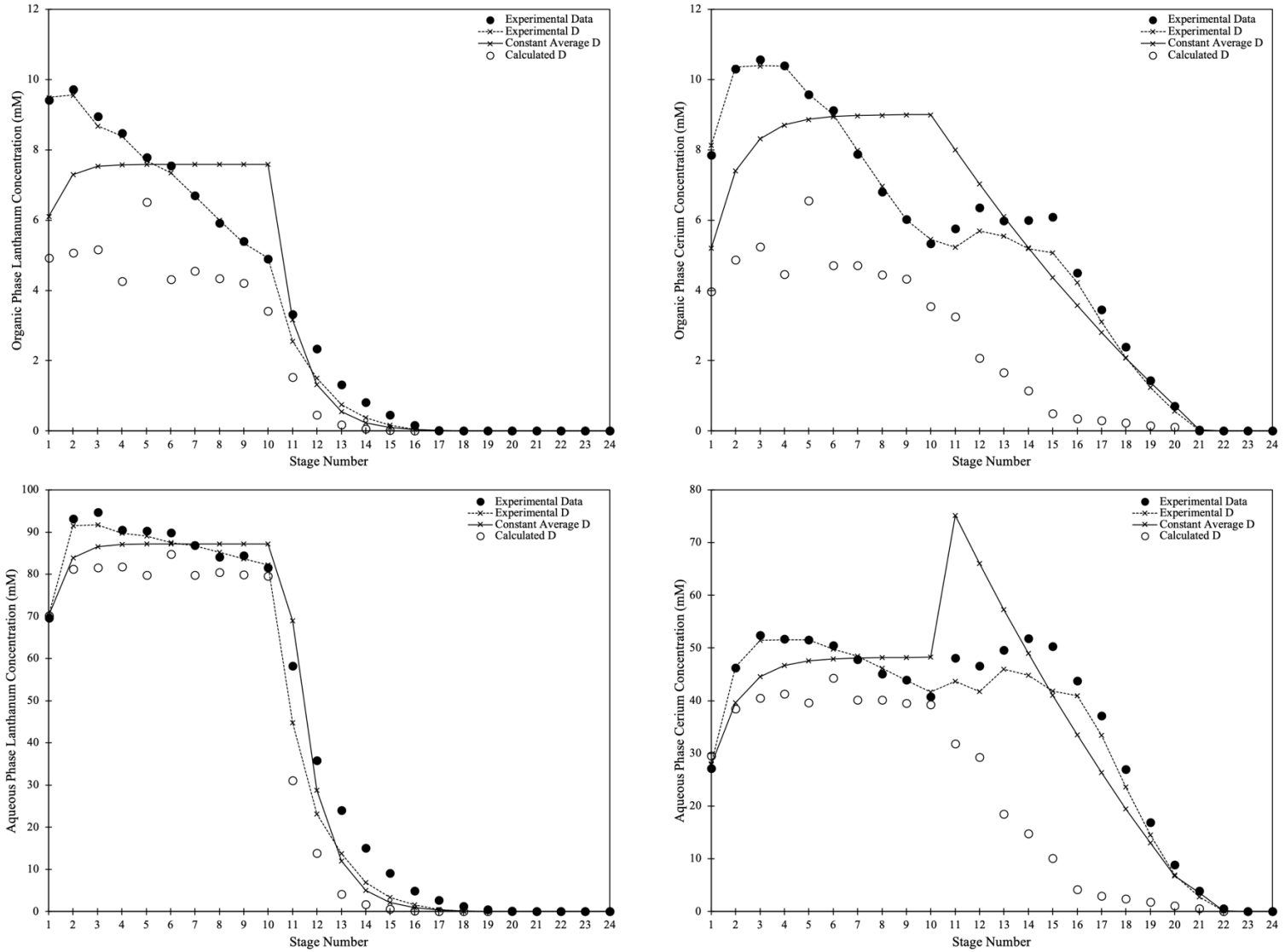

Figure 7.14: MATLAB model comparisons for stage-wise organic and aqueous phase La and Ce concentration profiles.

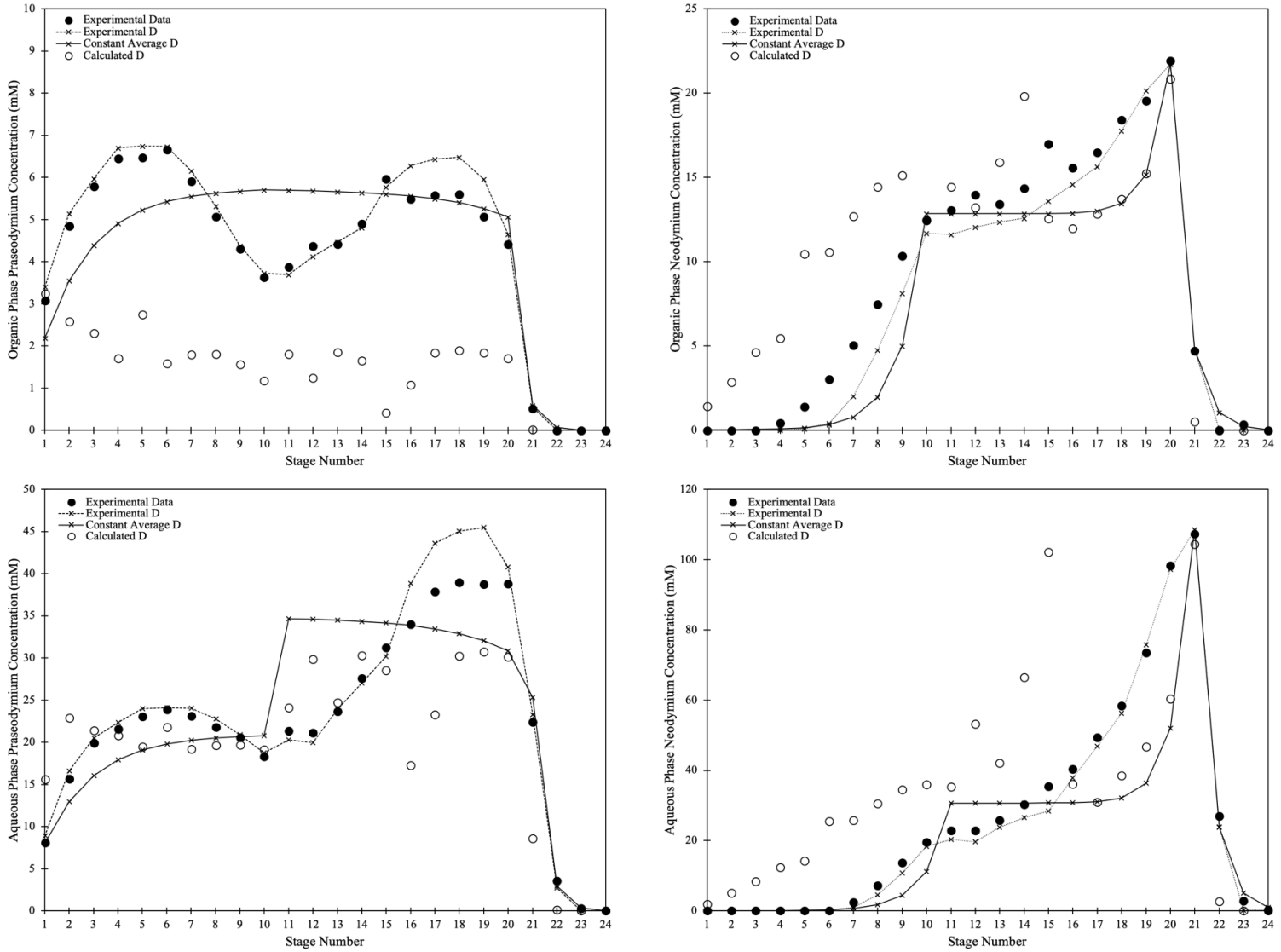

Figure 7.15: MATLAB model comparisons for stage-wise organic and aqueous phase Pr and Nd concentration profiles.

The organic phase is fully saturated across the entire cascade, therefore distribution ratios for Pr are inherently predicted to be significantly lower because the empirical expression is extrapolating well beyond limitations of the experimental data set. Similar for Ce, extraction data at 3 M HCl did not achieve saturation loading in single metal experiments and therefore there is a deviation due to extrapolation of free TODGA concentration under saturated loading conditions for selective scrubbing. However, the overall partitioning trend was modeled much more accurately for Ce than Pr, albeit predicting concentrations almost 50% lower than experimentally observed.

The single-metal correlations to calculate distribution ratios were dependent on aqueous phase equilibrium chloride concentration and organic phase equilibrium free TODGA concentration. However, the counter-current mixer-settler test results reveal that TODGA maintains saturation loading across the entire cascade, with the exception of the first stage where fresh solvent contacts the predominantly La and Ce-bearing aqueous stream. Furthermore, TODGA's extremely low affinity for HCl extraction results in a near-constant aqueous phase chloride concentration across the circuit, particularly once the solvent is saturated and metal-metal exchange is taking place. All trivalent lanthanides in the aqueous phase are treated as metal chloride complexes, consequently exchanging one mole of metal for another does not impact the overall chloride balance in the aqueous phase. Single metal equilibrium expressions that rely upon chloride and TODGA concentrations will not provide any degree of accuracy to predict distribution ratios under saturation conditions, and thus a new approach must be considered for TODGA's selective scrubbing mechanism under saturation conditions.

Predicting Equilibrium at Saturation: Pseudo-Single Metal Concept

The extract-scrub sections of the counter-current light rare earth separation cascade operated under the following chemical conditions:

1. TODGA organic phase loading capacity was at saturation across the entire cascade.
2. Average aqueous phase HCl concentration was 3.1 M with ± 2% calculated deviation.
3. Average free TODGA concentration at saturation was 0.022 M with ± 8% calculated deviation, assuming a three-to-one mole ratio for ligand:metal complexation.

The only exception to this observation was the first extraction stage where fresh incoming solvent contacted the PrNd-depleted aqueous phase containing primarily La and Ce, at which point the theoretical loading capacity only reached 61%. Calculated free TODGA concentration in stage 15 also appeared to be an outlier at 0.011 M, with all surrounding stages having calculated free TODGA more in line with the average value. Based on the three chemical conditions described above, a model to calculate distribution ratios under saturated organic phase loading conditions is not adequate if it relies upon total chloride concentration and free TODGA at equilibrium. That being said, these two reactants must be considered to accurately capture extraction behavior at the opposing ends of the extract-scrub cascade when initial loading occurs and when metal-bearing feeds enter the system.

A new alternative method, herein referred to as the "Pseudo-Single Metal Concept," was developed to calculate distribution ratios in a complex multicomponent system by breaking out the individual contribution of each rare earth species to the total aqueous phase chloride ionic strength and organic phase free TODGA concentration. For rare earth species *i*, the pseudo-single metal total chloride ionic strength was calculated using:

$$(x_{Cl^-})_i = x_{HCl} + 3x_i \quad \text{(Eq. 41)}$$

Where x_{HCl} is the equilibrium aqueous phase HCl concentration and x_i is the equilibrium aqueous phase lanthanide concentration of species *i* (M). The pseudo-single metal total chloride concentration essentially computes each REE's contribution to ionic strength beyond the contribution from HCl. Similarly, the pseudo-single metal free TODGA concentration is calculated using:

$$(y_{DGA})_i = 0.1 - 3y_i \quad \text{(Eq. 42)}$$

Where 0.1 is the total TODGA concentration in the organic phase (M) and y_i is the equilibrium organic phase lanthanide concentration of species *i* (M). Again, the pseudo-single metal free TODGA concentration only accounts for that particular component's contribution to the organic phase loading.

Equilibrium data from the counter-current mixer-settler test provides a rich data set comprising a wide variety of REE loading conditions at saturation when facilitating metal-metal exchange. Logarithmic surface plots were generated for this data set using

MATLAB's curve fitting application for each lanthanide, utilizing the same approach previously described. Linear polynomial expressions were determined for each lanthanide, culminating in a new "pseudo-single metal" equation to calculate distribution ratios. Coefficients determined from the curve fitting application and the corresponding distribution ratio equations are shown in Table 7.7.

Table 7.7: Coefficients from MATLAB curve fitting of "pseudo-single metal" equilibrium data from mixer-settler testing and corresponding empirical distribution ratio expressions.

Element	log(K_i)	α_1	α_2	"Pseudo" D_i Expression
La	-4.58	-4.26	-5.20	$D_{La} = (2.61\text{E}-05)[(x_{Cl^-})_{La}]^{-4.26}[(y_{DGA})_{La}]^{-5.20}$
Ce	-4.72	1.59	-2.79	$D_{Ce} = (1.92\text{E}-05)[(x_{Cl^-})_{Ce}]^{1.59}[(y_{DGA})_{Ce}]^{-2.79}$
Pr	-2.30	1.51	-0.81	$D_{Pr} = (4.97\text{E}-03)[(x_{Cl^-})_{Pr}]^{1.51}[(y_{DGA})_{Pr}]^{-0.81}$
Nd	1.24	2.91	2.40	$D_{Nd} = (1.75\text{E}+01)[(x_{Cl^-})_{Nd}]^{2.91}[(y_{DGA})_{Nd}]^{2.40}$

Empirical curve fitting techniques are not indicative of any correlation to physical and chemical properties of the solvent system. However, comparison of the coefficients determined with the MATLAB surface fitting tool for single metal extraction experiments and the saturated multicomponent counter-current cascade provide insight about which parameters exert the strongest influence on distribution ratio calculations. A comparison of MATLAB curve fitting coefficients is shown in Table 7.8.

Table 7.8: Comparison of empirically fit coefficients for single metal extraction experiments and the saturated multicomponent solvent extraction cascade.

	Single Metal Extraction			Saturated Multicomponent Cascade		
Element	K_i	α_1	α_2	K_i	α_1	α_2
La	2.77E-03	5.32	1.02	2.63E-05	-4.26	-5.2
Ce	3.72E-03	5.20	0.87	1.91E-05	1.59	-2.79
Pr	3.02E-01	5.50	2.20	5.01E-03	1.51	-0.81
Nd	1.03E-01	5.73	1.55	1.74E+01	2.91	2.4

For single metal extraction experiments, chloride concentration is the dominating parameter until the free TODGA concentration approaches zero, at which point the calculated distribution ratio approaches zero. K_i values are two orders of magnitude higher for the pseudo empirical fits; the fit also forces the impacts of pseudo chloride concentration and

pseudo free TODGA concentration to be reduced when compared to single metal extraction parameters. Interestingly, all pseudo coefficients are positive for Nd, which was readily extractable under the conditions in the counter-current test. La, being relatively non-extractable under these conditions, had stronger negative coefficients. Ce and Pr, both being on the cusp of extractability, had a similar dependence on pseudo chloride concentration with Ce exhibiting a higher dependence on free TODGA at saturation. A plot of experimental distribution ratios versus calculated distribution ratios using the pseudo-single metal approach is shown in Figure 7.16.

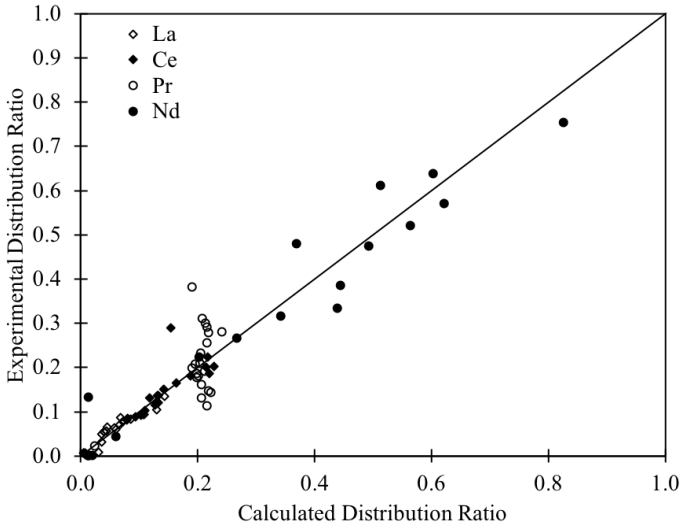

Figure 7.16: Comparison of experimental distribution ratios and calculated distribution ratios under saturated organic phase loading conditions using empirical "pseudo-single metal" correlation approach with mixer-settler equilibrium data.

The empirical fit appears to have reasonable agreement with experimental data, especially for less extractable La and Ce. There is some scatter associated with Nd distribution ratio calculations, and the pseudo approach essentially calculated a near-constant distribution ratio for Pr under all conditions. The calculated distribution ratios were used as inputs to the MATLAB mass balance model to see if the revised approach for saturation conditions improved agreement for stage-wise organic and aqueous REE concentration profiles. The revised calculations are plotted against experimental mixer-settler results for comparison; La and Ce organic and aqueous phase stage-wise concentration profiles are shown in Figure 7.17 with Pr and Nd organic and aqueous stage-wise concentration profiles being shown in Figure 7.18.

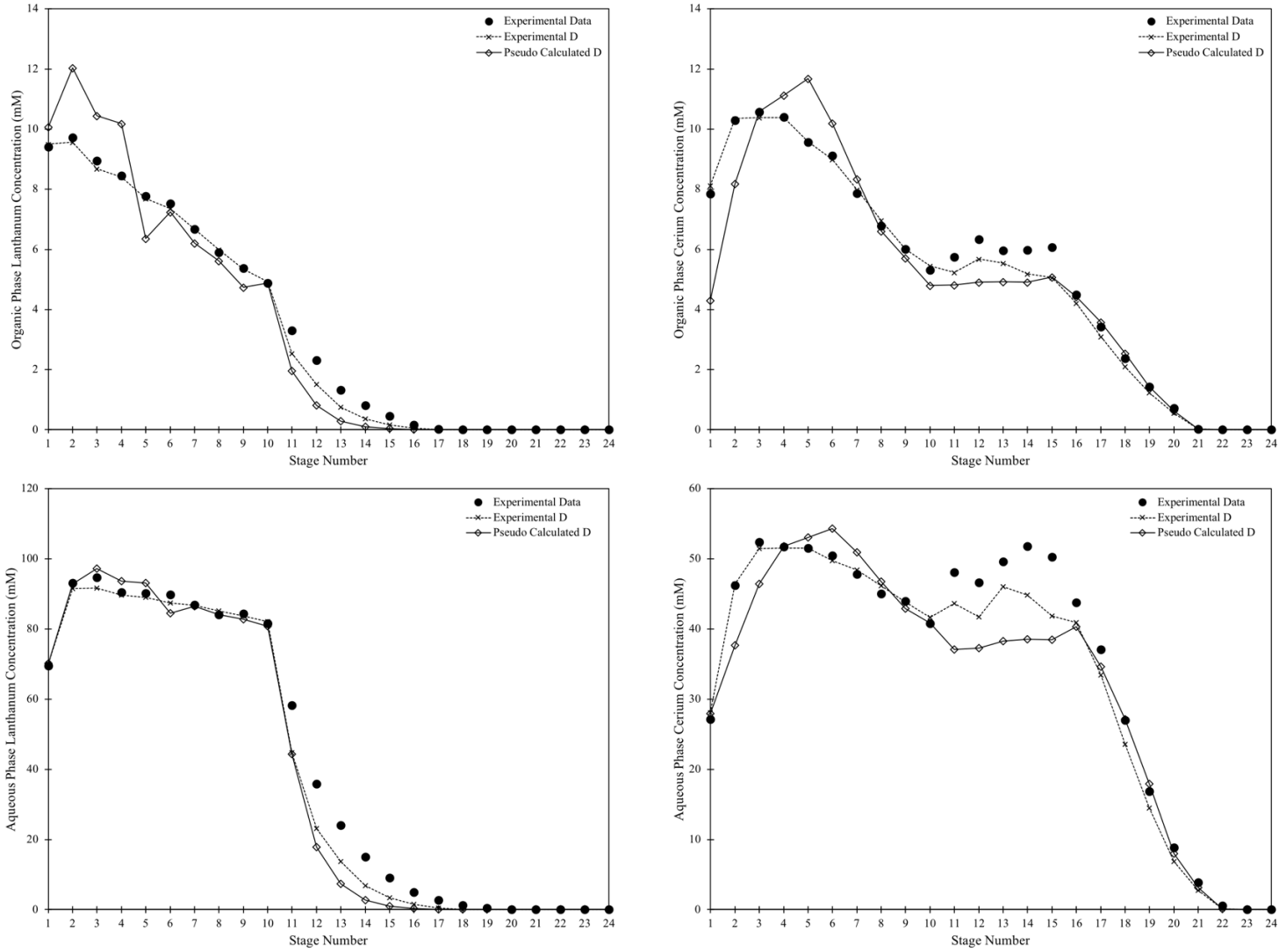

Figure 7.17: "Pseudo-single metal" MATLAB model comparisons for stage-wise organic and aqueous phase La and Ce concentration profiles.

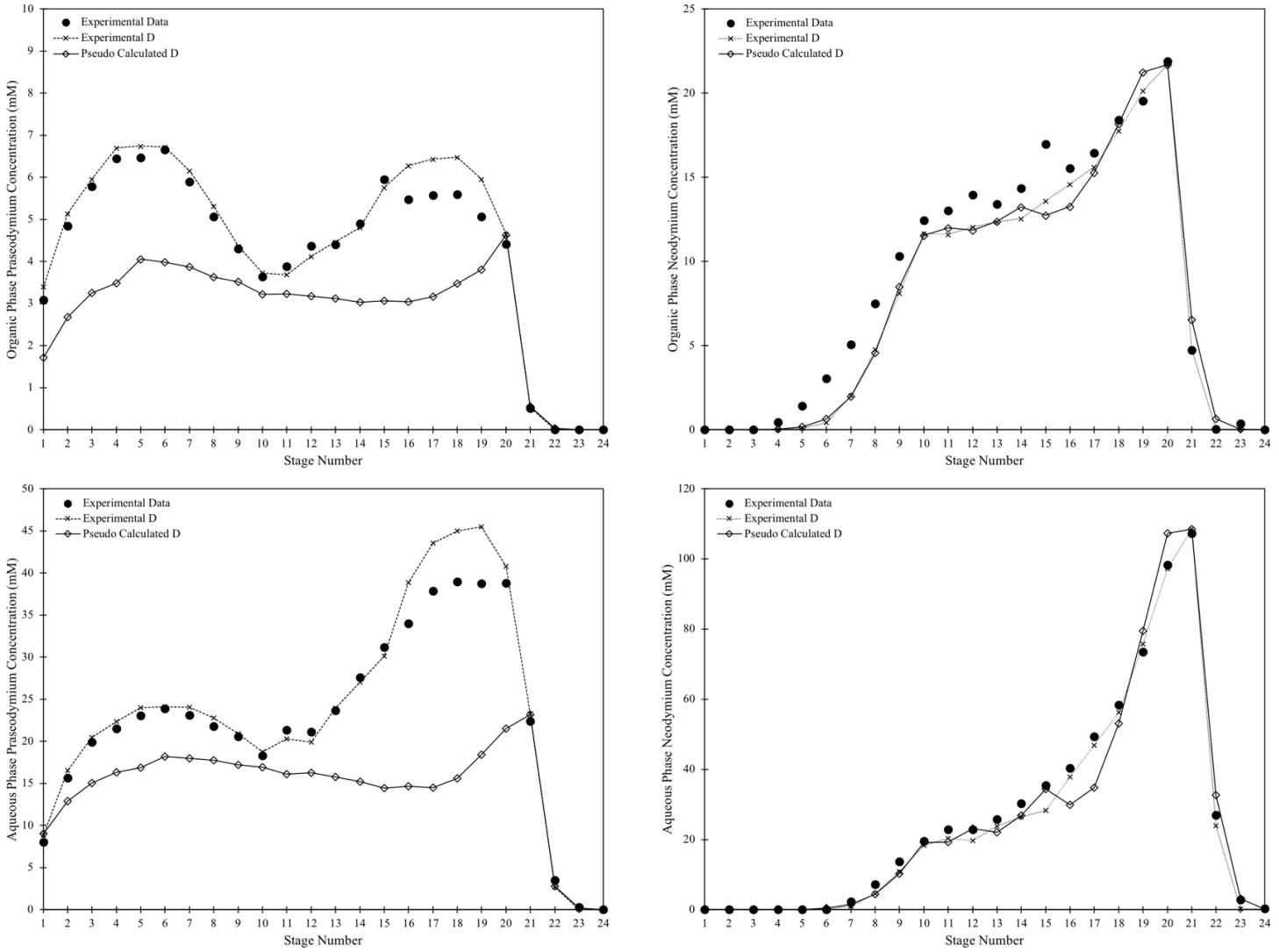

Figure 7.18: "Pseudo-single metal" MATLAB model comparisons for stage-wise organic and aqueous phase Pr and Nd concentration profiles.

The modified approach provides remarkable agreement with experimental results, perhaps with the exception of Pr. Pr is the minor component in the system, comprising only 9.2% of the total rare earth concentration in the feed. Therefore, larger errors in the distribution ratio calculation manifest as significant deviations in the predicted concentration profile. That being said, the revised modeling approach qualitatively captured Pr loading trends across the extract-scrub portion of the cascade, albeit with concentrations predicted to be nearly 50% lower than the experimentally observed result in some cases. The remaining REEs bring the predicted concentration profiles in line with the experimentally measured profiles, with some error associated with overestimating La extraction and underestimating Ce extraction in stage 1. This result is not unexpected, as the empirically determined correlations for distribution ratios were calculated from this data set, which does not exhibit dramatic deviations in distribution ratio values.

In summary, developing an accurate model to calculate equilibrium parameters in a complex multicomponent system remains a significant challenge, requiring experimental validation and empirical fitting of data to reasonably estimate extraction behavior. Single metal extraction data provides reasonable results for simple extraction systems but cannot capture the complexity of metal-metal exchange reactions presumed to take place during selective scrubbing to purify rare earths. Assuming constant distribution ratios may capture some generic extraction trends, but ultimately is not useful as a predictive modeling tool. The newly proposed “pseudo-single metal” fitting technique significantly improves the agreement between calculated equilibrium parameters and experimental results, but is limited as a predictive modeling tool because data is derived from counter-current mixer-settler testing and is valid only within the bounds of the chemical conditions at which the test was conducted. Extrapolation of distribution ratios will likely yield non-realistic results and is not recommended. Confirmation of counter-current performance using laboratory mixer-settlers is a critical component for the development of REE separation processes using TODGA.

CHAPTER 8: PERFORMANCE OF DIGLYCOLAMIDE EXTRACTANTS FOR RARE EARTH SEPARATIONS

Introduction

The culmination of batch equilibrium data, selective scrubbing experiments, counter-current solvent extraction modeling and simulation, and mixer-settler experiments presented herein suggest that TODGA may indeed be used in a continuous counter-current solvent extraction cascade for the separation and purification of rare earth elements, notably for the processing of light rare earth minerals such as bastnäsite. Careful process control of ionic strength, organic phase solvent loading conditions, and strip product recycle (with proper feed adjustment) may feasibly produce separated rare earths at high degrees of recovery and purity. As a neutral solvating extractant, TODGA does not require the use of saponification to control pH and achieve high degrees of rare earth recovery, and its improved separation factors suggest that separations may be achieved in a reduced number of stages as compared to phosphonic acids.

While the use of a selective electroneutral solvating extractant has several advantages over current state of the art solvent extraction processes using phosphonic acid, there are several drawbacks that at the time of this writing potentially limit its viability at an industrial scale. TODGA favors highly acidic conditions for trivalent lanthanide extraction from hydrochloric acid media. More generally, TODGA extracts trivalent lanthanides from solutions with a high chloride ionic strength. Stripping lanthanides from the organic phase is easily achieved by contacting the loaded organic phase with a dilute acid stream. This is precisely the opposite chemical conditions required for extraction and stripping of phosphonic acids such as PC88A, which extract well from dilute acid solutions and require highly acidic strip solutions to recover rare earths from the organic phase. This poses a potential drawback for TODGA-based solvent extraction circuits because the raffinate solutions from each circuit will contain molar quantities of HCl and/or NaCl, requiring significant reagent regeneration and recycle within the overall mining process flowsheet to maintain viable economics. Additionally, the extraction-scrub sections of a solvent extraction cascade contain significantly more stages than the strip section, which would remain inventoried with said high molarity solutions, potentially increasing corrosion and emission concerns. It is also

anticipated that operating the extraction and scrub under high chloride ionic strength conditions may actually increase reagent consumption within a solvent extraction circuit. Reagent requirements will be further explored in this chapter within the context of industrial separation processes, emphasizing chemical reagent requirements, equipment requirements, and process throughput.

Selective scrubbing techniques investigated in this work successfully demonstrated the ability to purify higher affinity lanthanides from co-extracted lanthanide impurities through a "crowding" net metal-metal exchange mechanism. However, practical application of this technique is further complicated due to the nature of the extraction-stripping ionic strength conditions discussed above. Strip product solutions generated from a TODGA counter-current solvent extraction process will contain purified rare earth chlorides (concentration is dependent upon the chosen strip section O/A ratio and the organic phase loading capacity) in a dilute HCl stream, nominally ranging from 0.1 to 0.5 M for the experiments conducted in this work. If such a solution were directly refluxed into the scrub section, the low ionic strength would strip all lanthanides from the organic phase and result in a complete loss of recovery and separation capability, potentially reaching a pinch point between the extraction and scrub sections. Therefore, feed adjustment of the portion of refluxed strip product is required prior to introduction to the scrub section. This step adds complexity due to the required holdup and process control of an adjustment scrub feed tank. Furthermore, the driving force for selective metal-metal exchange is reduced due to the dilution effect from feed adjustment, potentially requiring additional scrub stages to achieve target purity requirements. This may be compensated to a certain extent by stripping the solvent at a higher O/A ratio to further concentrate the strip product but has an upper bounding limit due to equipment limitations for operability at extreme phase ratios and acceptable entrainment in the system. Furthermore, as the stripping O/A ratio increases, the number of required strip stages may potentially increase due to reduced stripping efficiency.

TODGA concentrations explored in the present work were limited to 0.1 M extractant or less in mixer-settler testing for a specific reason that will be explored in this chapter: increasing TODGA concentration in the organic phase results in gelling, precipitation, and/or poor phase disengagement and is unsuitable for use in solvent extraction equipment under high

organic phase loading conditions. This severely limits the throughput capacity for a fixed mixer-settler equipment size as compared to the throughput that may be achieved using PC88A due to the limited organic phase loading capacity. This chapter contains qualitative (and semi-quantitative) assessments of experimental hydrodynamic performance of the TODGA-Ln(III)-HCl solvent system.

Despite the fact that TODGA has been exhaustively investigated for f-element separations chemistry for applications in the nuclear fuel cycle, there are no major industrial hydrometallurgical applications currently using DGA chemistry at scale. Consequently, synthesis and commercial availability of the extractant is typically limited to kilogram-scale quantities at a cost that would be significantly higher than commercially available extractants.

This chapter serves as a critical review to compare and contrast the innovative TODGA-Ln(III)-HCl solvent system with industrial separation processes with an emphasis on reagent requirements, equipment requirements, and process throughput.

Hydrodynamic Properties and Organic Phase Loading Capacity

Industrial rare earth solvent extraction circuits typically utilize PC88A concentrations ranging from 1-1.5 M extractant in a kerosene diluent [45]. Chemical manufacturing suppliers of phosphonic acid extractants advise that gelling will occur if the solvent is overloaded during extraction, recommending that solvent loading does not exceed 30% of the stoichiometric theoretical loading capacity [26]. Using a three to one metal:ligand extraction stoichiometry, this corresponds to a theoretical maximum organic phase loading capacity of 0.33 M for a 1 M PC88A solvent system. By comparison, assuming a three to one extraction stoichiometry for a 0.1 M TODGA solvent, the maximum theoretical loading capacity is 0.033 M. This is further limited by the experimental observation that TODGA saturates at approximately 80% theoretical loading assuming this stoichiometry, effectively limiting the organic phase loading capacity to 0.027 M. The implications of organic phase loading capacity ultimately manifest as a reduction in process throughput for a fixed mixer-settler size, or conversely a significantly larger mixer-settler size and solvent inventory to achieve the same degree of throughput as a phosphonic acid system in smaller mixer-settlers. Therefore, it is critical to achieve competitive loading capacities in the TODGA solvent

system to maintain process throughput and realize any potential reduction in capital and operating costs due to the apparent enhanced selectivity of TODGA for adjacent light rare earth separations.

The ability of a biphasic liquid-liquid system to separate by gravitational forces within industrial solvent extraction equipment depends on many complex variables, including phase densities, viscosities, and interfacial surface tension, ultimately dictating process throughput to avoid flooding conditions caused by inadequate phase separation in the settling section. Leonard outlined a procedure to calculate a dimensionless "dispersion number," N_{Di}, to characterize phase separation performance and subsequent suitability for scale-up in solvent extraction equipment [51]. The procedure utilizes measurements of the liquid-liquid interface and total liquid (organic plus aqueous) column height in a graduated cylinder. The two phases are mixed for a set period of time, and the period of time required for the dispersion band to completely coalesce is recorded. The dispersion number is then calculated according to Equation 43.

$$N_{Di} = \frac{1}{t_B}\sqrt{\frac{\Delta Z}{g}} \qquad \text{(Eq. 43)}$$

Where

t_B = Time for dispersion band to break, seconds

ΔZ = Initial thickness of the dispersion band, mm

g = Gravitational constant, m/s^2

Relative values of the dispersion number were utilized to assign a qualitative metric for performance, ranging from "excellent" to "unacceptable". Dispersion number metrics are defined in Table 8.1.

Table 8.1: Dispersion number metrics for solvent performance [51].

N_{Di} x 10^4	Rating
16	Excellent
8	Good
4	Fair
2	Poor
< 20	Unacceptable

These measurements may also be utilized to estimate the degree of entrainment of one phase in another as indicated by differences in the final liquid-liquid interface position after mixing and phase separation. Leonard presents a variety of dispersion number correlations for batch shakeouts and continuous operation in centrifugal contactors and mixer-settlers, as well as correlations for solvent systems that do not fully disengage, i.e. a dispersion band remains after phase disengagement. Due to the limited availability and quantity of DGA extractants, a modified dispersion number procedure was developed for the present work to evaluate solvent performance in small batch shakeout experiments. These experiments are largely qualitative in nature, especially due to the restricted sizes of the batch contacts due to extractant availability. However, calculation of the dispersion number and observation of the physical behavior during phase disengagement provides valuable insight into the suitability of a given solvent system for use in solvent extraction equipment.

Dispersion number measurements were calculated for the TODGA-Ln(III)-HCl solvent system using batch shakeout experiments. For comparison, commercially available DGA extractants N,N'-dimethyl-N,N'-dioctyl diglycolamide (DMDODGA) and N,N,N′,N′-tetra-2-ethylhexyl diglycolamide (T2EHDGA) were also evaluated under the same conditions as TODGA. Chemical structures of DMDODGA and T2EHDGA are shown in Figure 8.1.

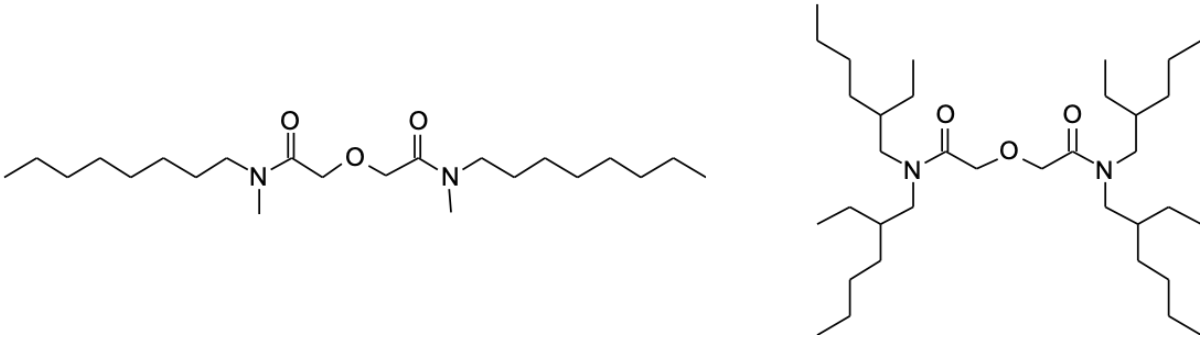

Figure 8.1: N,N'-dimethyl-N,N'-dioctyl diglycolamide (DMDODGA, left) and N,N,N′,N′-tetra-2-ethylhexyl diglycolamide (T2EHDGA, right).

Five batch shakeouts were conducted in series on the same organic phase solvent to calculate dispersion numbers under various conditions anticipated to be encountered in a solvent extraction cascade. Each batch shakeout was closely monitored during phase disengagement to identify issues with dispersion coalescence, entrainment, gelling or precipitation. Solvents were prepared at three different DGA concentrations for the dispersion tests to determine the

impact on solvent loading; DGA concentrations of 0.1, 0.3, and 0.5 M were tested. All solvents contained 5% Exxal-13 in Isopar-L diluent. Aqueous REE feed solutions were prepared in 3 M HCl for the dispersion tests containing 64% La, 5% Ce, 8% Pr, and 23% Nd (molar basis). The REE concentrations were prepared such that the molar ratio of DGA in the organic phase to total REE in the aqueous phase was 1.4. This corresponded to total REE feed concentrations of 73, 218, and 363 mM for the 0.1, 0.3, and 0.5 M DGA dispersion tests, respectively. All shakeouts were conducted at O/A = 1 using 5 mL per phase. First, the organic phase was contacted with 3 M HCl as a pre-equilibration contact. Second, the pre-equilibrated organic solvent was carried forward into a batch contact with the respective REE feed in 3 M HCl. Third, the REE-loaded organic solvent was carried forward to a second contact with fresh REE feed in 3 M HCl to ensure complete saturation loading, simulating the loading conditions expected to be encountered during both extraction and scrubbing in a counter-current cascade. Fourth, the REE-loaded organic solvent was carried forward into a contact with pH 1 HCl to simulate stripping conditions. Finally, the stripped solvent was contacted one last time with fresh pH 1 HCl, simulating conditions anticipated in the final strip stage prior to solvent recycle. The phases were allowed to separate by gravity and the time required for the phases to disperse was recorded to calculate the dispersion number. Samples were centrifuged and cleanly separated between each contact, carrying the organic phase continuously through all five contacts described above.

All contacts were shaken by hand for 30 seconds and immediately placed in a laboratory clamp stand to record the required time for the dispersion band to coalesce. Dispersion number results are presented in Table 8.2.

Table 8.2: Dispersion Numbers for TODGA, DMDODGA, and T2EHDGA under extraction and stripping conditions.

	Contact Description	0.1 M DGA N_{Di} x 10^4	0.3 M DGA N_{Di} x 10^4	0.5 M DGA N_{Di} x 10^4
TODGA	3 M HCl	11.4	7.7	5.8
	3 M HCl + REE	13.3	Gelling	Gelling
	3 M HCl + REE	13.3	N/A	N/A
	pH 1 HCl	15.4	N/A	N/A
	pH 1 HCl	3.5	N/A	N/A
DMDODGA	3 M HCl	1.9	3rd Phase	3rd Phase
	3 M HCl + REE	Gelling	Gelling	Gelling
	3 M HCl + REE	N/A	N/A	N/A
	pH 1 HCl	N/A	N/A	N/A
	pH 1 HCl	N/A	N/A	N/A
T2EHDGA	3 M HCl	16.5	13.1	7.6
	3 M HCl + REE	17.8	11.5	6.0
	3 M HCl + REE	19.2	10.7	10.7
	pH 1 HCl	10.5	11.5	12.6
	pH 1 HCl	11.0	9.6	7.2

T2EHDGA was the only extractant tested that achieved dispersion numbers that would be ranked as excellent or good under all anticipated chemical equilibrium conditions in a counter-current solvent extraction cascade. DMDODGA gelled upon contact with metal at all DGA concentrations tested and ranked unacceptable for HCl pre-equilibration at 0.1 M DGA. DMDODGA also formed a clean third phase at higher concentrations upon contact with 3 M HCl. Dispersion numbers for 0.1 M TODGA ranked in the good to excellent category for all contacts tested with the exception of the final pH 1 HCl contact. This is the reason 0.5 M HCl was chosen for stripping TODGA in the counter-current mixer-settler test described in Chapter 7. As previously discussed, stripping conditions with limited ionic strength in the aqueous phase typically exhibit significant amounts of entrainment in both phases as well as poor phase disengagement. Generally speaking, dispersion testing performance ranked T2EHDGA > TODGA > DMDODGA under the conditions tested. The results also indicate a general trend of degradation in phase separation performance with increasing DGA concentration. Photographs of the dispersion shakeout experiments are

shown in Appendix F; these photos provide useful qualitative insight regarding third phase formation, gelling, and entrainment that occurred during phase disengagement.

The next set of dispersion number experiments aimed to see if an increased concentration of Exxal-13 phase modifier would eliminate gelling and improve the phase separation performance as compared to the solvent systems that were tested at 5% Exxal-13 by volume. It is postulated that the gelling/precipitation experimentally observed contains insoluble metal:ligand complexes that precipitated out of the organic phase upon extraction. This assumption is reasonable, as the gels changed color from white/off-white to light purple when moved from fluorescent lighting to incandescent lighting or natural sunlight in the laboratory, indicating the presence of neodymium chloride [52]. The role of a phase modifier is to stabilize and maintain solubility of the extracted metal:ligand complex in the organic phase, therefore the dispersion tests were repeated using 30% by volume Exxal-13 in Isopar-L diluent. Four contacts were conducted for each solvent in this set of experiments; results are shown in Table 8.3.

Table 8.3: Dispersion Numbers for TODGA, DMDODGA, and T2EHDGA under extraction and stripping conditions. Solvents prepared with 30% v/v Exxal-13 in Isopar-L.

	Contact Description	0.1 M DGA N_{Di} x 10^4	0.3 M DGA N_{Di} x 10^4	0.5 M DGA N_{Di} x 10^4
TODGA	3 M HCl	18.5	21.8	9.5
	3 M HCl + REE	20.1	19.5	Gelling
	pH 1 HCl	18.5	21.8	N/A
	pH 1 HCl	15.8	20.6	N/A
DMDODGA	3 M HCl	5.9	4.2	N/A
	3 M HCl + REE	Gelling	Gelling	N/A
	pH 1 HCl	N/A	N/A	N/A
	pH 1 HCl	N/A	N/A	N/A
T2EHDGA	3 M HCl	11.7	11.0	11.0
	3 M HCl + REE	10.1	12.8	9.8
	pH 1 HCl	12.9	10.6	11.2
	pH 1 HCl	11.8	9.6	9.4

These results reveal that the 0.3 M TODGA system does not gel in the presence of additional phase modifier, yet still gels at the highest target loading of 0.5 M. DMDODGA still gelled

in all cases tested. T2EHDGA maintained dispersion numbers within the ranking of excellent and good under all conditions tested.

TODGA, DMDODGA, and T2EHDGA all have identical tridentate donor groups and chemical backbone structure responsible for coordinating trivalent lanthanides, with the only notable difference being the alkyl chain substituents branching off from the amide nitrogen atoms. Results from dispersion number measurements as a function of DGA concentration suggest that phase separation performance improves for molecular structures that contained branched aliphatic substituents. Long straight-chain alkyl substituents will function at low DGA concentrations (as validated for all TODGA mixer-settler experiments conducted in this work), but short chain alkyl substituents gel under all solvent extraction conditions tested in the presence of rare earth chloride solutions.

This poses an important question: is TODGA the most suitable DGA extractant for rare earth separations in light of the fact that the branched aliphatic substituents on T2EHDGA exhibited satisfactory phase separation performance under high loading conditions? Preliminary extraction experiments were conducted by colleagues at ORNL for TODGA, DMDODGA, and T2EHDGA to evaluate their selectivity trends across the lanthanide series at various HCl concentrations. Their experiments were conducted using 0.1 M DGA with 30% Exxal-13 in Isopar-L diluent. The aqueous feed contained 0.1 mM of each lanthanide, La-Lu + Y, for a total of 1.5 mM TREE. The aqueous feeds were prepared at 1, 3, and 5 M HCl. Contacts were all performed at O/A = 1, mixing for 1 hour on a rotary wheel mixer followed by centrifugation to separate the phases. The aqueous feed's low TREE concentration ensured that organic phase loading conditions were maintained well below saturation, allowing an objective comparison of extraction performance for each DGA. ORNL colleagues have graciously provided their experimental data for interpretation, results for La-Sm are shown in Figure 8.2.

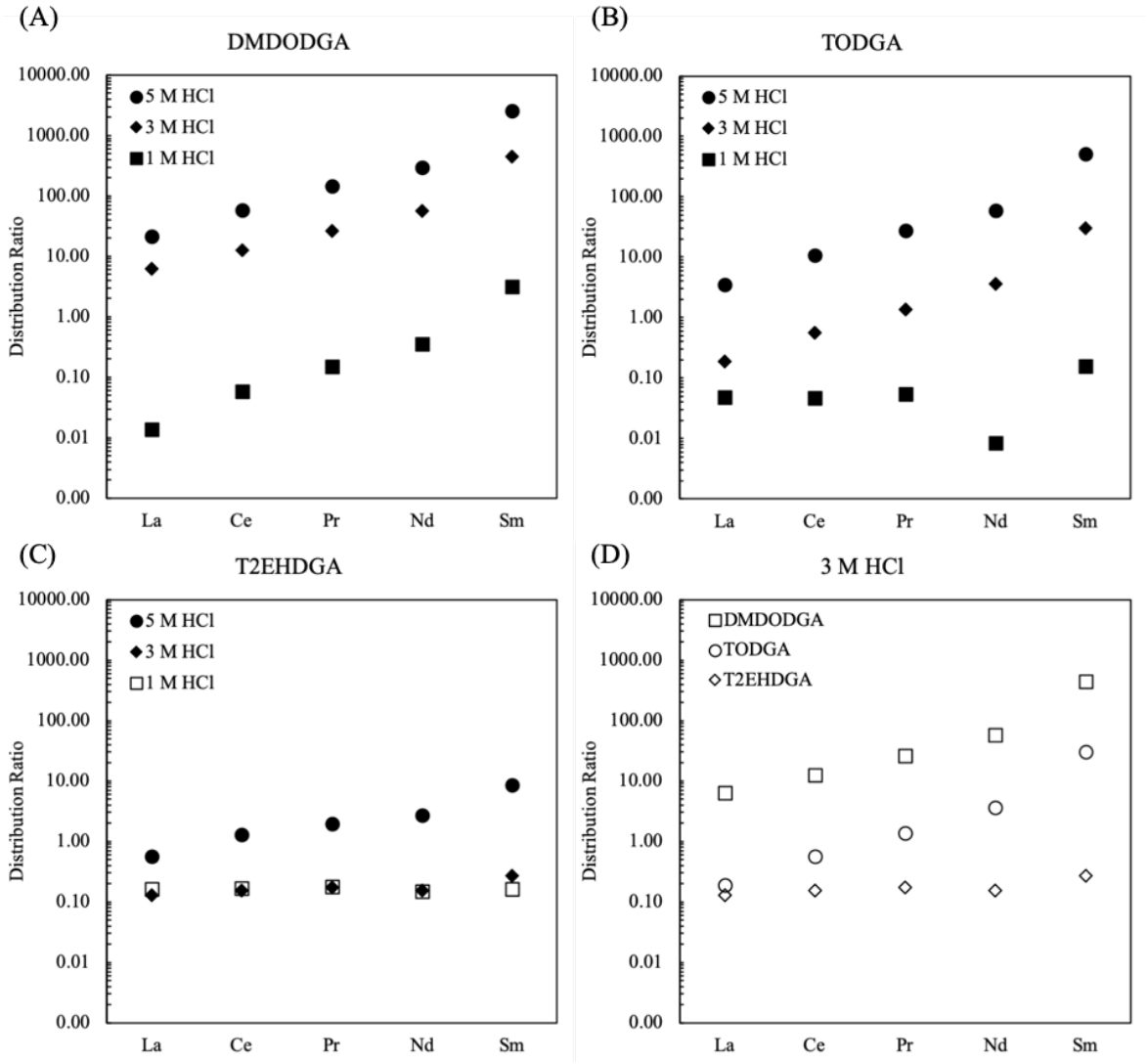

Figure 8.2: Extraction selectivity trends of La-Sm for TODGA, T2EHDGA, and DMDODGA. Experimental data courtesy of D. Brigham, ORNL.

There are several conclusions that can be drawn from the extraction equilibrium data in Figure 8.2. Comparison of Figures 8.2(A), 8.2(B), and 8.2(C) indicates that the overall extraction strength from the strongest to weakest extractant is ranked DMDODGA > TODGA > T2EHDGA. ORNL researchers did not observe gelling or precipitation with 0.1 M DMDODGA, presumably due to the extremely dilute loading conditions targeted in this study. Figure 8.2(D) plots 3M HCl extraction results for all three extractants; not only is T2EHDGA significantly weaker as an extractant but the slope of the distribution data trendline drops off dramatically. As previously discussed, the slope of the distribution ratio trendline represents the adjacent lanthanide separation factor, suggesting that T2EHDGA is

non-selective under these conditions for adjacent lanthanide separations. Calculated average adjacent lanthanide separation factors for Nd-La and Sm/Nd are shown in Table 8.4.

Table 8.4: Lanthanide separation factors for TODGA, DMDODGA, and T2EHDGA at varying HCl concentrations.

HCl (M)	TODGA	DMDODGA	T2EHDGA
5 M LREE $\beta_{Average}$	2.6	2.4	1.7
3 M LREE $\beta_{Average}$	2.7	2.1	1.1
1 M LREE $\beta_{Average}$	0.8	3.1	1.0
5 M $\beta_{Sm/Nd}$	8.7	8.8	3.1
3 M $\beta_{Sm/Nd}$	8.3	7.9	1.7
1 M $\beta_{Sm/Nd}$	18.9	9.0	1.1

Separation factors confirm the selectivity trend for each extractant. TODGA has the highest average separation factor among light rare earths, followed closely by DMDODGA. TODGA loses light REE selectivity at 1 M HCl, which is in good agreement with the stripping equilibrium data presented in Chapter 6. Both TODGA and DMDODGA maintain excellent separation factors between Nd and Sm under all conditions tested. Figure 8.2(A) and the DMDODGA separation factors in Table 8.4 indicate that reducing HCl concentration down to 1 M does not significantly alter separation factors as it does with TODGA. T2EHDGA is essentially non-selective for adjacent lanthanides under all conditions tested, with 5 M HCl being the only acid concentration with measurable distribution ratios greater than unity. T2EHDGA's observed selectivity trends are in agreement with literature data, where its primary use has been as a group lanthanide extractant from nitric acid media relevant to nuclear fuel reprocessing [31, 32]. Lanthanide extraction from nitric acid using DGAs is significantly stronger than extraction from hydrochloric acid. Therefore, T2EHDGA may be a suitable extractant if the objective is group lanthanide separations, such as the separation of fission product lanthanides from trivalent minor actinides such as americium and curium.

Revisiting dispersion number experiments within the added context of DGA selectivity, a unique trend begins to emerge for DGAs. DMDODGA is the strongest extractant of the three, yet gels under all REE loading conditions tested. TODGA is still a relatively strong extractant and does not gel under high loading conditions, so long as the TODGA

concentration is sufficiently low. Addition of phase modifier allows slightly higher TODGA concentrations before gelling is observed. T2EHDGA does not gel under any condition tested but is a very weak extractant that is essentially non-selective for the application of adjacent lanthanide separations. Due to the low selectivity and extraction strength of T2EHDGA, it is also possible that the solvent was not fully loaded with REEs during dispersion number testing, which may influence the observed phase separation behavior and avoidance of gelling. The following conclusions are postulated about DGA behavior:

1) DGAs with short alkyl chain substituents are the strongest extractants.
2) Increasing DGA alkyl chain length reduces the overall extraction strength but retains lanthanide selectivity.
3) Branching of the DGA alkyl chain prevents gelling and improves phase separation but comes at the cost of a loss of adjacent lanthanide selectivity.

There is a precedent set in literature to corroborate these conclusions. Sasaki et. al. reported the effects of alkyl substituents on DGA lanthanide extraction from nitric acid, concluding that 1) increasing the alkyl chain length increased the organic phase loading capacity, 2) DGAs with the shortest alkyl chains exhibited the highest distribution ratios, and 3) branched chain DGAs such as T2EHDGA exhibit both lower distribution ratios and organic phase loading capacity as compared to TODGA [53]. Sasaki's work targeted 3M nitric acid specifically as it relates to minor actinide recovery from acidic high-level waste associated with a PUREX-type raffinate in nuclear fuel reprocessing, which is a fundamentally different separation objective when compared to separating adjacent lanthanides in hydrochloric acid media. The conclusions of Sasaki are specific to loading capacities achieved in 3 M nitric acid. Sengupta et. al. further corroborated these findings, reporting that increasing the alkyl chain length decreases extraction efficiency [54]. Their work postulated that lipophilicity of the DGAs increases as the length of the alkyl chain substituents increases, adversely impacting the ligand's ability to approach the organic-aqueous interface for metal complexation. Furthermore, they postulated that T2EHDGA's 2-ethylhexyl substituents causes significant steric crowding around the binding site, suppressing distribution ratios.

The concept of steric hindrance has been further elucidated by others using a blend of liquid-liquid extraction experiments, EXAFS spectroscopy, density functional theory calculations, and classical molecular dynamics simulations [55, 11, 36]. As previously discussed in Chapter 3, TODGA acts as a tridentate donor, binding trivalent lanthanides at a 3:1 ligand:metal stoichiometry. This creates "clefts" between the DGA alkyl group substituents where counter-anions are located in the outer coordination sphere [36]. Baldwin et. al. further demonstrated that lanthanide extraction from nitric acid media also extracts water which may be bound via hydrogen bonding to the counter anion nitrate groups [55]. Therefore, it may be rationalized that extraction limitations encountered in the present hydrochloric acid system with T2EHDGA are likely due to steric hindrance around the binding site. Branching so close to the binding site interferes with the accommodation of chloride counter-anions, phase modifier molecules that help solubilize the metal:ligand complex, and any co-extracted water. This could potentially be alleviated by moving branching further away from the binding site, reducing steric hindrance to boost extraction efficiency while maintaining suitable phase disengagement behavior (this topic will be discussed in additional detail in Chapter 9).

A final consideration relative to phase disengagement performance is the tendency for DGAs to self-aggregate or form reverse micelles under certain extraction conditions. Nave et. al. used a combination of liquid-liquid extraction experiments, interfacial tensiometry, small angle X-ray scattering (SAXS), and small-angle neutron scattering (SANS) to demonstrate that TODGA aggregates into spherical reverse micelles in dilute nitric acid, with the micelle consisting of a polar core with extracted water and ions in the center [56]. Their work confirmed that four TODGA molecules aggregate around extracted water and nitric acid, with van der Waals forces between the aggregated micelles being responsible for third phase formation as the nitric acid concentration is increased. They also concluded that the presence of hydrogen bond networks induced by phase modifiers aid in quenching dispersion forces between aggregate cores. Jensen et. al. identified a critical micelle acidity of 0.7 M, noting that TODGA exists primarily as monomers and dimers at low acidity, yet aggregate into the reverse micelle TODGA tetramer at the critical micelle acidity. Their work demonstrated that this is the dominant TODGA species in the organic phase at acidities exceeding 1 M nitric acid. Curiously, their work also showed that the presence of trivalent Nd in extraction

maintained a stoichiometry of four TODGA monomers to one Nd ion. The $Nd(TODGA)_4$ complex was observed across a wide range of acidities, with metal-bearing and metal-free TODGA tetramers both existing at highly acidic nitric acid conditions [48]. Aggregation behavior provides a possible rationale for the gelling/precipitation behavior observed under high loading conditions in hydrochloric acid, as the formation of aggregate complexed metal species are less likely to remain soluble in the organic phase. This suggests that the presence of additional phase modifier aids to increase TODGA's organic phase loading capacity before gelling occurs, as Exxal-13 contains a mixture of branched aliphatic alcohols capable of providing the requisite hydrogen bonding network to disrupt interactions among aggregated TODGA species in the organic phase.

Reagent Requirements

As previously discussed, industrial rare earth separation processes and the detailed processing parameters (number of stages, O/A phase ratios, throughput, equipment sizing) are typically proprietary and treated as closely guarded as trade secrets with little to no published information available in literature. Zhang et. al. has published summaries of parameters for overall processing schemes [45], but this does not provide the requisite detailed information to make a like-for-like comparison with DGA extractants. Therefore, known processing parameters for the two extractants will be qualitatively compared with discussion surrounding the reagent requirements for each system. Table 8.5 shows a summary of process parameters for PC88A and TODGA required for extraction and stripping of PrNd.

Table 8.5: Process parameters for PC88A, 0.1 M TODGA, and 0.5 M generic DGA.

	1.5 M PC88A in kerosene[1]	0.1 M TODGA/30% Exxal-13/Isopar-L[4]	0.5 M DGA/30% Exxal-13/Isopar-L[4]
Aqueous Feed TREO	1.5 M[1]	0.1 M[4]	1.5 M[4]
Aqueous Feed Acidity	pH 3-4[1]	3 M HCl[4]	3 M HCl[4]
Raffinate Acidity	pH 1 HCl[3]	3 M HCl[4]	3 M HCl[4]
Scrub Section Acidity	pH 1 HCl[3]	3 M HCl[4]	3 M HCl[4]
Strip Feed Required	0.73 M HCl[2]	pH 1 HCl[4]	pH 1 HCl[4]
Saponification Required	Yes	No	No
Organic Phase Loading Capacity	30%[2]	80%[4]	80%[4]
Solvent Required (L)*	39.6	222.9	44.6

**Basis: liters of solvent required to extract 1 kg of Nd2O3, calculated using loading capacity and ligand concentration*

1: [45]

2: [26]

3: [39]

4: present work

First, the most important comparison to evaluate is the limitation in organic phase loading capacity. A generic basis for liters of solvent required to extract 1 kg of Nd_2O_3 was calculated to highlight this stark difference based on the maximum loading capacity and ligand concentration. The 0.1 M TODGA system requires over five times the volume of solvent for this extraction basis as compared to PC88A. This has dramatic implications for the design of a solvent extraction cascade: for a fixed mixer-settler size, the PC88A system can achieve throughputs over five times higher than that obtainable using 0.1 M TODGA. Conversely, the solvent inventory and equipment sizing would be significantly larger for 0.1 M TODGA than PC88A to achieve the same process throughput. If a novel modified DGA could achieve a ligand concentration of 0.5 M without gelling and simultaneously demonstrating favorable phase disengagement behavior, this would provide comparable throughput to the PC88A system. Extractant concentration limitations can be mitigated to a certain extent through the use of high O/A phase ratios, but PC88A circuits are typically designed to operate at high O/A phase ratios to minimize solvent inventory, reduce capital equipment costs, and minimize downstream processing costs. There is likely little to no practical margin using O/A ratios for such a dramatic difference in ligand concentration for 0.1 M TODGA.

As previously discussed, electroneutral solvating ligands and acidic cation exchange ligands extract and strip under exactly opposite chemical conditions. TODGA extraction efficiency increases with increasing chloride salting strength, either through the use of HCl or NaCl. The use of NaCl may be limited to specific separation circuits due to its solubility limit, which is further limited due to the common-ion effect in the presence of highly concentrated rare earth chloride salts [57]. Lanthanides are easily stripped from the solvent through contact with a dilute acid. Phosphonic acids, however, extract from dilute HCl and strip under highly acidic conditions. The raffinate and strip product solutions are always product streams in rare earth processing, therefore the chemical reagent impact of using electroneutral ligands versus phosphonic acids is dependent upon the process configuration. For example, consider the separation cascades required for bastnäsite processing shown in Figure 2.7. The raffinate from a light-heavy rare earth separation would contain approximately 2-2.5 M HCl along with light rare earths La-Nd. If this raffinate were directly fed into a light rare earth separation circuit, additional feed adjustment would be required to boost the ionic strength such that extractability of Nd and Pr are favorable. The present work indicates this separation takes place at approximately 3 M HCl, so the acid concentration must be increased by 0.5-1 M. Additional HCl must also be consumed for feed adjustment of the portion of refluxed strip product prior to its use as a scrub feed to prevent the complete stripping of lanthanides from the organic phase. If the strip product is 0.1 M HCl, concentrated acid or salt must be added to reach 3 M for the light rare earth separation. By contrast, phosphonic acids utilize saponification to mitigate the release of proton during extraction, effectively performing an overall net neutralization of acid to facilitate the recovery of rare earths into the organic phase. The raffinate for light-heavy rare earth separations is variable depending on actual circuit design, but it is reasonable to assume the raffinate acid concentration is approximately pH 1 HCl. Adjustment of this raffinate prior to introduction into an PrNd separations cascade would require significantly less acid than feed adjustments for TODGA. The strip product is typically optimized in phosphonic acid circuits for direct recycle into the scrub section and does not require further feed adjustment. As previously discussed, TODGA does not require consumption of base for saponification, providing a caustic reagent savings compared to PC88A.

Downstream processing of separated rare earth chloride streams also plays a significant role when considering the composition of the raffinate and strip product solutions. Typically, rare earths are precipitated from aqueous solution using sodium carbonate or oxalic acid, followed by calcination to produce rare earth oxides. Significantly larger amounts of sodium carbonate would be required to neutralize highly acidic rare earth streams associated with TODGA before precipitation could occur. Alternately, precipitation with oxalic acid is optimized when the starting pH and rare earth concentrations are as high as possible because an HCl mother liquor is produced as rare earth oxalates are formed [58]. Recovery and precipitation efficiency are anticipated to decrease if the starting solutions are highly acidic. Finally, in many instances modern mining practices are being driven toward a "zero liquid waste" discharge philosophy for environmental stewardship and increasing regulatory requirements [59]. Optimized closed loop recycle streams are utilized whenever practical, and process water effluents may require regeneration of chemical reagents and further treatment/purification to permit the discharge of treated water to the environment. The use of TODGA is anticipated to require recovery and recycle of acidic or salt-bearing effluent streams within the mine if it is to maintain any competitive advantage over PC88A. Many sectors in the mining industry are being proactive to implement this philosophy in anticipation of future stresses on the environment at the cost of higher capital and operating costs. However, margins in the rare earth market are razor-thin, potentially limiting additional capital and operating costs as required by a new solvent system for rare earth separations.

Qualitative analysis of reagent consumption and process throughput would be highly dependent upon the overall mining process flowsheet configuration and does not account for many unit operations required for rare earth separations such as impurity removal, cerium management, and downstream processing. Additionally, integration of an alternative separation process would require optimization across the mine site to include upstream beneficiation and leaching, as well as effluent process water management. Furthermore, while TODGA is a commercially available product from various vendors, it is currently only available at the kg-scale level. By comparison, Zhang reports that a light rare earth separations cascade requires 214 cubic meters of 1.5 M PC88A in kerosene diluent per 1000 tons of rare earth produced annually [45], or just over 56,000 gallons of solvent per 1000 tons

REO! While economies of scale would theoretically reduce solvent costs if ever implemented in an industrial setting, the technical maturation and availability of TODGA are nowhere near the production requirements for even just a small piloting facility. This is anticipated to be exacerbated if a novel DGA is discovered that can achieve specified metrics for selectivity, loading capacity, and hydrodynamic performance. Overall conclusions regarding reagent consumption, throughput, and solvent choice are summarized below:

1) TODGA does not consume base because saponification is not required.
2) TODGA will likely increase acid consumption when compared to PC88A due to high ionic strength requirements for extraction and scrubbing.
3) TODGA requires an additional feed adjustment step to enable selective scrubbing with refluxed strip product solutions.
4) The organic phase loading capacity of 0.1 M TODGA is not practical for industrial applications because of throughput limitations. DGA concentrations would need to approach 0.5 M while retaining a high loading capacity to achieve comparable throughput to PC88A solvent systems.
5) The use of an electroneutral solvating extractant for separations will have significant implications on both upstream and downstream unit operations.
6) DGA extractants are not commercially available at scales required for industrial rare earth separations. Risk-adverse stakeholders in the rare earth industry would likely be resistant to dramatic modifications to processing technologies in such a volatile market for incremental process improvements.

Stage Requirements

Accurate assessment of stage requirements for PC88A and TODGA solvent systems is highly subjective for two primary reasons. First, stage requirements for specific separations and the associated processing parameters are not available in published literature. Second, the

disparity in organic phase extractant concentrations for PC88A and TODGA would call into question the validity of any quantitative comparison, especially because rare earth chloride concentrations and solvent TODGA concentrations are an order of magnitude lower for TODGA-based solvent extraction processes.

While a direct quantitative comparison cannot be made for equilibrium stage requirements, the impact of enhanced separation factors can be demonstrated using the counter-current cascade model and equilibrium data from the light rare earth separation mixer-settler experiment discussed in Chapter 7. For example, consider a hypothetical scenario where Ce distribution ratios are scaled by a factor of 0.75 and Pr distribution ratios are scaled by a factor of 2 in the 24-stage counter-current cascade. This increases the average Pr/Ce separation factor in the extraction section from 1.2 to 3.3. Results from the MATLAB mass balance model using these modified hypothetical distribution ratios indicate that the purity of the PrNd strip product solution would increase from 97.1% to 99.7%, and the overall PrNd recovery increases from 86% to 96% in the same 24-stage configuration. While definitive conclusions cannot be made regarding TODGA equilibrium stage requirements as compared to PC88A separation processes, it is reasonable to say that a stage reduction is anticipated due to the enhanced adjacent light rare earth separation factors observed in the TODGA-Ln(III)-HCl solvent system.

CHAPTER 9: CONCLUSIONS

Conclusions

Separation and purification of REEs is often regarded as one of the most significant technical and environmental challenges in the REE supply chain to produce manufactured components used in clean energy and national security applications. Industrial processes primarily utilize counter-current solvent extraction for separation and purification of individual REE; these processes are notorious for excessive equilibrium stage requirements, chemical reagent consumption, and environmental impacts. Novel extractant chemistries that reduce capital and operating costs for a REE separations plant will help enable a secure and resilient domestic REE supply chain amid global concerns regarding materials criticality and supply chain disruption. Recent advances in diglycolamide (DGA) extraction chemistry have shown that this family of extractants exhibit unique selectivity trends across the lanthanide series that may be exploited for REE separations, thereby reducing equilibrium stage requirements in a solvent extraction cascade and reducing chemical reagent consumption through elimination of saponification.

The methodology developed in this work marks the first use of the electroneutral solvating extractant N,N,N',N'-Tetraoctyl Diglycolamide (TODGA) and its enhanced light atomic weight rare earth selectivity in hydrochloric acid media to separate rare earths from each other using a selective scrubbing technique that achieves high degrees of recovery and purity in a continuous counter-current solvent extraction cascade. TODGA organic phase loading conditions required to facilitate selective scrubbing for separating adjacent lanthanides were identified; experimental results indicate that TODGA loads REEs with minimal selectivity and will undergo selective scrubbing via metal-metal exchange once the organic phase is completely saturated with extracted REE. Selective scrubbing is performed through reflux of purified strip product solution in the solvent extraction cascade; TODGA separation processes require a feed adjustment step prior to reflux to raise the ionic strength and retain REEs in the organic phase.

Equilibrium data for the TODGA-Ln(III)-HCl extraction system was measured for single-metal REE extraction experiments at various REE and HCl feed concentrations. Empirical multidimensional surface fitting of the equilibrium data was used to generate expressions to

calculate distribution ratios as a function of equilibrium aqueous phase chloride ionic strength and organic phase free TODGA concentration. These correlations, coupled with batch counter-current simulation experiments and process modeling, were used to design a counter-current solvent extraction process to produce purified didymium (75% Nd, 25% Pr) from a mixed light rare earth feed (La, Ce, Pr, Nd) using TODGA. Purified didymium oxide is an important precursor material for the production of rare earth permanent magnets; this separation is of significant industrial importance to produce critical REEs for clean energy applications. Experimental results from mixer-settler testing revealed that the single metal distribution ratio expressions do not accurately predict lanthanide partitioning between the aqueous and organic phase under saturated loading conditions. An alternative empirical fitting technique, colloquially referred to as a "pseudo single-metal" concept, utilized equilibrium data from the mixer-settler cascade operating under saturated loading conditions to develop new empirical distribution ratio expressions that account for each REE's contribution to the solvent composition and ionic strength. This technique dramatically improved mass balance modeling for the counter-current cascade, but caution should be exercised as the empirical fit is only valid for the specified chemistry conditions in the solvent extraction cascade.

The organic phase solvent requires extractant concentrations upwards of 0.5 M DGA to achieve competitive loading capacity, and by extension process throughput, when compared to industry standard phosphonic acids. It was determined that TODGA gels under high REE solvent loading conditions and cannot achieve requisite REE loading capacities. A structure-property relationship has been discovered under high loading conditions in HCl media for the family of DGA extractants based upon the molecule's alkyl chain substituents in collaboration with Oak Ridge National Laboratory (ORNL). Structure-property relationship suggests that DGAs with short alkyl chain substituents are the strongest extractants and have high selectivity, but easily gel under high loading conditions. Increasing DGA alkyl chain length reduces the overall extraction strength but retains favorable REE selectivity. Branching of the DGA alkyl chain prevents gelling and poor phase separation but comes at the cost of a loss of adjacent lanthanide selectivity; evidence in literature indicates that the loss of selectivity is due to steric hindrance caused by alkyl substituent branching in close proximity to the coordination environment during metal:ligand complexation.

Definitive conclusions regarding chemical reagent consumption and equilibrium stage requirements for TODGA solvent extraction processes as compared to industry standard phosphonic acid separation processes have not been determined at the time of this writing. The low TODGA organic phase loading capacity requires significantly reduced REE feed concentrations to the separation cascade; therefore, a direct quantitative comparison with concentrated PC88A cascade operations does not provide meaningful insight into DGA performance. However, semi-qualitative assessments were conducted, concluding that caustic consumption is eliminated for the neutral DGA solvent system, but the high ionic strength required for extraction and scrub is anticipated to require reagent recycle or regeneration within the overarching mineral processing flowsheet. It was also concluded that TODGA's improved light REE separation factors will likely achieve separations in a reduced number of equilibrium stages, but the stage reduction is likely not as optimistic as originally hypothesized due to reduced selectivity under saturated loading conditions and dilution effects as a result of scrub feed ionic strength adjustment prior to reflux.

Future Outlook and Ongoing Research Efforts

TODGA's applicability for industrial rare earth separations based on counter-current solvent extraction processes may be limited, primarily due to the low organic phase loading capacity. However, DGA structure/property relationships identified in this work have spawned a new direction for research and development efforts for a new class of modified DGA extractants. Ongoing research efforts are focusing on the synthesis and testing of novel modified DGA extractants in collaboration with ORNL. The rationale for these research efforts stemmed from conclusions identified in this dissertation surrounding organic phase loading conditions and operability in industrial solvent extraction equipment. Results from Chapter 6 revealed that TODGA will essentially co-extract non-selectively until the organic phase loading capacity is reached, at which point selective metal-metal exchange scrubbing will occur to achieve high degrees of purity and recovery in a counter-current solvent extraction cascade. Structure-property relationships identified in this research indicate that branched aliphatic substituents help stabilize the extracted metal:ligand complex but must be tailored such that adjacent light lanthanide selectivity is not compromised, especially under saturated loading conditions. Consequently, ongoing research is focusing on branched aliphatic substituents

with branching that is further removed from the binding site. Such a chemical structure is postulated to have minimal steric interference with the binding functional groups and outer coordination sphere that must accommodate counter-anions, co-extracted water, and phase modifiers. An entire suite of modified DGAs is under investigation to elucidate structure-property relationships, ultimately aiming to discover a novel DGA ligand that exhibits enhanced light rare earth selectivity, robust extraction strength at varying chloride concentrations, competitive loading capacity, and hydrodynamic properties suitable for use in solvent extraction equipment.

Modified DGAs that satisfy this set of criteria will be benchmarked under relevant process conditions for light rare earth separations. This includes development of distribution ratio expressions and their integration with a counter-current mass balance model to predict cascade performance. As discussed in Chapter 7, predicting equilibrium partitioning behavior for a complex multicomponent mixture operating at saturated organic phase loading conditions is extremely challenging and will likely require additional experimentation for process-specific validation. The process outlined in this research provides a framework for the collection of laboratory equilibrium data, as well as modeling and simulation methods to determine stage requirements and process configurations to achieve high degrees of product recovery and purity. Finally, mixer-settler experiments are utilized not only to confirm predicted separation performance but also to provide a rigorous basis for comparison to existing state-of-the-art solvent extraction processes through the evaluation of stage requirements, chemical reagent consumption, and implications on process water effluents.

REFERENCES

[1] J. Gambogi, "Mineral Commodity Summaries," U.S. Geological Survey, January 2020.

[2] J. Gambogi, "Mineral Commodity Summaries," U.S. Geological Survey, 2013.

[3] D. Bauer, "U.S. Department of Energy Critical Materials Strategy," U.S. Department of Energy, 2011.

[4] World Trade Organization, *China- Measures Related to the Exportation of Rare Earths, Tungsten, and Molybdenum,* 2014.

[5] J. W. Miller, "Molycorp Files for Bankruptcy Protection," MarketWatch, 25 June 2015. [Online]. Available: https://www.marketwatch.com/story/molycorp-files-for-bankruptcy-protection-2015-06-25-71032419.

[6] F. Els, "Chinese Rare Earth Giant Born," Mining.com, 16 December 2014. [Online]. Available: https://www.mining.com/chinese-rare-earth-giant-born-62354/.

[7] D. J. Trump, *Presidential Executive Order on a Federal Strategy to Ensure Secure and Reliable Supplies of Critical Minerals,* 2017.

[8] D. J. Trump, *Presidential Determination Pursuant to Section 303 of the Defense Production Act of 1950, as amended,* 2019.

[9] C. K. Gupta and N. Krishnamurthy, Extractive Metallurgy of Rare Earths, CRC Press, 2005.

[10] Critical Materials Institute, "About CMI," December 2013. [Online]. Available: http://cmi.ameslab.gov.

[11] R. J. Ellis, D. M. Brigham, L. Delmau, A. S. Ivanov, N. J. Williams, M. N. Vo, B. Reinhart, B. A. Moyer and V. S. Bryantsev, ""Straining" to Separate the Rare Earths: How the Lanthanide Contraction Impacts Chelation by Diglycolamide Ligands," *Inorganic Chemistry,* pp. 1152-1160, 2016.

[12] M. Okada, S. Sugimoto, C. Ishizaka, T. Tanaka and M. Homma, "Didymium-Fe-B Sintered Permanent Magnets," *Journal of Applied Physics,* pp. 4146-4148, 1985.

[13] J. Zhang, B. Zhao and B. Schreiner, Separation Hydrometallurgy of Rare Earth Elements, Switzerland: Springer International Publishing, 2016.

[14] Rare Element Resources, "Rare Element Resources," 2016. [Online]. Available: http://www.rareelementresources.com/.

[15] Ucore Rare Metals, "Ucore Rare Metals," 2015. [Online]. Available: https://ucore.com/.

[16] United States Department of Energy, "Report on Rare Earth Elements from Coal and Coal Byproducts," United States Department of Energy, Washington, D.C., 2017.

[17] S. Wu, L. Wang, L. Zhao, P. Zhang, H. El-Shall, B. Moudgil, X. Huang and L. Zhang, "Recovery of rare earth elements from phosphate rock by hydrometallurgical processes- A critical review," *Chemical Engineering Journal,* no. 335, pp. 774-800, 2018.

[18] MP Materials, "MP Materials," 2019. [Online]. Available: https://mpmaterials.com/about/.

[19] N. V. Thakur, "Separation of Rare Earths by Solvent Extraction," *Mineral Processing and Extractive Metallurgy Review,* vol. 21, no. 1, pp. 277-306, 2000.

[20] J. D. Law and T. A. Todd, "Liquid-Liquid Extraction Equipment," Idaho National Laboratory, 2008.

[21] K. L. Lyon, "Separation of Adjacent Rare Earth Elements Using Solvent Extraction," University of Idaho, Moscow, ID, 2016.

[22] F. A. Cotton and G. Wilkinson, Advanced Inorganic Chemistry- A Comprehensive Text, 3rd Edition, John Wiley and Sons, 1972.

[23] F. Xie, T. A. Zhang, D. Dreisinger and F. Doyle, "A Critical Review on Solvent Extraction of Rare Earths from Aqueous Solutions," *Minerals Engineering,* vol. 56, pp. 10-28, 2014.

[24] M. S. Lee, J. Y. Lee, J. S. Kim and G. S. Lee, "Solvent Extraction of Neodymium Ions from Hydrochloric Acid Solution Using PC88A and Saponified PC88A," *Separation and Purification Technology,* vol. 46, pp. 72-78, 2005.

[25] M. D. Soderstrom, T. McCallum, B. Jakovljevic and A. J. Quilodrán, "Solvent Extraction of Rare Earth Elements Using Cyanex® 572," in *Conference of Metallurgists Proceedings*, Vancouver, B.C., 2014.

[26] Cytec Industries, Inc., *Cyanex® 572 Solvent Extraction Reagent Product Data Sheet,* Cytec Industries, Inc., 2013.

[27] L. Chunsheng, W. Sheng, C. Fuxiang, W. Songling, L. Yan, Z. Bo and Y. Chunhua, "Clean Separation Technologies of Rare Earth Resources in China," *Journal of Rare Earths,* pp. 331-336, 2013.

[28] Prometia, "Criteria, Limits, and Advantages of Rare Earths Recycling," 17 December 2014. [Online]. Available: http://prometia.eu/wp-content/uploads/2014/02/3-PROMETIA-Rollat.pdf.

[29] C. G. Brown and L. G. Sherrington, "Solvent Extraction Used in Industrial Separation of Rare Earths," *Journal of Chemical Technology & Biotechnology,* no. 29, pp. 193-209, 1978.

[30] J. A. Gray, *An Equilibrium Study of the Chloride and Nitrate Systems of Praseodymium and Neodymium with Tributyl Phosphate and Acid,* Ames, IA: Iowa State University, 1965.

[31] A. V. Gelis and G. J. Lumetta, "Actinide Lanthanide Separation Process- ALSEP," *Industrial & Engineering Chemistry Research,* pp. 1624-1631, 2014.

[32] D. Magnusson, A. Geist, R. Malmbeck, G. Modolo and A. Wilden, "Flow-sheet design for an innovative SANEX process using TODGA and SO3-Ph-BTP," *Procedia Chemistry,* vol. 7, pp. 245-250, 2012.

[33] M. Gregoric, C. Ekberg, M. R. Foreman, B. Steenari and T. Retegan, "Characterization and Leaching of Neodymium Magnet Waste and Solvent Extraction of the Rare-Earth Elements Using TODGA," *Journal of Sustainable Metallurgy,* pp. 638-645, 2017.

[34] M. Husain, S. A. Ansari, P. K. Mohapatra, R. K. Gupta, V. S. Parmar and V. K. Manchanda, "Extraction chrmoatography of lanthanides using N,N,N',N'-tetraoctyl diglycolamide (TOGDA) as the stationary phase," *Desalination,* no. 229, pp. 294-301, 2008.

[35] M. E. Case, R. V. Fox, D. L. Baek, B. J. Mincher and C. M. Wai, "Extraction behavior of selected rare earth metals from acidic chloride media using tetrabutyl diglycolamide," *Solvent Extraction and Ion Exchange,* vol. 35, no. 7, pp. 496-506, 2017.

[36] D. M. Brigham, A. S. Ivanov, B. A. Moyer, L. H. Delmau, V. S. Bryantsev and R. J. Ellis, "Trefoil-Shaped Outer-Sphere Ion Clusters Mediate Lanthanide(III) Ion Transport with Diglycolamide Ligands," *Journal of the American Chemical Society,* no. 139, pp. 17350-17358, 2017.

[37] D. D. Dicholkar, P. Kumar, P. K. Heer, V. G. Gaikar, S. Kumar and R. Natarajan, "Synthesis of N,N,N',N'-Tetraoctyl-3-oxapentane-1,5-diamide (TODGA) and its Steam Thermolysis-Nitrolysis as a Nuclear Waste Solvent Minimization Method," *Industrial & Chemical Engineering Research,* no. 52, pp. 2457-2469, 2013.

[38] ExxonMobil, "Branched Alcohols," ExxonMobil, 2020. [Online]. Available: https://www.exxonmobilchemical.com/en/products/branched-alcohols.

[39] K. L. Lyon, V. P. Utgikar and M. R. Greenhalgh, "Dynamic Modeling for the Separation of Rare Earth Elements Using Solvent Extraction: Predicting Separation Performance Using Laboratory Equilibrium Data," *Industrial & Engineering Chemical Research,* pp. 1048-1056, 2017.

[40] W. Groenier, "Calculation of Transient Behavior of a Dilute-Purex Solvent Extraction Process Having Application to the Reprocessing of LMFBR Fuels," Oak Ridge National Laboratory, 1972.

[41] C. Bendixsen, "ICPSEF: A User's Manual for the Computer Mathematical Model of the ICPP PUREX Solvent Extraction System," Exxon Nuclear Idaho Company, Inc., November 1982.

[42] H. S. Fogler, Elements of Chemical Reaction Engineering, Prentice Hall, 2006.

[43] R. A. Leonard and M. C. Regalbuto, "A Spreadwise Algorithm for Stagewise Solvent Extraction," Argonne National Laboratory, 1993.

[44] M. Regalbuto, J. Copple, R. Leonard, C. Pereira and G. Vandergrift, "Solvent Extraction Process Development for Partitioning and Transmutation of Spent Fuel," Nuclear Energy Agency of the OECD (NEA): Oranisation for Economic Co-Operation and Development- Nuclear Energy Agency, 2005.

[45] Y. Zhang, J. Cohen, A. A. Davidson and J. D. Owens, "Chapter 11 - A Hybrid Method for Solving Tridiagonal Systems on the GPU," in *GPU Computing Gems Jade Edition*, Morgan Kaufmann, 2012, pp. 117-132.

[46] M. Benedict, T. H. Pigford and H. W. Levi, Nuclear Chemical Engineering, 2nd Edition, McGraw-Hill, Inc., 1981.

[47] J. Rydberg, G. R. Choppin, C. Musikas and T. Sekine, "Solvent Extraction Equilibria," in *Solvent Extraction Principles and Practice, 2nd Edition*, New York, Marcel Dekker, Inc, 2004, pp. 109-201.

[48] M. P. Jensen, T. Yaita and R. Chiarizia, "Reverse-Micelle Formation in the Partitioning of Trivalent f-Element Cations by Biphasic Systems Containing a Tetraalkyldiglycolamide," *Langmuir,* no. 23, pp. 4765-4774, 2007.

[49] P. J. D. Lloyd, "Principles of Industrial Solvent Extraction," in *Solvent Extraction Principles and Practice, 2nd Edition*, New York, Marcel Dekker, Inc., 2004, pp. 339-366.

[50] R. E. Treybal, Mass-Transfer Operations, 3rd Edition, McGraw-Hill Book Company, 1981.

[51] R. A. Leonard, "Solvent Characterization Using the Dispersion Number," in *Eighth Symposium on Separation Science and Technology for Energy Applications*, Gatlinburg, TN, 1993.

[52] M. O'Donoghue, Gems, 6th Edition, NAG Press, 2008.

[53] Y. Sasaki, Y. Sugo, K. Morita and K. L. Nash, "The Effect of Alkyl Substituents on Actinide and Lanthanide Extraction by Diglycolamide Compounds," *Solvent Extraction and Ion Exchange,* no. 33, pp. 625-641, 2015.

[54] A. Sengupta, A. Bhattacharyya, W. Verboom, S. Musharaf Ali and K. M. Prasanta, "Insight into the Complexation of Actinides and Lanthanides with Diglycolamide Derivatives: Experimental and Density Functional Theoretical Studies," *The Journal of Physical Chemistry,* no. 121, pp. 2640-2649, 2017.

[55] A. G. Baldwin, A. S. Ivanov, N. J. Williams, R. J. Ellis, B. A. Moyer, V. S. Bryantsev and J. C. Shafer, "Outer-Sphere Water Clusters Tune the Lanthanide Selectivity of Diglycolamides," *ACS Central Science,* no. 4, pp. 739-747, 2018.

[56] S. Nave, G. Modolo, C. Madic and F. Testard, "Aggregation Properties of N,N,N',N'-Tetraoctyl-3-oxapentanediamide (TODGA) in n-Dodecane," *Solvent Extraction and Ion Exchange,* vol. 22, no. 4, pp. 527-551, 2004.

[57] D. D. Ebbing and S. D. Gammon, General Chemistry, 8th Edition, New York: Houghton Mifflin Company, 2005.

[58] R. Chi and Z. Xu, "A Solution Chemistry Approach to the Study of Rare Earth Element Precipitation by Oxalic Acid," *Metallurgical and Materials Transactions B,* vol. 30B, pp. 189-195, 1999.

[59] M. Yaqub and W. Lee, "Zero-liquid discharge (ZLD) technology for resource recovery from wastewater: A review," *Science of the Total Environment,* no. 681, pp. 551-563, 2019.

APPENDIX A: IONIC RADII OF RARE EARTH ELEMENTS

Table A.1: Lanthanide M^{3+} ion size [22].

Atomic Number	Element	M^{3+} Radii (Å)
57	Lanthanum	1.061
58	Cerium	1.034
59	Praseodymium	1.013
60	Neodymium	0.995
61	Promethium	0.979
62	Samarium	0.964
63	Europium	0.950
64	Gadolinium	0.938
65	Terbium	0.923
66	Dysprosium	0.908
67	Holmium	0.894
68	Erbium	0.881
69	Thulium	0.869
70	Ytterbium	0.858
71	Lutetium	0.848
88	Yttrium	0.88

APPENDIX B: SINGLE METAL EXTRACTION EQUILIBRIUM DATA

Table B.1: Single metal extraction equilibrium data. All experiments conducted at O/A = 1 using 0.1 M TODGA/30% v/v Exxal-13/Isopar-L solvent

Element	Feed HCl (M)	Feed Ln (mM)	AQ EQ (mM)	ORG EQ (mM)	D_i	% Extraction	% DGA Loading	Free $[DGA]_{EQ}$ (M)	Total $[Cl^-]_{EQ}$ (M)	K_{EQ}
Lanthanum	4.23	197.33	171.67	29.12	0.170	15%	87%	0.013	4.75	783.7
	3.51	243.43	220.12	23.72	0.108	10%	71%	0.029	4.17	62.0
	2.53	247.17	232.86	13.55	0.058	5%	41%	0.059	3.23	8.2
	4.78	100.77	74.74	24.04	0.322	24%	72%	0.028	5.00	118.7
	3.86	125.29	104.87	19.16	0.183	15%	57%	0.043	4.17	32.8
	2.80	125.71	117.61	9.53	0.081	8%	29%	0.071	3.15	7.1
	4.62	62.64	41.96	19.41	0.462	31%	58%	0.042	4.75	59.3
	4.09	50.74	35.98	13.95	0.388	28%	42%	0.058	4.20	26.6
	2.92	63.49	56.52	6.86	0.121	11%	21%	0.079	3.09	8.2
Cerium	4.96	214.95	182.44	32.51	0.178	15%	98%	0.002	5.51	71363.5
	3.90	224.16	195.22	28.94	0.148	13%	87%	0.013	4.49	714.5
	2.80	223.20	203.44	19.76	0.097	9%	59%	0.041	3.41	36.3
	5.01	106.16	76.01	30.15	0.397	28%	90%	0.010	5.24	3171.6
	4.01	111.32	87.45	23.87	0.273	21%	72%	0.028	4.27	153.4
	2.94	113.51	99.90	13.61	0.136	12%	41%	0.059	3.24	19.3
	5.06	50.90	27.43	23.47	0.856	46%	70%	0.030	5.15	242.6
	4.02	54.26	36.07	18.19	0.504	34%	55%	0.045	4.13	76.4
	2.97	53.12	43.87	9.25	0.211	17%	28%	0.072	3.10	18.7
Praseodymium	4.23	18.94	5.92	12.28	2.074	65%	37%	0.063	4.25	107.4
	3.15	18.88	11.81	6.58	0.557	35%	20%	0.080	3.19	33.3
	2.07	18.63	16.95	1.48	0.088	8%	4%	0.096	2.12	10.5
	4.03	9.19	2.08	6.45	3.102	70%	19%	0.081	4.04	89.9
	3.15	9.38	5.31	3.61	0.680	38%	11%	0.089	3.17	30.2
	2.00	9.01	8.22	0.63	0.076	7%	2%	0.098	2.02	9.8
	4.03	2.30	0.83	3.36	4.062	146%	10%	0.090	4.03	85.1
	3.08	2.26	2.56	1.77	0.693	78%	5%	0.095	3.08	27.8
	1.80	2.30	4.20	0.33	0.080	15%	1%	0.099	1.82	13.7
Neodymium	4.16	61.00	30.66	27.48	0.896	45%	82%	0.018	4.26	2147.5
	3.01	57.09	38.79	18.37	0.473	32%	55%	0.045	3.13	171.4
	2.04	56.76	49.79	7.95	0.160	14%	24%	0.076	2.19	34.7
	4.12	29.21	8.57	19.87	2.320	68%	60%	0.040	4.14	495.3
	3.10	29.35	16.02	12.03	0.751	41%	36%	0.064	3.15	92.4
	2.03	29.63	25.10	4.23	0.168	14%	13%	0.087	2.10	27.2
	4.12	14.43	2.01	11.98	5.949	83%	36%	0.064	4.13	321.4
	3.09	14.44	6.08	7.92	1.303	55%	24%	0.076	3.11	98.0
	2.03	14.70	11.93	2.41	0.202	16%	7%	0.093	2.06	28.9
Samarium	2.82	7.53	1.31	6.02	4.596	80%	18%	0.082	2.82	373.0
	1.89	7.36	4.13	3.08	0.744	42%	9%	0.091	1.91	143.6
	0.91	7.52	7.07	0.45	0.064	6%	1%	0.099	0.93	82.0
	2.97	3.72	0.33	3.28	9.864	88%	10%	0.090	2.97	511.6
	1.95	3.66	1.80	1.78	0.989	49%	5%	0.095	1.96	154.9
	0.94	3.69	3.41	0.28	0.081	7%	1%	0.099	0.95	96.6
	2.94	1.75	0.13	1.57	11.916	90%	5%	0.095	2.94	540.1
	1.98	1.72	0.99	0.93	0.937	54%	3%	0.097	1.99	129.8
	0.96	1.78	1.60	0.15	0.096	9%	0%	0.100	0.97	107.1

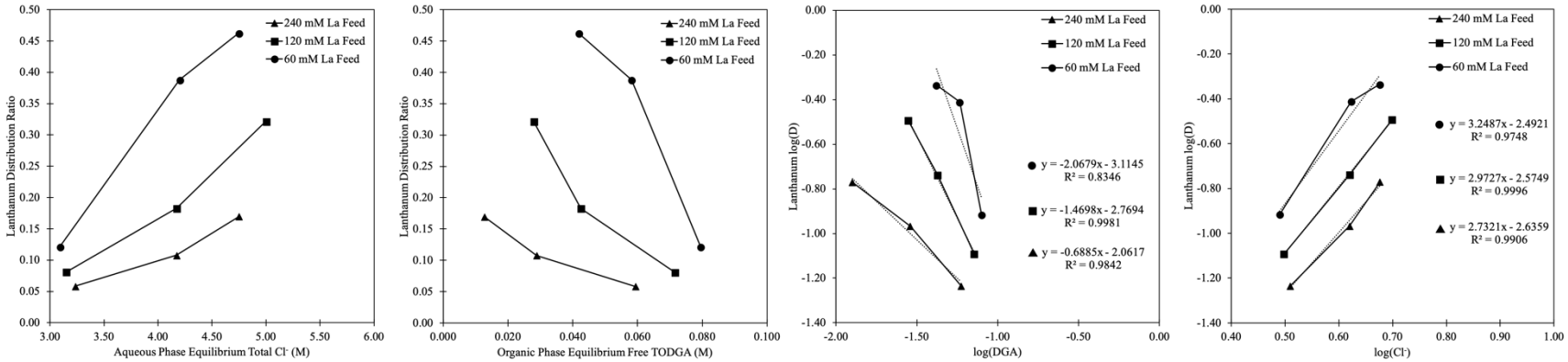

Figure B.1: Lanthanum distribution ratio trends as a function of equilibrium aqueous phase chloride concentration and organic phase free TODGA concentration.

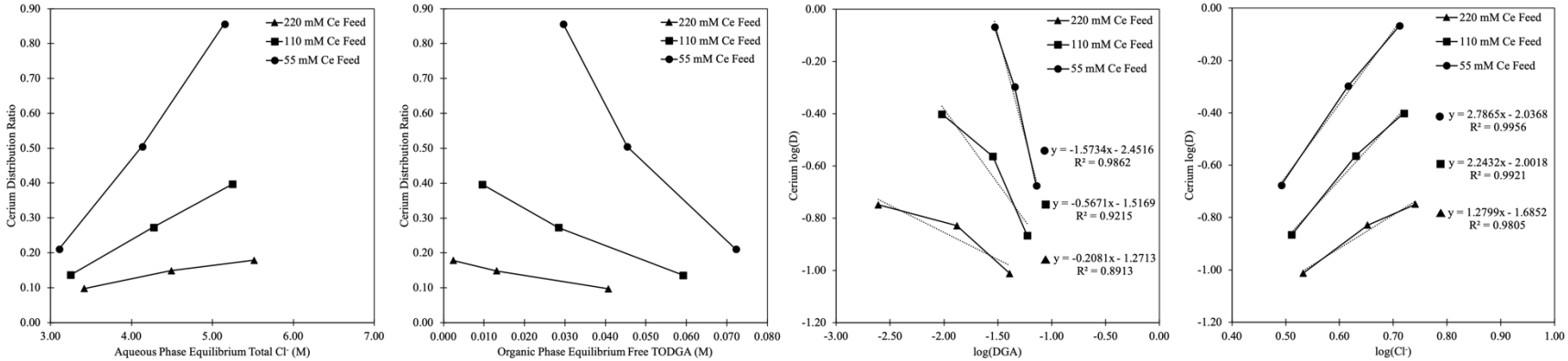

Figure B.2: Cerium distribution ratio trends as a function of equilibrium aqueous phase chloride concentration and organic phase free TODGA concentration.

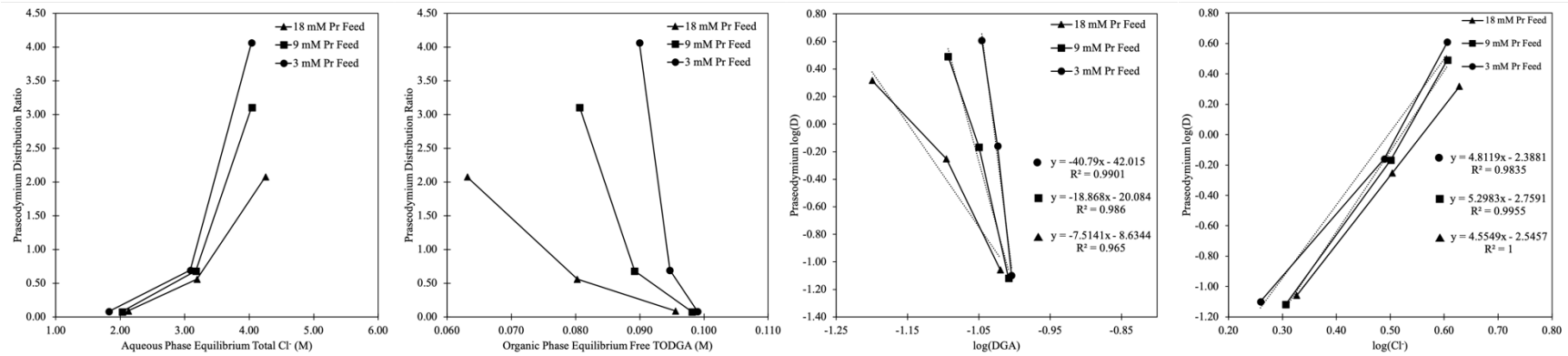

Figure B.3: Praseodymium distribution ratio trends as a function of equilibrium aqueous phase chloride concentration and organic phase free TODGA concentration.

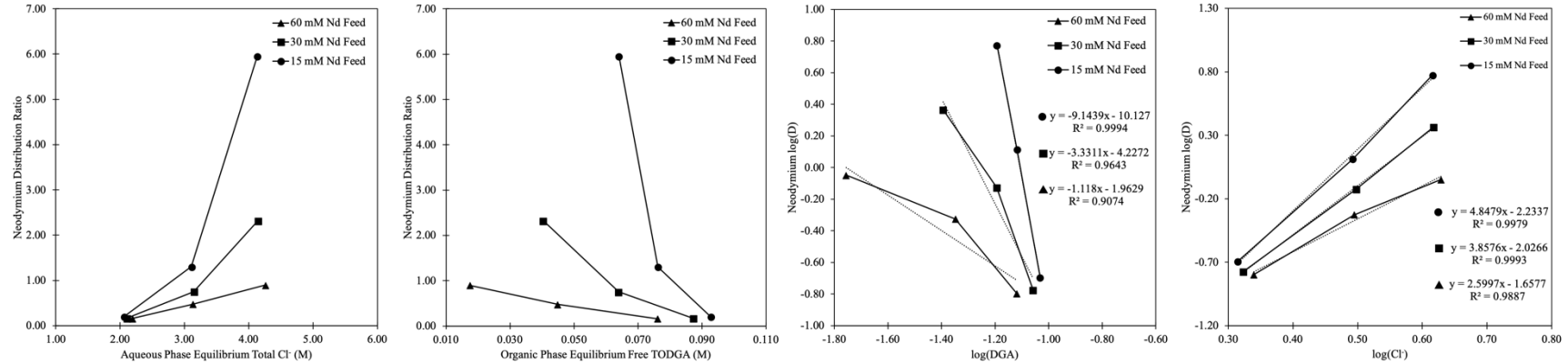

Figure B.4: Neodymium distribution ratio trends as a function of equilibrium aqueous phase chloride concentration and organic phase free TODGA concentration.

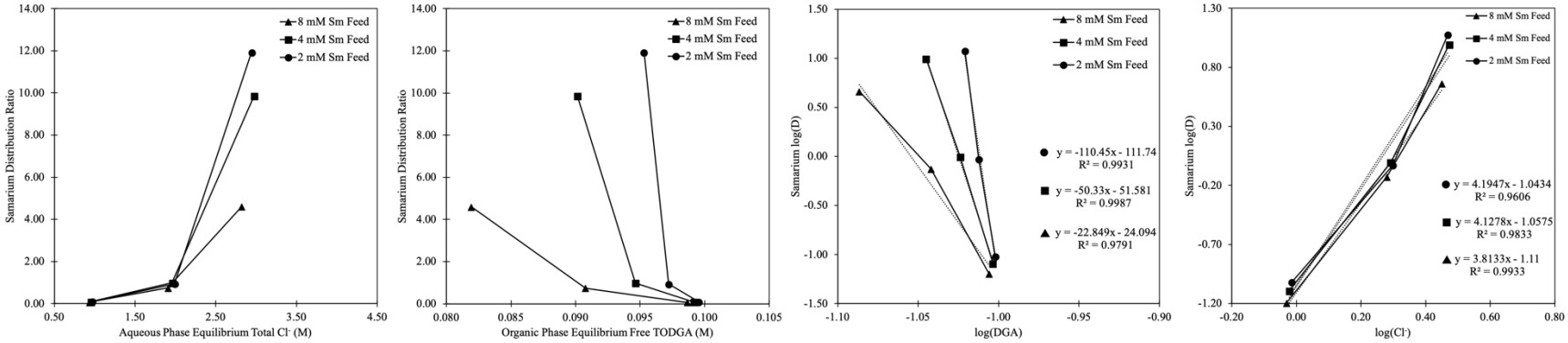

Figure B.5: Samarium distribution ratio trends as a function of equilibrium aqueous phase chloride concentration and organic phase free TODGA concentration

APPENDIX C: IDEAL LIGHT RARE EARTH SEPARATION CASCADE DESIGN FLOW DIAGRAM

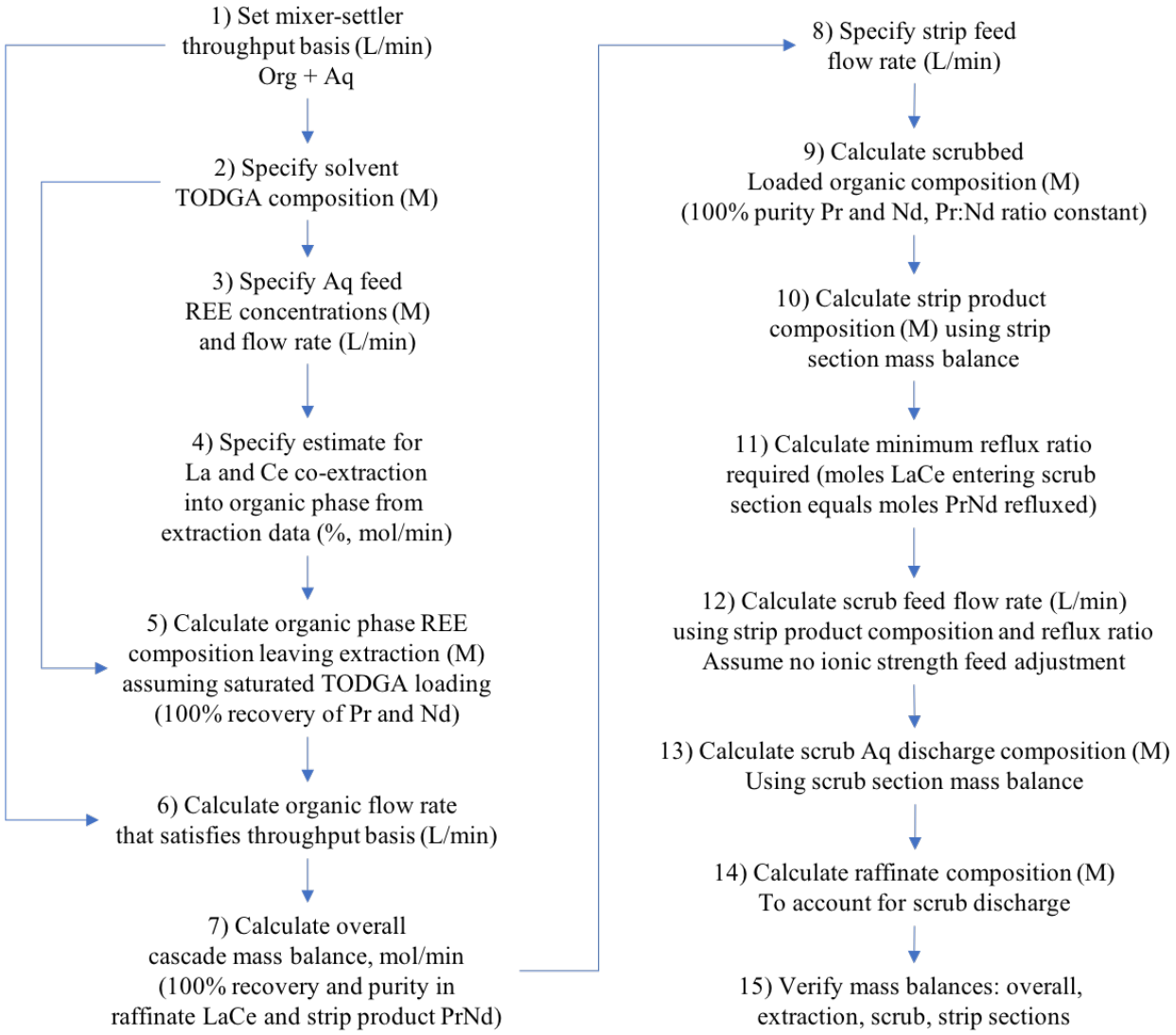

Figure C.1: Flow diagram for ideal cascade design calculations.

APPENDIX D: EQUILIBRIUM DATA FOR LIGHT RARE EARTH BATCH COUNTER-CURRENT EXPERIMENTS

Table D.1: Equilibrium data for light REE batch counter-current simulation extraction and scrub experiments.

	Simulated Stage	Aqueous Equilibrium (mM)					Organic Equilibrium (mM)					Theoretical Loading
		La	Ce	Pr	Nd	TOTAL	La	Ce	Pr	Nd	TOTAL	
Extraction	1	55.85	10.24	0.52	0.05	66.66	10.45	4.55	0.49	0.16	15.64	47%
	2	93.88	24.53	2.02	0.54	120.97	11.11	6.93	1.14	0.69	19.87	60%
	3	95.38	35.77	4.53	2.26	137.95	9.23	8.17	2.07	2.28	21.75	65%
	4	90.35	38.76	6.92	6.43	142.46	7.23	7.20	2.58	5.22	22.23	67%
	5	84.64	38.71	9.29	14.52	147.17	5.88	5.85	2.79	9.48	24.00	72%
Scrub	6	57.29	37.89	11.15	21.32	127.66	3.47	5.61	3.15	12.81	25.04	75%
	7	40.93	41.84	15.78	25.26	123.81	2.43	5.51	4.14	14.18	26.26	79%
	8	21.30	37.19	24.71	37.95	121.15	1.08	4.17	5.03	16.72	27.01	81%
	9	10.53	27.45	33.56	58.18	129.72	0.40	2.32	5.27	19.50	27.48	82%
	10	2.61	11.60	38.73	81.02	133.95	0.09	0.88	5.07	22.09	28.12	84%

Table D.2: Distribution ratios and separation factors for light REE batch counter-current simulation extraction and scrub experiments.

	Simulated Stage	Distribution Ratios				Separation Factors					
		D_{La}	D_{Ce}	D_{Pr}	D_{Nd}	β Ce-La	β Pr-Ce	β Nd-Pr	β Pr-La	β Nd-La	β Nd-Ce
Extraction	1	0.187	0.445	0.932	2.902	2.4	2.1	3.1	5.0	15.5	6.5
	2	0.118	0.283	0.562	1.285	2.4	2.0	2.3	4.7	10.9	4.5
	3	0.097	0.228	0.457	1.007	2.4	2.0	2.2	4.7	10.4	4.4
	4	0.080	0.186	0.373	0.811	2.3	2.0	2.2	4.7	10.1	4.4
	5	0.070	0.151	0.300	0.653	2.2	2.0	2.2	4.3	9.4	4.3
Scrub	6	0.061	0.148	0.282	0.601	2.4	1.9	2.1	4.7	9.9	4.1
	7	0.059	0.132	0.263	0.561	2.2	2.0	2.1	4.4	9.5	4.3
	8	0.051	0.112	0.204	0.441	2.2	1.8	2.2	4.0	8.7	3.9
	9	0.038	0.084	0.157	0.335	2.2	1.9	2.1	4.2	8.9	4.0
	10	0.034	0.075	0.131	0.273	2.2	1.7	2.1	3.9	8.0	3.6

APPENDIX E: EQUILIBRIUM DATA FOR 24 STAGE LIGHT RARE EARTH MIXER-SETTLER TEST

Table E.1: Equilibrium data for 24-stage counter-current mixer-settler experiment for the separation of PrNd from a light REE mixture.

	Stage	HCl	Aqueous Phase				Organic Phase				Distribution Ratios				Adjacent Separation Factors			% TODGA
		(mol/L)	La (mM)	Ce (mM)	Pr (mM)	Nd (mM)	La (mM)	Ce (mM)	Pr (mM)	Nd (mM)	La	Ce	Pr	Nd	Ce/La	Pr/Ce	Nd/Pr	Loading
EXTRACTION	1	3.08	69.568	27.128	8.062	-	9.424	7.857	3.085	-	0.135	0.290	0.383	-	2.14	1.32	-	61%
	2	3.15	93.180	46.235	15.635	-	9.738	10.314	4.856	-	0.105	0.223	0.311	-	2.13	1.39	-	75%
	3	3.16	94.655	52.396	19.910	-	8.960	10.584	5.796	-	0.095	0.202	0.291	-	2.13	1.44	-	76%
	4	3.08	90.470	51.699	21.531	-	8.473	10.415	6.453	0.457	0.094	0.201	0.300	-	2.15	1.49	-	77%
	5	3.35	90.224	51.502	23.050	-	7.789	9.584	6.477	1.427	0.086	0.186	0.281	-	2.16	1.51	-	76%
	6	3.12	89.838	50.492	23.872	-	7.545	9.136	6.662	3.038	0.084	0.181	0.279	-	2.15	1.54	-	79%
	7	3.14	86.864	47.799	23.093	2.364	6.692	7.879	5.909	5.073	0.077	0.165	0.256	2.146	2.14	1.55	8.39	77%
	8	3.08	84.061	45.056	21.763	7.164	5.916	6.797	5.076	7.494	0.070	0.151	0.233	1.046	2.14	1.55	4.48	76%
	9	3.13	84.415	43.952	20.583	13.733	5.394	6.022	4.312	10.355	0.064	0.137	0.209	0.754	2.14	1.53	3.60	78%
	10	3.02	81.596	40.793	18.309	19.555	4.888	5.331	3.638	12.476	0.060	0.131	0.199	0.638	2.18	1.52	3.21	79%
SCRUB	11	3.12	58.225	48.082	21.335	22.849	3.314	5.761	3.880	13.059	0.057	0.120	0.182	0.572	2.11	1.52	3.14	78%
	12	3.03	35.836	46.601	21.122	22.853	2.333	6.352	4.376	13.976	0.065	0.136	0.207	0.612	2.09	1.52	2.95	81%
	13	3.05	24.008	49.586	23.670	25.801	1.316	5.976	4.417	13.429	0.055	0.121	0.187	0.520	2.20	1.55	2.79	75%
	14	3.02	15.089	51.828	27.579	30.297	0.817	5.997	4.908	14.371	0.054	0.116	0.178	0.474	2.14	1.54	2.67	78%
	15	3.08	9.084	50.274	31.201	35.436	0.455	6.087	5.964	16.996	0.050	0.121	0.191	0.480	2.42	1.58	2.51	89%
	16	3.04	4.935	43.757	33.980	40.329	0.159	4.503	5.488	15.573	0.032	0.103	0.162	0.386	3.20	1.57	2.39	77%
	17	3.14	2.679	37.108	37.840	49.382	0.021	3.445	5.583	16.486	0.008	0.093	0.148	0.334	11.85	1.59	2.26	77%
	18	3.17	1.227	27.012	38.945	58.355	-	2.391	5.603	18.439	-	0.089	0.144	0.316	-	1.63	2.20	79%
	19	3.06	0.444	16.859	38.744	73.505	-	1.437	5.076	19.558	-	0.085	0.131	0.266	-	1.54	2.03	78%
	20	3.18	0.093	8.824	38.792	98.248	-	0.712	4.427	21.926	-	0.081	0.114	0.223	-	1.41	1.96	81%
STRIP	21	0.75	-	3.900	22.385	107.321	-	0.029	0.519	4.740	-	0.008	0.023	0.044	-	3.08	1.91	16%
	22	0.56	-	0.555	3.523	26.918	-	-	-	0.050	-	-	-	0.002	-	-	-	0%
	23	0.55	-	0.047	0.291	2.834	-	-	-	0.378	-	-	-	0.133	-	-	-	1%
	24	0.55	-	0.001	0.033	0.339	-	-	-	-	-	-	-	-	-	-	-	0%

APPENDIX F: DGA DISPERSION TESTING PHOTOGRAPHS

These representative photographs were taken after phase disengagement by gravity was complete for batch shakeout experiments used to calculate the dispersion number in Table 8.2. Photographs were also taken after centrifugation for samples that gelled. Actual photographs list REE concentrations using a total rare earth oxide (TREO) basis in g/L; this is the standard unit reported in the rare earth industry for specifying rare earth concentrations in solvent extraction. Concentrations reported in this work predominantly use a molar basis. Therefore, the following conversions are provided for clarity: 12 g/L TREO = 73 mM REE, 36 g/L TREO = 218 mM REE, and 60 g/L TREO = 363 mM REE. TREO composition using a mass basis is 63% La_2O_3, 5% CeO_2, 9% Pr_6O_{11}, and 24% Nd_2O_3. Elemental REE composition using a molar basis is 64% La, 5% Ce, 8% Pr, and 23% Nd.

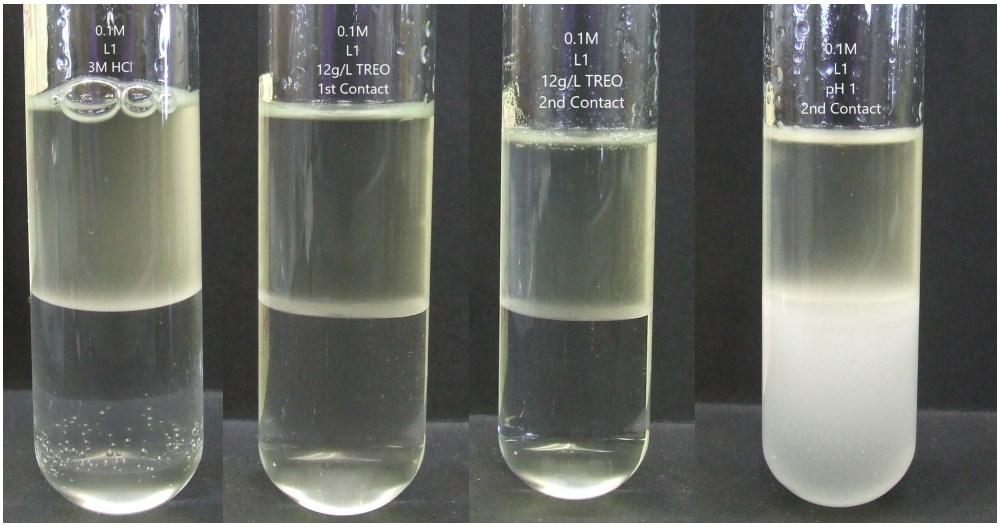

Figure F.1: 0.1 M TODGA/5% Exxal-13/Isopar-L dispersion number experiments. From left to right: 3 M HCl contact, 73mM REE in 3 M HCl contact, 2nd 73mM REE in 3 M HCl contact, and 2nd pH 1 HCl contact (1st pH 1 contact not shown).

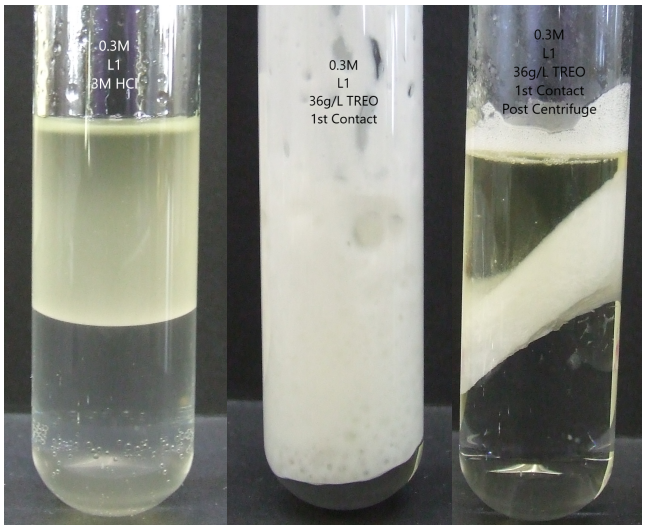

Figure F.2: 0.3 M TODGA/5% Exxal-13/Isopar-L dispersion number experiments. From left to right: 3 M HCl contact, 218 mM REE in 3 M HCl contact, 218 mM REE in 3 M HCl contact post-centrifuge.

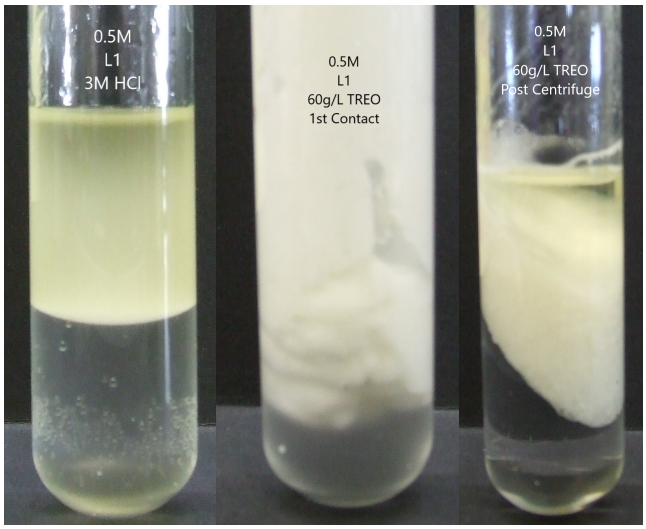

Figure F.3: 0.5 M TODGA/5% Exxal-13/Isopar-L dispersion number experiments. From left to right: 3 M HCl contact, 363 mM REE in 3 M HCl contact, 363 mM REE in 3 M HCl contact post-centrifuge.

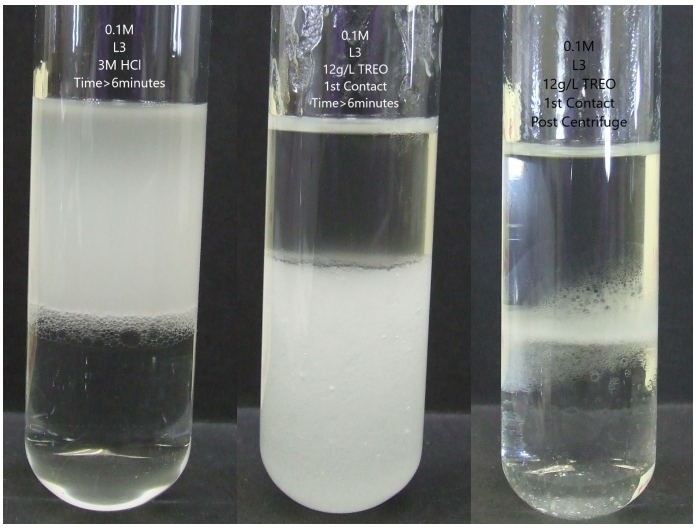

Figure F.4: 0.1 M DMDODGA/5% Exxal-13/Isopar-L dispersion number experiments. From left to right: 3 M HCl contact, 73mM REE in 3 M HCl contact, 73mM REE in 3 M HCl contact post-centrifuge.

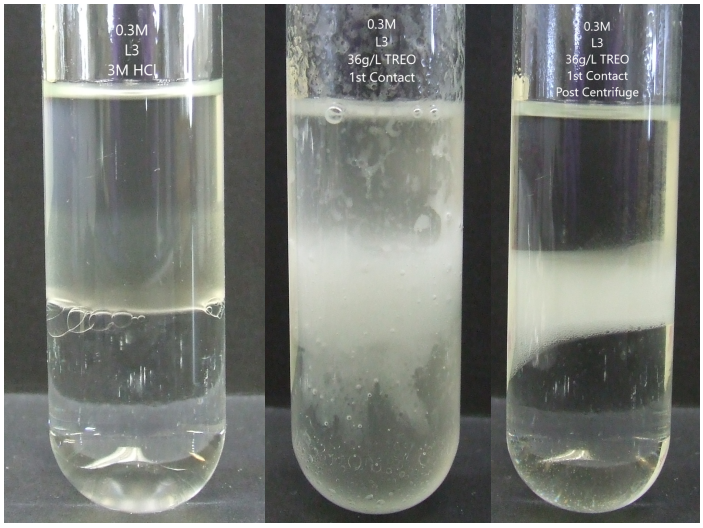

Figure F.5: 0.3 M DMDODGA/5% Exxal-13/Isopar-L dispersion number experiments. From left to right: 3 M HCl contact, 218 mM REE in 3 M HCl contact, 218 mM REE in 3 M HCl contact post-centrifuge.

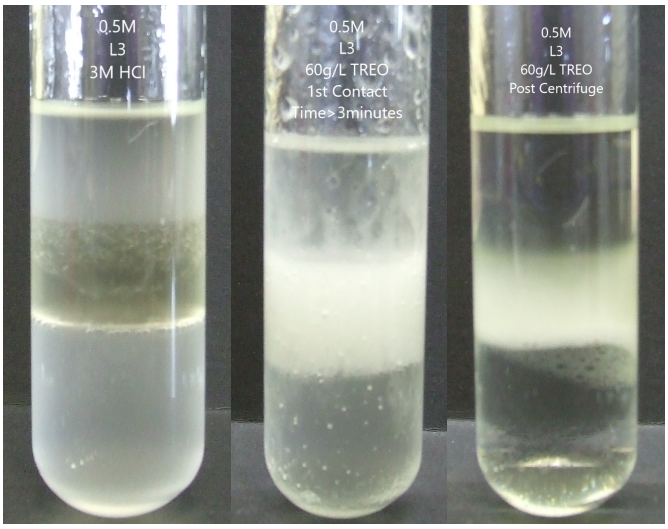

Figure F.6: 0.5 M DMDODGA/5% Exxal-13/Isopar-L dispersion number experiments. From left to right: 3 M HCl contact, 363 mM REE in 3 M HCl contact, 363 mM REE in 3 M HCl contact post-centrifuge.

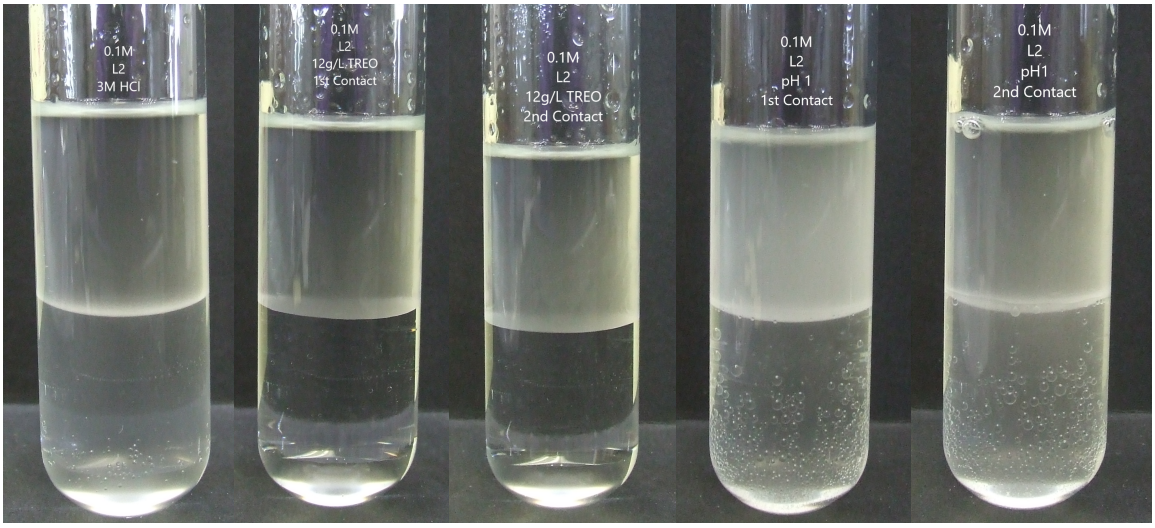

Figure F.7: 0.1 M T2EHDGA/5% Exxal-13/Isopar-L dispersion number experiments. From left to right: 3 M HCl contact, 73mM REE in 3 M HCl contact, 2nd 73mM REE in 3 M HCl contact, pH 1 HCl contact, and 2nd pH 1 HCl contact.

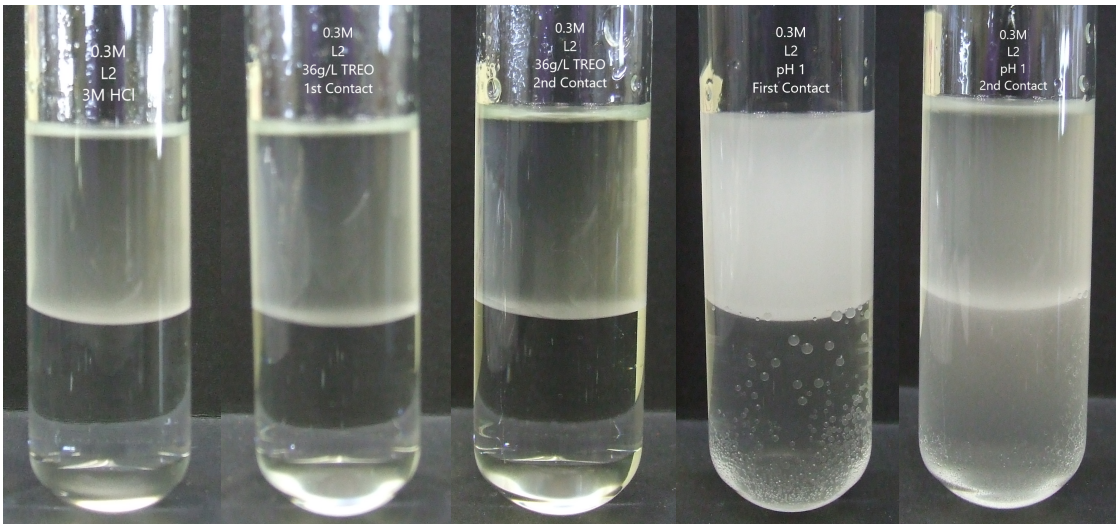

Figure F.8: 0.3 M T2EHDGA/5% Exxal-13/Isopar-L dispersion number experiments. From left to right: 3 M HCl contact, 218 mM REE in 3 M HCl contact, 2nd 218 mM REE in 3 M HCl contact, pH 1 HCl contact, and 2nd pH 1 HCl contact.

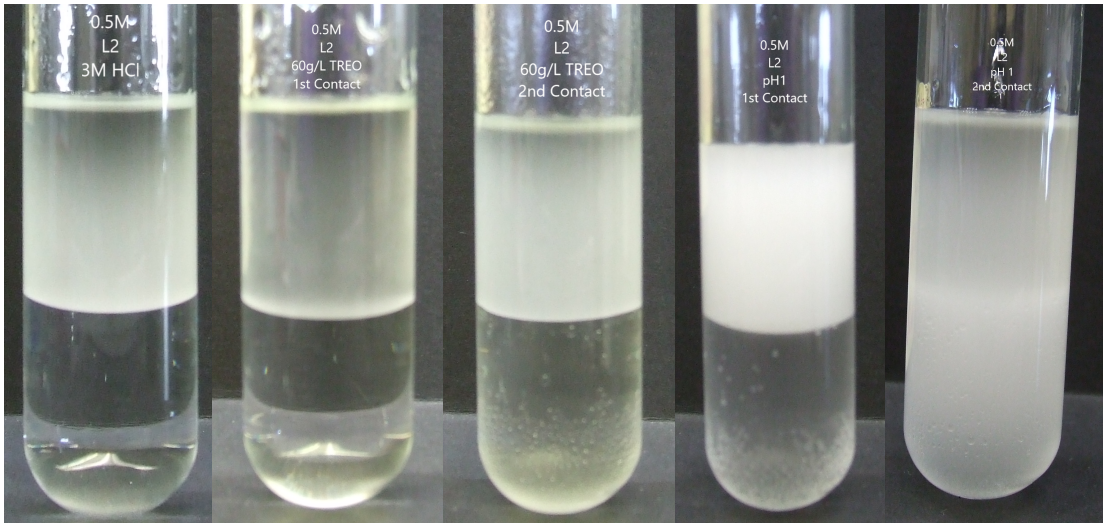

Figure F.9: 0.5 M T2EHDGA/5% Exxal-13/Isopar-L dispersion number experiments. From left to right: 3 M HCl contact, 363 mM REE in 3 M HCl contact, 2nd 363 mM REE in 3 M HCl contact, pH 1 HCl contact, and 2nd pH 1 HCl contact.